

BPHZ renormalisation and vanishing subcriticality asymptotics of the fractional Φ_d^3 model

Nils Berglund and Yvain Bruned

February 21, 2024

Abstract

We consider stochastic PDEs on the d -dimensional torus with fractional Laplacian of parameter $\rho \in (0, 2]$, quadratic nonlinearity and driven by space-time white noise. These equations are known to be locally subcritical, and thus amenable to the theory of regularity structures, if and only if $\rho > d/3$. Using a series of recent results by the second named author, A. Chandra, I. Chevyrev, M. Hairer and L. Zambotti, we obtain precise asymptotics on the renormalisation counterterms as the mollification parameter ε becomes small and ρ approaches its critical value. In particular, we show that the counterterms behave like a negative power of ε if ε is superexponentially small in $(\rho - d/3)$, and are otherwise of order $\log(\varepsilon^{-1})$. This work also serves as an illustration of the general theory of BPHZ renormalisation in a relatively simple situation.

2010 *Mathematical Subject Classification.* 60H15, 35R11 (primary), 81T17, 82C28 (secondary).

Keywords and phrases. Stochastic partial differential equations, regularity structures, fractional Laplacian, BPHZ renormalisation, subcriticality boundary.

1 Introduction

The last years have witnessed tremendous progress in the theory of singular stochastic partial differential equations (SPDEs). The theory of regularity structures, introduced by Martin Hairer in [19], provides a functional analysis framework in which many so-called locally subcritical singular SPDEs can be shown to admit (local in time) solutions. The theory has been successfully applied to a number of different SPDEs, including the KPZ equation [18, 27, 30] and its generalisations to polynomial nonlinearities [25] and non-polynomial nonlinearities [29], the dynamic Φ_3^4 model [19, 28], the continuum parabolic Anderson model [22], the Navier–Stokes equation [34], the motion of a random string on a curved surface [20, 5], the FitzHugh–Nagumo SPDE [2], the dynamical Sine–Gordon model [26, 9], the heat equation driven by space-time fractional noise [14], reaction-diffusion equations with a fractional Laplacian [3], and the multiplicative stochastic heat equation [24, 23].

A limitation of the theory introduced in [19] is that, while it provides function spaces allowing to prove fixed-point theorems in a very general setting, the applications to SPDEs also require a renormalisation procedure, which had to be carried out in an *ad hoc* manner in each case. This situation has been remedied in a series of papers by the second named author, Ajay Chandra, Ilya Chevyrev, Martin Hairer and Lorenzo Zambotti [6, 8, 4]. These works provide a kind of black box, allowing to automatically renormalise any locally subcritical SPDE. Owing to its great generality, however, this theory is rather abstract, making it somewhat difficult of access.

A first goal of the present work is to illustrate the general theory in one of the simplest possible, yet interesting examples. This example is the Φ^3 model with fractional Laplacian $\Delta^{\rho/2}$ on the d -dimensional torus, driven by space-time white noise ξ , whose equation before renormalisation reads

$$\partial_t u - \Delta^{\rho/2} u = u^2 + \xi . \quad (1.1)$$

A family of SPDEs with fractional Laplacian, including the above example, was considered in [3]. Results in that work imply in particular that the above equation is locally subcritical if and only if $\rho > \rho_c = \frac{d}{3}$. As the parameter ρ of the fractional Laplacian decreases towards its critical value ρ_c , the size of the model space describing a regularity structure for (1.1) diverges exponentially fast in $1/(\rho - \rho_c)$. As we shall see, this has an effect on the renormalisation procedure for the equation, since the counterterms entering this procedure involve sums over elements of the model space having negative degree (see [6, Thm. 2.21] and (3.3) below). This should be a general phenomenon for models approaching the subcriticality threshold.

The fact that the nonlinearity in (1.1) is quadratic entails a number of significant simplifications when applying the general theory of [6, 8, 4], owing to the fact that the model space can be described precisely in terms of binary trees. This considerably simplifies a number of combinatorial arguments. Throughout the analysis, we provide numerous examples, which should help to illustrate the general abstract theory.

A second goal of this work is to analyse in detail the limit $\rho \searrow \rho_c$, i.e. when approaching the threshold where local subcriticality is lost. The hope is that this will improve the understanding of the role of subcriticality in renormalisation of singular SPDEs and the theory of regularity structures. The renormalisation procedure requires to modify the SPDE (1.1) by mollifying space-time noise ξ on scale ε , and adding ε -dependent counterterms to the equation. Our main result, Theorem 2.1, analyses the asymptotic behaviour of these counterterms as a function of ε and $\rho - \rho_c$. We obtain that if ε is superexponentially small in terms of $\rho - \rho_c$, the counterterms scale like a negative power of ε , while for larger ε , they have order $\log(\varepsilon^{-1})$.

Note that fractional models near criticality have been studied before, in particular in the context of constructive Quantum Field Theory (QFT). For instance, the large-volume (infrared) behaviour of the static $\Phi_{4-\delta}^4$ model has been studied in [7], by modifying the Laplacian of the Φ_4^4 model in order to make it subcritical. The picture that emerges from a renormalisation group (RG) analysis is that while for $\delta = 0$, the RG flow converges to a Gaussian fixed point, for $\delta > 0$, this fixed point becomes unstable, and a non-Gaussian fixed point appears. Recently, in [1] Aizenman and Duminil–Copin proved that by taking both the large-volume and zero-spacing (ultraviolet) limit of a lattice model converging to the Φ_4^4 model, one converges to a model with Gaussian fluctuations. It is thus of interest to try to connect what is known on static models at and near criticality, with what happens to the renormalisation procedure in near-critical dynamical models.

A final motivation for this article is that the equation (1.1) is interesting in its own right. For instance, it approximates the Fisher–KPP equation for population dynamics [16, 31] for intermediate population values. Note that the real Fisher–KPP equation contains a factor of the form $\sqrt{u(1-u)}$ in front of the noise ξ , and it currently seems unlikely that such a nonlinearity could be handled with the help of regularity structures. However, an understanding of the equation with additive noise may provide some useful first insights on its dynamics. See also [3] for further motivation on considering SPDEs with fractional Laplacians as a way to regularise coupled SPDE–ODE systems.

The remainder of this article is organised as follows. Section 2 gives a detailed description of the model, and states the main result, Theorem 2.1, on the asymptotic behaviour of counterterms. Section 3 summarises the construction of the model space, and the main results from [6, 8, 4] needed to compute the renormalised equation. The most difficult step in applying the general theory is to compute the expectation of the renormalised canonical model elements, and is presented in the next

three sections. Section 4 describes how these expectations can be represented in terms of Feynman diagrams (see Definition 4.11). Section 5 introduces the notions of forests (see Definition 5.5) and Hepp sectors (see Definition 5.11), needed to apply ideas from BPHZ renormalisation theory, as explained in [21] in the Euclidean case. Most of our formalism is taken from [21], which transposes the algebraic construction in [6] and the proof of the renormalised model convergence in [8] to Feynman diagrams. It has a strong connection with the algebraic structures observed by Connes and Kreimer in [12, 13]. The main difference comes from the presence of Taylor expansions, which are encoded at the level of the diagrams by changing decorations. In our model, we can to a large extent circumvent these Taylor expansions and thus be closer to the extraction-contraction renormalisation procedure on Feynman diagrams. The actual bounds on the expectations are then obtained in Section 6, and the asymptotic analysis completing the proof of the main result is given in Section 7.

Acknowledgments

We would like to thank Christian Kuehn for many useful discussions. Part of this work was carried out while the authors attended the programme ‘‘Scaling limits, rough paths, quantum field theory’’ (SRQ) held at the Isaac Newton Institute (INI) in Cambridge. We would like to thank the organisers of this trimester for putting together a stimulating programme, and the members of INI for providing a friendly working atmosphere. NB thanks the School of Mathematics at the University of Edinburgh, and YB thanks the Institut Denis Poisson at the University of Orléans for hospitality during mutual visits. YB gratefully acknowledges funding support from the European Research Council (ERC) through the ERC Starting Grant Low Regularity Dynamics via Decorated Trees (LoRDeT), grant agreement No. 101075208. Finally, we thank the anonymous referees for their remarks, which led to an improvement in the presentation.

2 Model and results

We are interested in the SPDE

$$\partial_t u - \Delta^{\rho/2} u = u^2 + \xi \quad (2.1)$$

for the unknown $u = u(t, x)$ with $(t, x) \in \mathbb{R}_+ \times \mathbb{T}^d$, where $\Delta^{\rho/2} = -(-\Delta)^{\rho/2}$ denotes the fractional Laplacian with $0 < \rho \leq 2$, and ξ denotes space-time white noise. As such, this equation is not well-posed in general, and a renormalisation procedure is required. The general form of the renormalised equation is expected to be

$$\partial_t u - \Delta^{\rho/2} u = u^2 + C(\varepsilon, \rho, u) + \xi^\varepsilon, \quad (2.2)$$

where $\xi^\varepsilon = \varrho^\varepsilon * \xi$ denotes space-time white noise mollified on scale ε , and $C(\varepsilon, \rho, u)$ is a counterterm which diverges as $\varepsilon \searrow 0$. Here $\varrho^\varepsilon(t, x) = \varepsilon^{-(\rho+d)} \varrho(\varepsilon^{-\rho} t, \varepsilon^{-1} x)$ for a smooth, compactly supported mollifier ϱ integrating to 1, and $*$ denotes space-time convolution.

The theory of regularity structures introduced in [19] applies, provided the equation (2.1) is *locally subcritical*, or superrenormalisable in physicist’s terms. As shown in [3, Theorem 4.3], (2.1) is locally subcritical for

$$\rho > \rho_c(d) = \frac{d}{3}.$$

Note that $\rho_c < 2$ imposes $d \leq 5$ (Figure 1). One can guess this threshold by a scaling argument. Indeed, let us set $\bar{u}(t, x) = \lambda^\alpha u(\lambda^\beta t, \lambda x)$ with $\lambda > 0$ and $\alpha, \beta \in \mathbb{R}$. Then, \bar{u} solves the equation

$$\partial_t \bar{u} - \lambda^{\beta-\rho} \Delta^{\rho/2} \bar{u} = \lambda^{\beta-\alpha} \bar{u}^2 + \lambda^{\alpha+\beta} \xi_{\lambda^\beta, \lambda} = \lambda^{\beta-\alpha} \bar{u}^2 + \lambda^{\alpha+\frac{\beta}{2}-\frac{d}{2}} \xi, \quad (2.3)$$

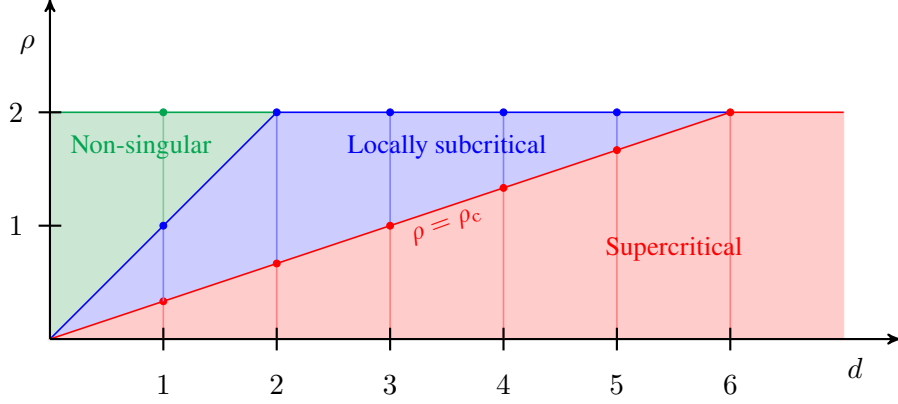


FIGURE 1: Parameter space (d, ρ) . Results in this article apply to the locally subcritical regime $\rho_c = \frac{d}{3} < \rho < d$, with $\rho \leq 2$.

where the second equality is in law, and $\xi_{\lambda^\beta, \lambda}$ denotes scaled space-time white noise given by

$$\langle \xi_{\lambda^\beta, \lambda}, \varphi \rangle = \langle \xi, \varphi^{\lambda^\beta, \lambda} \rangle, \quad \varphi^{\lambda^\beta, \lambda}(t, x) = \frac{1}{\lambda^{\beta+d}} \varphi\left(\frac{t}{\lambda^\beta}, \frac{x}{\lambda}\right)$$

for any compactly supported test function φ . Setting $\alpha = \frac{d-\beta}{2}$, the noise intensity is the same in (2.1) and (2.3). Then one has $\beta - \alpha = \frac{3}{2}(\beta - \rho_c)$, so that

$$\partial_t \bar{u} - \lambda^{\beta-\rho} \Delta^{\rho/2} \bar{u} = g \bar{u}^2 + \xi, \quad g = \lambda^{\frac{3}{2}(\beta-\rho_c)}. \quad (2.4)$$

The natural choice is then $\beta = \rho$, which corresponds to the fractional scaling $\mathfrak{s} = (\rho, 1, \dots, 1)$ (cf. (4.2)). One thus obtains two regimes:

- If $\rho > \rho_c$ and we let λ tend to 0, then g tends to 0, i.e. (2.4) converges to a linear equation. This is exactly the definition of local subcriticality.
- If $\rho = \rho_c$, we recover the non-linear equation we started with, i.e. the system is invariant under this particular scaling. This is reminiscent of what is called a fixed point of the Wilsonian renormalisation group in the language of physicists.

The counterterm $C(\varepsilon, \rho, u)$ in (2.2) is expected to diverge also in the limit $\rho \searrow \rho_c$, and the main goal of this work is to determine how $C(\varepsilon, \rho, u)$ behaves as a function of ε and $\rho - \rho_c$ for small values of these parameters.

In order to formulate the main result, we define, for $a \in \mathbb{R}$ and $k > 0$, the threshold value

$$\varepsilon_c(\rho, a, k) = \exp\left\{-\frac{1}{\rho - \rho_c} \left[\log k + a - \frac{\log(k+1)}{2k} \right]\right\}.$$

Then we set

$$\varepsilon_c(\rho, a) = \varepsilon_c(\rho, a, k_{\max}), \quad \bar{\varepsilon}_c(\rho, a) = \varepsilon_c(\rho, a, \bar{k}_{\max}),$$

where

$$k_{\max} = \frac{d - \rho}{3(\rho - \rho_c)} \quad \text{and} \quad \bar{k}_{\max} = \frac{d - 2\rho}{3(\rho - \rho_c)}.$$

The integer parts of k_{\max} and \bar{k}_{\max} measure the size of the model space of the regularity structure (cf. [3, Thm. 4.18]), where k_{\max} is associated with the part of the counterterm $C(\varepsilon, \rho, u)$ that does

not depend on u , while \bar{k}_{\max} determines its part linear in u . Note that $\varepsilon_c(\rho, a) > \bar{\varepsilon}_c(\rho, a)$, and that as ρ decreases to ρ_c , $\varepsilon_c(\rho, a)$ and $\bar{\varepsilon}_c(\rho, a)$ both go to zero superexponentially fast, namely like

$$\exp\left\{-\frac{1}{\rho - \rho_c}\left[\log\left(\frac{1}{\rho - \rho_c}\right) + \mathcal{O}(1)\right]\right\}. \quad (2.5)$$

Finally, for $\eta < 0$, we denote by $\mathcal{C}^\eta(\mathbb{T}^d)$ the Besov–Hölder space defined as the set of distributions ζ on \mathbb{T}^d such that $\lambda^{-\eta}|\langle \zeta, \mathcal{S}_x^\lambda \varphi \rangle|$ is bounded uniformly in $\lambda \in (0, 1]$ for any $x \in \mathbb{T}^d$ and any compactly supported test function φ of class $\mathcal{C}^{\lceil -\eta \rceil}$, where $(\mathcal{S}_x^\lambda \varphi)(y) = \lambda^{-d} \varphi(\lambda^{-1}(y - x))$.

Our main result is then the following.

Theorem 2.1 (Main result). *Assume $\rho < \frac{d}{2}$ and $\rho \in (\rho_c, 2]$. Then there exist functions $C_i(\varepsilon, \rho)$, $i \in \{0, 1\}$, such that for any initial condition $u_0 \in \mathcal{C}^\eta(\mathbb{T}^d)$ with $\eta > -\frac{\rho}{2}$, the regularised renormalised SPDE (2.2) with counterterm*

$$C(\varepsilon, \rho, u) = C_0(\varepsilon, \rho) + C_1(\varepsilon, \rho)u$$

admits a sequence of local solutions u^ε , converging in probability to a limiting process as $\varepsilon \rightarrow 0$. Furthermore, there exist constants a, M, A_0 and \bar{A}_0 , all independent of ε and ρ , such that, writing $\varepsilon_c = \varepsilon_c(\rho, a)$ and $\bar{\varepsilon}_c = \bar{\varepsilon}_c(\rho, a)$, the first counterterm satisfies

$$\begin{aligned} |C_0(\varepsilon, \rho)| &\leq M \varepsilon_c^{-(d-\rho)} \left[\log(\varepsilon^{-1}) + \frac{1}{\rho - \rho_c} \left(\frac{\varepsilon_c}{\varepsilon} \right)^{3(\rho - \rho_c)} \right] && \text{if } \varepsilon \geq \varepsilon_c, \\ \left| \frac{C_0(\varepsilon, \rho)}{A_0 \varepsilon^{-(d-\rho)}} - 1 \right| &\leq \frac{M}{\rho - \rho_c} \left(\frac{\varepsilon}{\varepsilon_c} \right)^{3(\rho - \rho_c)} && \text{if } \varepsilon < \varepsilon_c, \end{aligned} \quad (2.6)$$

while the second counterterm satisfies

$$\begin{aligned} |C_1(\varepsilon, \rho)| &\leq M \bar{\varepsilon}_c^{-(d-2\rho)} \left[\log(\varepsilon^{-1}) + \frac{1}{\rho - \rho_c} \left(\frac{\bar{\varepsilon}_c}{\varepsilon} \right)^{3(\rho - \rho_c)} \right] && \text{if } \varepsilon \geq \bar{\varepsilon}_c, \\ \left| \frac{C_1(\varepsilon, \rho)}{\bar{A}_0 \varepsilon^{-(d-2\rho)}} - 1 \right| &\leq \frac{M}{\rho - \rho_c} \left(\frac{\varepsilon}{\bar{\varepsilon}_c} \right)^{3(\rho - \rho_c)} && \text{if } \varepsilon < \bar{\varepsilon}_c. \end{aligned} \quad (2.7)$$

Remark 2.2. Convergence is in probability in $\mathcal{C}_s^\alpha([0, T], \mathbb{T}^d)$, for any fixed $T > 0$, and for the process stopped when its \mathcal{C}_s^α -norm exceeds a fixed large cut-off L . Here α is any real number satisfying $\alpha < -\frac{1}{2}(d - \rho)$, and \mathcal{C}_s^α is the scaled Hölder–Besov space associated with the scaling of the fractional Laplacian. This space is defined in an analogous way as $\mathcal{C}^\alpha(\mathbb{T}^d)$, but with a fractional scaling given by $(\mathcal{S}_{(t,x),s}^\lambda \varphi)(s, y) = \lambda^{-(\rho+d)} \varphi(\lambda^{-\rho}(s - t), \lambda^{-1}(y - x))$. \diamond

Remark 2.3. The condition $\rho < \frac{d}{2}$ is due to the fact that we focus here on the asymptotic regime when the counterterms are given by sums of many divergent terms that are indexed by Feynman diagrams. More precisely, the results are meaningful when k_{\max} and \bar{k}_{\max} are both large. What happens for $\rho \geq \frac{d}{2}$ is in fact well known. When $\rho = d$, only the counterterm $C_0(\varepsilon, \rho)$ is required, and it diverges like $\log(\varepsilon^{-1})$. When $\frac{d}{2} < \rho < d$, $C_0(\varepsilon, \rho)$ is still the only required counterterm, but it diverges like $\varepsilon^{-(d-\rho)}$. When $\rho = \frac{d}{2}$, it becomes necessary to include the second counterterm $C_1(\varepsilon, \rho)$, which then diverges like $\log(\varepsilon^{-1})$. \diamond

Remark 2.4. The condition $\eta > -\frac{\rho}{2}$ is a consequence of the critical regularity of the initial condition in the fractional heat equation. Indeed, the scaling property $P_\rho(t, x) = t^{-d/\rho} P_\rho(1, t^{-1/\rho} x)$ of the fractional heat kernel implies that if $u_0 \in \mathcal{C}^\eta$ with $\eta < 0$, then $(P_\rho u_0)(t, x)$ blows up like $t^{\eta/\rho}$.

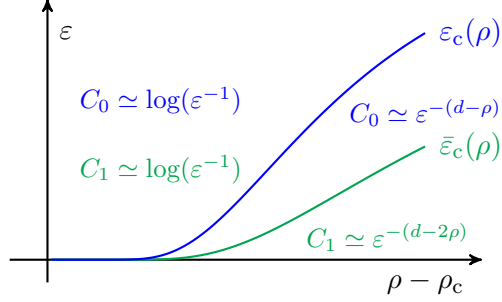


FIGURE 2: Behaviour of the counterterms as a function of $\rho - \rho_c$ and ε . The small- ε asymptotics of C_0 changes on the blue curve $\varepsilon = \varepsilon_c(\rho)$, while the asymptotics of C_1 changes on the green curve $\varepsilon = \bar{\varepsilon}_c(\rho)$.

Therefore, $(P_\rho u_0)(t, x)^2$ blows up like $t^{2\eta/\rho}$, and its space-time convolution with P_ρ is bounded if and only if $\eta > -\frac{\rho}{2}$.

More technically, the condition is related to the exponents of the space $\mathcal{D}^{\gamma, \eta}$ of modelled distributions in which one solves a fixed-point equation, where γ measures the Hölder regularity, while η controls the singularity at time zero (cf. [19, Def. 6.2]). Indeed, [19, Lemma 7.5] shows that if $u_0 \in \mathcal{C}^\eta(\mathbb{T}^d)$, then its convolution with the Green function of the fractional Laplacian can be identified with an element of $\mathcal{D}^{\gamma, \eta}$ for every $\gamma > \max\{\eta, 0\}$. The fixed point U cannot be more regular than the fractional stochastic convolution, which has regularity α for any $\alpha < -\frac{1}{2}(d - \rho)$ (cf. [2, Sect. 4.1]). If $U \in \mathcal{D}^{\gamma, \eta}$ has regularity $\alpha < 0$, then U^2 has regularity $\bar{\alpha} = 2\alpha$, while [19, Prop. 6.12] shows that $U^2 \in \mathcal{D}^{\bar{\gamma}, \bar{\eta}}$ with $\bar{\gamma} = \gamma + \alpha$ and $\bar{\eta} = \eta + \min\{\alpha, \eta\}$. In order to apply [19, Thm. 7.8] yielding existence of a unique fixed point, one needs to fulfill the condition $\min\{\bar{\eta}, \bar{\alpha}\} > -\rho$, which holds if $-\frac{\rho}{2} < \eta \leq \alpha$. (The other required condition $\eta < \min\{\bar{\eta}, \bar{\alpha}\} + \rho$ is automatically satisfied if $\eta < 0$.) \diamond

In less technical terms, the first estimate in Theorem 2.1 shows that, up to error terms which are small unless ε is close to ε_c ,

$$C_0(\varepsilon, \rho) \simeq \begin{cases} \varepsilon_c^{-(d-\rho)} \log(\varepsilon^{-1}) & \text{if } \varepsilon \geq \varepsilon_c, \\ A_0 \varepsilon^{-(d-\rho)} & \text{if } \varepsilon < \varepsilon_c. \end{cases}$$

In the same spirit, the second counterterm satisfies

$$C_1(\varepsilon, \rho) \simeq \begin{cases} \bar{\varepsilon}_c^{-(d-2\rho)} \log(\varepsilon^{-1}) & \text{if } \varepsilon \geq \bar{\varepsilon}_c, \\ \bar{A}_0 \varepsilon^{-(d-2\rho)} & \text{if } \varepsilon < \bar{\varepsilon}_c. \end{cases}$$

We thus obtain a saturation effect at values of the mollification parameter ε which are not superexponentially small: for ε larger than its critical value, the counterterms are of order $\log(\varepsilon^{-1})$, with a prefactor becoming very large when ρ approaches ρ_c (Figure 2). For superexponentially small ε , on the other hand, the counterterms diverge respectively like $\varepsilon^{-(d-\rho)}$ and $\varepsilon^{-(d-2\rho)}$. This is due to the fact that both counterterms can be written as the sum of a large number of contributions. Only one of these terms, which has the strongest singular behaviour as ε goes to 0, dominates for superexponentially small ε . The vast majority of the terms diverge only logarithmically, but their number is large enough for them to dominate when ε is larger than its critical value.

The constants A_0 and \bar{A}_0 can be characterised more precisely. Assuming that the mollifier has the form $\varrho^\varepsilon(t, x) = \varrho_0^\varepsilon(t) \varrho_1^\varepsilon(x)$ with $\varrho_0^\varepsilon(t) = \varepsilon^{-\rho} \varrho_0(\varepsilon^{-\rho} t)$, $\varrho_1^\varepsilon(x) = \varepsilon^{-d} \varrho_1(\varepsilon^{-1} x)$, and ϱ_1 even, we have

$$A_0 = -\frac{1}{2} \lim_{\varepsilon \rightarrow 0} \varepsilon^{d-\rho} (\varrho_1^\varepsilon *_x G_\rho)(0) = -\frac{1}{2} \lim_{\varepsilon \rightarrow 0} \int_{\mathbb{R}^d} \varrho_1(x) \varepsilon^{d-\rho} G_\rho(\varepsilon x) dx, \quad (2.8)$$

where $G_\rho = (\Delta^{\rho/2})^{-1}$ is the Green function of the fractional Laplacian and $*_x$ denotes convolution in space. Scaling properties of G_ρ (see for instance [32, Section 4]) imply that A_0 is indeed finite. We also have

$$\bar{A}_0 = -2 \lim_{\varepsilon \rightarrow 0} \varepsilon^{d-2\rho} \int_{\mathbb{R}^{d+1}} P_\rho(t, x) (G_\rho^\varepsilon *_x \tilde{P}_\rho^\varepsilon)(|t|, x) dt dx, \quad (2.9)$$

where P_ρ is the fractional heat kernel, $G_\rho^\varepsilon = \varrho_1^\varepsilon *_x G_\rho$, and $\tilde{P}_\rho^\varepsilon = P_\rho * \varrho^\varepsilon * \varrho^\varepsilon$.

The main insight provided by Theorem 2.1 is as follows. The usual way of renormalising the singular SPDE (1.1) is to fix $\rho > \rho_c$, and then to take the limit $\varepsilon \rightarrow 0$. Our result then shows that a well-defined limit exists, provided one adds counterterms to the equation that behave logarithmically in ε as long as ε is not too small, but ultimately diverge like a negative power of ε . On the other hand, one could also fix a small positive value of ε and look at the limit $\rho \searrow \rho_c$. In physical terms, this would model a situation where space-time is discrete at very small scales, perhaps defined by Planck's scale. Since discrete models are usually harder to solve than continuous ones, the vanishing ε limit can be considered as an idealised mathematical object that really only approximates the real system. Note that for $\varepsilon > 0$, the SPDE is no longer singular, and local existence of solutions does not pose a problem at all. What our result says in this case, is that in order to have a chance to be close, for small ε , to a well-defined continuous model, one should add counterterms of order $\log(\varepsilon^{-1})$, but which diverge superexponentially fast in $\rho - \rho_c$ in the sense of (2.5).

A more ambitious goal would be to look at possible limiting dynamics when ε and $\rho - \rho_c$ simultaneously converge to zero, along some path in the (ρ, ε) plane, cf. Figure 2. There are two reasons why obtaining such a convergence result is currently out of reach. The first reason is that when changing ρ , one changes both the model space and the space of modelled distributions in which one tries to solve a fixed-point equation, so that the general theory of convergence in regularity structures does not immediately apply. The second, more serious reason is that as $\rho \searrow \rho_c$, the number of symbols in the model space having negative degree diverges exponentially. However, many arguments in the theory of regularity structures only apply when the number of these symbols remains bounded. This fact is then crucial in showing that the sequence of ε -dependent models converges in an appropriate topology to a well-defined limiting model. It is not clear at this point whether a similar convergence argument can be obtained when the number of symbols having negative degree is unbounded.

Before moving to the proof of Theorem 2.1, we list some extensions and interesting open questions related to our results.

- Obtaining a matching lower bound on the counterterms in the regime of large ε seems out of reach at this stage, because of the existence of cancellations in the sums defining these counterterms. However, as explained in Section 7.3, one can show that there exist terms in the sum defining $C_0(\varepsilon, \rho)$ which have the same asymptotic behaviour as the upper bound obtained above. Therefore, the counterterm can only be of smaller order in case unexpected cancellations occur in this sum.
- One can extend the results to the following generalisation of (1.1):

$$\partial_t u - \gamma \Delta^{\rho/2} u = g u^2 + \sigma \xi.$$

Its renormalised version reads

$$\partial_t u - \gamma \Delta^{\rho/2} u = g u^2 + C^{\gamma, g, \sigma}(\varepsilon, \rho, u) + \sigma \xi^\varepsilon,$$

where

$$C^{\gamma, g, \sigma}(\varepsilon, \rho, u) = C_0^{\gamma, g, \sigma}(\varepsilon, \rho) + C_1^{\gamma, g, \sigma}(\varepsilon, \rho) u.$$

One can then show (see Section 7.4) that

$$\begin{aligned} |C_0^{\gamma,g,\sigma}(\varepsilon, \rho)| &\lesssim \left(\frac{g^2\sigma^2}{\gamma^3}\right)^{k_{\max}} \frac{g\sigma^2}{\gamma} \widehat{C}_0(\varepsilon, \rho) && \text{if } \varepsilon \geq \varepsilon_c, \\ C_0^{\gamma,g,\sigma}(\varepsilon, \rho) &= \frac{g\sigma^2}{\gamma} \left[C_0(\varepsilon, \rho) + \mathcal{O}\left(\frac{g^2\sigma^2}{\gamma^3} \left(\frac{\varepsilon}{\varepsilon_c}\right)^{3(\rho-\rho_c)}\right) \right] && \text{if } \varepsilon < \varepsilon_c, \end{aligned} \quad (2.10)$$

where $\widehat{C}_0(\varepsilon, \rho)$ denotes the upper bound on $|C_0(\rho, \varepsilon)|$ in (2.6), and we write $a(\varepsilon, \rho) \lesssim b(\varepsilon, \rho)$ if there exists a constant $M \geq 1$, independent of ε and ρ , such that $a(\varepsilon, \rho) \leq Mb(\varepsilon, \rho)$ holds for ε and $\rho - \rho_c$ small enough. In a similar way, we have

$$\begin{aligned} |C_1^{\gamma,g,\sigma}(\varepsilon, \rho)| &\lesssim \left(\frac{g^2\sigma^2}{\gamma^3}\right)^{k_{\max}} \frac{g^2\sigma^2}{\gamma^2} \widehat{C}_1(\varepsilon, \rho) && \text{if } \varepsilon \geq \bar{\varepsilon}_c, \\ C_1^{\gamma,g,\sigma}(\varepsilon, \rho) &= \frac{g^2\sigma^2}{\gamma^2} \left[C_1(\varepsilon, \rho) + \mathcal{O}\left(\frac{g^2\sigma^2}{\gamma^3} \left(\frac{\varepsilon}{\bar{\varepsilon}_c}\right)^{3(\rho-\rho_c)}\right) \right] && \text{if } \varepsilon < \bar{\varepsilon}_c, \end{aligned} \quad (2.11)$$

where $\widehat{C}_1(\varepsilon, \rho)$ denotes the upper bound on $|C_1(\rho, \varepsilon)|$ in (2.7). Note that for $\varepsilon \geq \varepsilon_c$, the important parameter is $g^2\sigma^2\gamma^{-3}$. In particular, (2.5) implies

$$|C_0^{\gamma,g,\sigma}(\varepsilon, \rho)| \lesssim \frac{g\sigma^2}{\gamma} \exp\left\{ \frac{d-\rho}{\rho-\rho_c} \left[\log\left(\frac{g^{2/3}\sigma^{2/3}}{\gamma(\rho-\rho_c)}\right) + \mathcal{O}(1) \right] \right\}.$$

A similar relation holds for $C_1^{\gamma,g,\sigma}(\varepsilon, \rho)$ for $\varepsilon \geq \bar{\varepsilon}_c$. Thus if γ, g and σ are fixed, the counterterms diverge in the same way as for $\gamma = g = \sigma = 1$ as $\rho \searrow \rho_c$. However, if γ, g and σ are allowed to depend on ρ , new regimes can occur.

- The above choice of counterterms is not unique. In this work, we have chosen the BPHZ renormalisation, which is natural in some sense. However, as shown in [6], the set of all potential choices of counterterms is parametrised by a group, called the renormalisation group. This group can be very large, since its dimension as a Lie group is equal to the number of symbols in the model space having negative degree. However, in our case only a two-parameter family of counterterms really matters: this family is obtained by adding constants to both $C_0(\varepsilon, \rho)$ and $C_1(\varepsilon, \rho)$. It is interesting to note that a one-parameter family of these choices of counterterms can be realised by a simple shift $v = u + k$ of the random field, where k is a constant. Indeed, the equation for v reads

$$\partial_t v - \Delta^{\rho/2} v = v^2 + (C_0(\varepsilon, \rho) - C_1(\varepsilon, \rho)k + k^2) + (C_1(\varepsilon, \rho) - 2k)v + \xi^\varepsilon.$$

In fact, one can observe that this is nothing but the equation obtained by applying the BPHZ renormalisation to the equation

$$\partial_t v - \Delta^{\rho/2} v = v^2 - 2kv + k^2 + \xi.$$

Indeed, the term $C_1(\varepsilon, \rho)k$ comes from the fact that almost full binary trees (as defined in Section 3 below) can be generated by kv , and they will come with a factor k . Note that time-dependent shifts are currently out of the scope of the general theory, though one may expect that they lead to time-dependent renormalisation constants.

- A common way to analyse the effect of the interaction term as $\rho \searrow \rho_c$ is to study moments of the solution of the form

$$\mathbb{E}\{u(t, x_1)u(t, x_2)u(t, x_3)\}.$$

So far, such moments have been computed only for very specific models such as the two-dimensional parabolic Anderson model, see [17]. The main issue of such an approach is that in our case, the solutions are only local in time. However, it may be possible to obtain moment estimates for the process stopped when its Hölder norm exceeds some large threshold, and analysing their behaviour as $\varepsilon \rightarrow 0$ and $\rho \searrow \rho_c$ may yield information on the potential convergence to a non-trivial model.

3 Model space and renormalised equation

In order to apply the theory of regularity structures, the first step is to introduce a model space. This is a graded vector space spanned by abstract symbols, which allow to represent solutions of (2.1) by an abstract fixed-point equation of the form

$$U = \mathcal{I}_\rho(\Xi + U^2) + P(U). \quad (3.1)$$

Here U represents the solution, Ξ stands for space-time white noise, \mathcal{I}_ρ is an abstract integration operator standing for convolution with the fractional heat kernel, and $P(U)$ is a polynomial part, required by a recentering procedure.

More precisely, let $\mathfrak{s} = (\rho, 1, \dots, 1) \in \mathbb{R}_+^{d+1}$ be the scaling associated with the fractional Laplacian. Then we construct a set of symbols τ , each admitting a degree $|\tau|_{\mathfrak{s}} \in \mathbb{R}$, in the following way.

- For each multiindex $k = (k_0, \dots, k_d) \in \mathbb{N}_0^{d+1}$, we define the polynomial symbol $\mathbf{X}^k = X_0^{k_0} \dots X_d^{k_d}$, which has degree $|\mathbf{X}^k|_{\mathfrak{s}} = |k|_{\mathfrak{s}} = \rho k_0 + k_1 + \dots + k_d$. In particular, \mathbf{X}^0 is denoted $\mathbf{1}$ and has degree $|\mathbf{1}|_{\mathfrak{s}} = 0$.
- The symbol Ξ representing space-time white noise has degree $|\Xi|_{\mathfrak{s}} = -\frac{1}{2}(\rho + d) - \kappa$, where $\kappa > 0$ is arbitrarily small.
- If τ, τ' are two symbols, then $\tau\tau'$ is a new symbol of degree $|\tau\tau'|_{\mathfrak{s}} = |\tau|_{\mathfrak{s}} + |\tau'|_{\mathfrak{s}}$.
- Finally, if τ is a symbol which is not of the form \mathbf{X}^k , then $\mathcal{I}_\rho(\tau)$ denotes a new symbol of degree $|\tau|_{\mathfrak{s}} + \rho$, while for $k \in \mathbb{N}_0^{d+1}$, $\partial^k \mathcal{I}_\rho(\tau)$, stands for a new symbol of degree $|\tau|_{\mathfrak{s}} + \rho - |k|_{\mathfrak{s}}$ (where we use the multiindex notation $\partial^k = \partial_t^{k_0} \partial_{x_1}^{k_1} \dots \partial_{x_d}^{k_d}$).

It is convenient to represent symbols by trees, in which edges stand for integration operators \mathcal{I}_ρ , leaves stand for noise symbols Ξ , and multiplication of symbols is represented by joining them at the root. For instance,

$$\vee = \mathcal{I}_\rho(\Xi)^2, \quad \begin{array}{c} \bullet \\ \swarrow \quad \searrow \\ \bullet \quad \bullet \\ \swarrow \quad \searrow \\ \bullet \end{array} = \left[\mathcal{I}_\rho \left(\mathcal{I}_\rho(\mathcal{I}_\rho(\Xi)^2) \mathcal{I}_\rho(\Xi) \right) \right]^2.$$

Multiplication by a polynomial symbol \mathbf{X}^k is represented by adding a node decoration k to the relevant node of the tree, while derivatives $\partial^\ell \mathcal{I}_\rho$ are denoted by edge decorations ℓ . Thus for instance

$$\begin{array}{c} \bullet \\ \swarrow \quad \searrow \\ \bullet \quad \bullet \\ \swarrow \quad \searrow \\ \bullet \end{array}^{\ell} = \mathcal{I}_\rho(\mathbf{X}^k \partial^\ell \mathcal{I}_\rho(\Xi)).$$

The degree of a tree with p leaves (for the noise), q edges (for integration operators), node decorations of total exponent k and edge decorations of total exponent ℓ is given by

$$|\tau|_{\mathfrak{s}} = \left(-\frac{\rho + d}{2} - \kappa \right) p + \rho q + |k|_{\mathfrak{s}} - |\ell|_{\mathfrak{s}}. \quad (3.2)$$

Not all symbols are needed to represent the abstract fixed-point equation (3.1). In fact, for its right-hand side, we only need the smallest set T such that

- $\mathbf{X}^k \in T$ for any $k \in \mathbb{N}_0^{d+1}$,
- $\Xi \in T$,
- if $\tau, \tau' \in T$, $k \in \mathbb{N}_0^{d+1}$, one has $X^k \mathcal{I}_\rho(\tau), \mathcal{I}_\rho(\tau) \mathcal{I}_\rho(\tau') \in T$,
- if $d > 2$ and $\tau \in T$, then $\partial_{x_i} \mathcal{I}_\rho(\tau) \in T$ for every $1 \leq i \leq d$.

We denote by \mathcal{T} the linear span of T . It is a consequence of local subcriticality that T has only finitely many symbols of degree smaller than any $\alpha < \infty$ (see [19, Lemma 8.10]). The difference between $d \leq 2$ and $d > 2$ is due to the fact that for $d \leq 2$, one has $\rho < 1$ when ρ is close to $\rho_c = \frac{d}{3} \leq \frac{2}{3}$. This means that the abstract operator $\partial_{x_i} \mathcal{I}_\rho$ decreases the degree of the tree. Therefore, if we were to keep this rule, we would break subcriticality. For both cases, we have exhibited rules which are complete in the sense that they are stable under the action of the renormalisation.

Let $T_- \subset T$ denote the set of symbols/decorated trees of negative degree, and \mathcal{T}_- (resp. $\hat{\mathcal{T}}_-$) the linear span of the forests composed of elements in T_- (resp. T). On \mathcal{T}_- we define a commutative and associative forest product. The product of two forests τ_1 and τ_2 is simply the forest containing all the trees of both forests, where the same tree may occur several times. The neutral element for this product is the empty forest, that we will denote by $\mathbb{1}$.

The structure of the trees in T_- will be very important later on to control the renormalisation constants, which will be expressed in terms of sums over all trees of negative degree. We know from [3, Prop. 4.17] that trees in T_- are necessarily either *full* binary trees (every vertex has either two children or no child), in which case $q = 2p - 2$, or full binary trees with one edge missing (then $q = 2p - 1$), which we will call *almost full* binary trees. It turns out that for symmetry reasons, full binary trees can only contribute to the renormalized equation if they contain no nontrivial node decoration, while the almost full ones can contain one node decoration k with $|k|_s = 1$. Furthermore, (3.2) implies that the latter can only have negative degree if $d > 3$.

The form of the renormalised equation can be determined using the methods introduced in [6] and expanded in [4]. As shown in [4, Thm. 2.21], it has the form (2.2) with

$$C(\varepsilon, \rho, u) = \sum_{\tau \in T_-^F} c_\varepsilon(\tau) \frac{\Upsilon^F(\tau)(u)}{S(\tau)}, \quad (3.3)$$

where the terms $\Upsilon^F(\tau)(u)$ describe the effect of the nonlinearity $F(u, \xi) = u^2 + \xi$, $S(\tau)$ is a symmetry factor, and $c_\varepsilon(\tau)$ is the expectation of the element of the Wiener chaos represented by τ .

More precisely, the terms $\Upsilon^F(\tau)(u)$ are elementary differential operators defined recursively by $\Upsilon^F(\Xi)(u) = 1$ and

$$\Upsilon^F\left(\mathbf{X}^k \prod_{j=1}^m \mathcal{I}_\rho[\tau_j]\right)(u) = \left(\prod_{j=1}^m \Upsilon^F(\tau_j)(u)\right) \partial^k \partial_u^m u^2. \quad (3.4)$$

We write T_-^F for the subset of elements of T_- for which Υ^F is non-zero, see [4, Def. 2.12]. We could extend the previous definition of Υ^F to elements of the form $\partial_{x_i} \mathcal{I}_\rho(\tau_j)$ by using the derivative $\partial_{\partial_{x_i} u}$. However, such a derivative applied to F gives zero, which is why we omit this case in the definition of Υ^F .

Lemma 3.1. *Let $n_{\text{inner}}(\tau)$ be the number of inner nodes of $\tau \in T_-$, where an inner node is any node which is not a leaf (including the root). Then*

$$\Upsilon^F(\tau)(u) = \begin{cases} 2^{n_{\text{inner}}(\tau)} & \text{if } \tau \text{ is a full binary tree,} \\ 2^{n_{\text{inner}}(\tau)} u & \text{if } \tau \text{ is an almost full binary tree without decoration } X_i, \\ 2^{n_{\text{inner}}(\tau)} \partial_{x_i} u & \text{if } \tau \text{ is an almost full binary tree with a decoration } X_i. \end{cases}$$

PROOF: By induction on the size of the tree. The base case follows from $n_{\text{inner}}(\Xi) = 0$. If τ is a full binary tree, then it can be written as $\tau = \mathcal{I}_\rho(\tau_1)\mathcal{I}_\rho(\tau_2)$, where each τ_i is a full tree with n_i inner nodes. Then (3.4) and the induction hypothesis yield $\Upsilon^F(\tau)(u) = 2^{n_1+n_2+1}$, where $n_1 + n_2 + 1$ is exactly the number of inner nodes of τ .

If τ is an almost full tree without decoration, there are two possibilities. Either $\tau = \mathcal{I}_\rho(\tau_1)$ is a planted tree, where τ_1 is a full tree with n_1 inner nodes. Then (3.4) yields $\Upsilon^F(\tau)(u) = 2^{n_1+1}u$, where $n_1 + 1$ is the number of inner nodes of τ . Or $\tau = \mathcal{I}_\rho(\tau_1)\mathcal{I}_\rho(\tau_2)$, where τ_1 is full with n_1 inner nodes, and τ_2 is almost full with n_2 inner nodes. In that case, we obtain $\Upsilon^F(\tau)(u) = 2^{n_1+n_2+1}u$, where $n_1 + n_2 + 1$ is again the number of inner nodes of τ .

The case of an almost full tree with decoration X_i is straightforward, because then $\partial^k = \partial_{x_i}$ commutes with the other terms. \square

The second new quantity appearing in (3.3) is the symmetry factor $S(\tau)$. It is defined inductively by setting $S(\Xi) = 1$, while if τ is of the form $\mathbf{X}^k(\prod_{j=1}^m \mathcal{I}_\rho[\tau_j]^{\beta_j})$ with $\tau_i \neq \tau_j$ for $i \neq j$, then

$$S(\tau) = k! \left(\prod_{j=1}^m S(\tau_j)^{\beta_j} \beta_j! \right).$$

Lemma 3.2. *Let $n_{\text{sym}}(\tau)$ be the number of inner nodes of $\tau \in T_-$ having two identical lines of offspring. Then $S(\tau) = 2^{n_{\text{sym}}(\tau)}$.*

PROOF: First note that $k! = 1$ for any $\tau \in T_-$. Then the proof proceeds by induction on the size of the tree, noting that $m = 1$ and $\beta_1 = 2$ whenever two identical trees are multiplied, while $m = 2$ and $\beta_1 = \beta_2 = 1$ when two different trees are multiplied, and $m = \beta_1 = 1$ when τ is a planted tree of the form $\mathcal{I}_\rho(\tau_1)$. \square

Remark 3.3. Note that $S(\tau)$ is exactly the order of the symmetry group of the tree, which is generated by the $n_{\text{sym}}(\tau)$ reflections around symmetric inner nodes. For instance, $S(\tau) = 2$ for a comb tree, that is, a full binary tree in which each generation but the root has exactly two individuals, i.e.

$$S(\heartsuit) = S(\heartsuit) = S(\heartsuit) = S(\heartsuit) = \dots = 2.$$

Maximal symmetry is reached for regular trees, in which all individuals of the s first generations have exactly two offspring, while those of the last generation have no offspring. For such a tree, $n_{\text{sym}}(\tau) = 2^s - 1$, and thus $S(\tau) = 2^{2^s - 1}$, e.g.

$$S(\heartsuit) = 2, \quad S(\heartsuit) = 2^3, \quad S(\heartsuit) = 2^7. \quad (3.5)$$

\diamond

The final new quantity appearing in (3.3) is the ε -dependent factor $c_\varepsilon(\tau)$, which is related to the expectation of the model of τ . We analyse it in the next sections.

4 Canonical model

As in [19, Section 5], we decompose the fractional heat kernel P_ρ as the sum

$$P_\rho(z) = K_\rho(z) + R_\rho(z), \quad (4.1)$$

where R_ρ is smooth and uniformly bounded in \mathbb{R}^{d+1} , while K_ρ is compactly supported and has special algebraic properties. More precisely, let

$$|z|_s = |z_0|^{1/\rho} + \sum_{i=1}^d |z_i| \quad (4.2)$$

be the pseudonorm associated with the fractional scaling. Then by [19, Lemma 5.5], we may assume that K_ρ is supported in the ball $\{z: |z|_s \leq 1\}$, that $K_\rho = P_\rho$ in the ball $\{z: |z|_s \leq \frac{1}{2}\}$, and that K_ρ integrates to zero all polynomials of degree up to 2. In addition, K_ρ and its derivatives satisfy a number of analytic bounds, cf. [3, (3.1)–(3.4)]. See also [10] for a derivation of the associated Schauder estimate. We also assume the following two properties for the kernel $K_\rho^\varepsilon = \varrho^\varepsilon * K_\rho$:

1. Non-anticipation: $K_\rho^\varepsilon(t, x) = 0$ for $t \leq -\varepsilon^\rho$;
2. Spatial symmetry: $K_\rho^\varepsilon(t, -x) = K_\rho^\varepsilon(t, x)$.

To any symbol $\tau \in T$, we associate the *canonical model* $\mathbf{\Pi}^\varepsilon \tau$, defined (cf. [19, proof of Prop. 8.27]) by

$$(\mathbf{\Pi}^\varepsilon \mathbf{1})(z) = 1, \quad (\mathbf{\Pi}^\varepsilon X_i)(z) = z_i, \quad (\mathbf{\Pi}^\varepsilon \Xi)(z) = \xi^\varepsilon(z), \quad (4.3)$$

and extended inductively by the relations

$$\begin{aligned} (\mathbf{\Pi}^\varepsilon \tau \bar{\tau})(z) &= (\mathbf{\Pi}^\varepsilon \tau)(z) (\mathbf{\Pi}^\varepsilon \bar{\tau})(z), \\ (\mathbf{\Pi}^\varepsilon \partial^k \mathcal{I}_\rho \tau)(z) &= \int \partial^k K_\rho(z - \bar{z}) (\mathbf{\Pi}^\varepsilon \tau)(\bar{z}) d\bar{z}. \end{aligned} \quad (4.4)$$

We then set

$$E(\tau) = \mathbb{E}\{(\mathbf{\Pi}^\varepsilon \tau)(0)\},$$

which has in general the form of a Gaussian iterated integral. The computations will be greatly simplified by removing symbols that are in the kernel of E . We denote by I_E the ideal generated by forests having at least one decorated tree τ satisfying one of the following properties:

- τ has an odd number of leaves;
- τ is a planted tree (i.e., of the form $\mathcal{I}_\rho(\tau')$ or $\partial_{x_i} \mathcal{I}_\rho(\tau')$);
- τ has one X_i as a node decoration and no edge of the form $\partial_{x_i} \mathcal{I}_\rho$.

Proposition 4.1. *Let τ be a decorated tree. Then $E(\tau) = 0$ whenever $\tau \in I_E$.*

PROOF: If τ has an odd number of leaves, then $(\mathbf{\Pi}^\varepsilon \tau)(0)$ is centered as the product of an odd number of centered Gaussians has zero mean. If $\tau = \mathcal{I}_\rho(\tau')$, then $E(\tau) = K_\rho * E(\tau') = E(\tau') K_\rho * 1$ by translation invariance. The term $K_\rho * 1$ is equal to zero by definition of the kernel K_ρ (K_ρ integrates polynomials to zero up to a certain order). For the last case, the conclusion follows by noticing that $(\mathbf{\Pi}^\varepsilon \tau)(t, -x) = -(\mathbf{\Pi}^\varepsilon \tau)(t, x)$. \square

4.1 Simplifying the twisted antipode

The ε -dependent coefficients $c_\varepsilon(\tau)$ are defined by

$$c_\varepsilon(\tau) = E(\tilde{\mathcal{A}}_- \tau), \quad (4.5)$$

where $\tilde{\mathcal{A}}_- : \mathcal{T}_- \rightarrow \hat{\mathcal{T}}_-$ is a linear map encoding the renormalisation procedure, called the *twisted antipode*. The twisted antipode is defined in [6, Proposition 6.6], in terms of a coaction $\Delta^- :$

$\hat{\mathcal{T}}_- \rightarrow \mathcal{T}_- \otimes \hat{\mathcal{T}}_-$ which is close in spirit to the Connes–Kreimer extraction-contraction coproduct introduced in [11]. However, the coaction Δ^- is more complicated than the one used in [11], because it acts on decorated trees, where the decorations encode multiplication by monomials and derivatives appearing in Taylor expansions. This results in rather complicated expressions for the twisted antipode, cf. Proposition 4.4 below. It turns out, however, that thanks to Proposition 4.1, in our case many terms of $\tilde{\mathcal{A}}_- \tau$ give a vanishing contribution when applying E . The purpose of this section is to derive the simplified expression (4.7) of $\tilde{\mathcal{A}}_-$, which only involves extraction of subtrees and contractions, without any decorations. Furthermore, this simplified expression allows to define $\tilde{\mathcal{A}}_-$ in an iterative way, which does not involve the coaction Δ^- at all.

In order to derive the simplified expression of the twisted antipode, we have to start with the general construction given in [6]. The twisted antipode can be defined inductively by setting $\tilde{\mathcal{A}}_-(\mathbb{1}) = \mathbb{1}$ for the empty forest $\mathbb{1}$, and

$$\tilde{\mathcal{A}}_- \tau = -\hat{\mathcal{M}}_-(\tilde{\mathcal{A}}_- \otimes \text{id})(\Delta^- \tau - \tau \otimes \mathbb{1}) ,$$

cf. [6, Prop. 6.6]. Here $\hat{\mathcal{M}}_-$ is the multiplication operator (acting on forests), and τ is a tree of negative degree (we have omitted the natural injection of \mathcal{T}_- into $\hat{\mathcal{T}}_-$ because we view \mathcal{T}_- as a subset of $\hat{\mathcal{T}}_-$). Elements of $\hat{\mathcal{T}}_-$ are of the form $(F, \mathbf{n}, \boldsymbol{\epsilon})$ where F is a forest with node set N_F and edge set E_F , $\mathbf{n} : N_F \rightarrow \mathbb{N}_0^{d+1}$ represents the node decoration and $\boldsymbol{\epsilon} : E_F \rightarrow \mathbb{N}_0^{d+1}$ represents the edge decoration. The forest product is defined by

$$(F, \mathbf{n}, \boldsymbol{\epsilon}) \cdot (G, \bar{\mathbf{n}}, \bar{\boldsymbol{\epsilon}}) = (F \cdot G, \bar{\mathbf{n}} + \mathbf{n}, \bar{\boldsymbol{\epsilon}} + \boldsymbol{\epsilon}) ,$$

where the sums $\bar{\mathbf{n}} + \mathbf{n}$ and $\bar{\boldsymbol{\epsilon}} + \boldsymbol{\epsilon}$ mean that decorations defined on one of the forests are extended to the disjoint union by setting them to vanish on the other forest. Then the map $\Delta^- : \mathcal{T} \rightarrow \mathcal{T}_- \otimes \mathcal{T}$ defined in [6] is given for $T_\epsilon^n \in \mathcal{T}$ by

$$\Delta^- T_\epsilon^n = \sum_{A \in \mathfrak{A}(T)} \sum_{\mathbf{n}_A, \boldsymbol{\epsilon}_A} \frac{1}{\boldsymbol{\epsilon}_A!} \binom{\mathbf{n}}{\mathbf{n}_A} (A, \mathbf{n}_A + \pi \boldsymbol{\epsilon}_A, \boldsymbol{\epsilon} \setminus E_A) \otimes (\mathcal{R}_A T, [\mathbf{n} - \mathbf{n}_A]_A, \boldsymbol{\epsilon} + \boldsymbol{\epsilon}_A) , \quad (4.6)$$

where we use the following notations.

- Factorials and binomial coefficients are understood in multiindex notation, and the latter vanish unless \mathbf{n}_A is pointwise smaller than or equal to \mathbf{n} .
- For $C \subset D$ and $f : D \rightarrow \mathbb{N}_0^{d+1}$, $f|_C$ is the restriction of f to C .
- The first sum runs over $\mathfrak{A}(T)$, the set of all subforests A of T , where A may be empty. The second sum runs over all $\mathbf{n}_A : N_A \rightarrow \mathbb{N}_0^{d+1}$ and $\boldsymbol{\epsilon}_A : \partial(A, T) \rightarrow \mathbb{N}_0^{d+1}$ where $\partial(A, T)$ denotes the edges in $E_T \setminus E_A$ that are adjacent to N_A as a child, not a parent.
- We write $\mathcal{R}_A T$ for the tree obtained by contracting the connected components of A . Then we have an action on the decorations, in the sense that for $f : N_T \rightarrow \mathbb{N}_0^{d+1}$ and $A \subset T$, one has $[f]_A(x) = \sum_{x \sim_A y} f(y)$, where x is an equivalence class of \sim_A , and $x \sim_A y$ means that x and y are connected in A . For $g : E_T \rightarrow \mathbb{N}_0^{d+1}$, we define for every $x \in N_T$, $(\pi g)(x) = \sum_{e=(x,y) \in E_T} g(e)$.

Remark 4.2. The name “twisted antipode” is due to the fact that $\tilde{\mathcal{A}}_-$ satisfies the relation

$$\hat{\mathcal{M}}_-(\tilde{\mathcal{A}}_- \otimes \text{id}) \Delta^- \tau = \mathbb{1}^*(\tau) \mathbb{1} ,$$

where $\mathbb{1}^*$ is the projection on the empty forest and Δ^- is a coaction (but not a coproduct). If the spaces \mathcal{T}_- and $\hat{\mathcal{T}}_-$ were equal, $(\mathcal{T}_-, \cdot, \Delta^-, \mathbb{1}, \mathbb{1}^*, \tilde{\mathcal{A}}_-)$ would be a Hopf algebra, similar to the extraction-contraction Connes–Kreimer Hopf algebra of [11] which involves trees without decoration. \diamond

Example 4.3. Consider the case $\tau = \heartsuit$ (with zero node and edge decorations). Then

$$\Delta^- \heartsuit = \mathbb{1} \otimes \heartsuit + 2 \sum_k \frac{1}{k!} \heartsuit_k \otimes \heartsuit_k + \heartsuit \otimes \mathbb{1},$$

where the sum is over $k \in \mathbb{N}_0^{d+1}$ such that the extracted symbol has negative degree. Here the first term corresponds to extracting $A = \mathbb{1}$, the second one to $A = \heartsuit$, and the last one to $A = \heartsuit$.

Consider now a case when the tree has one node decoration, say $\tau = \heartsuit_k$. Then

$$\Delta^{-k} \heartsuit_k = \mathbb{1} \otimes \heartsuit_k + \sum_m \frac{1}{m!} \heartsuit_m \otimes \heartsuit_m^k + \sum_\ell \binom{k}{\ell} \heartsuit_\ell \otimes \heartsuit_{k-\ell},$$

where we first extract $A = \mathbb{1}$, then $A = \heartsuit$ and finally $A = \heartsuit_k$. As before, the sums on ℓ and m are restricted by the fact that the extracted symbol has to have a negative degree. \clubsuit

As a short-hand notation for (4.6), we use

$$\Delta^- T_\epsilon^n = \sum_{A \in \mathfrak{A}(T)} \sum_{\epsilon_A, n_A} \frac{1}{\epsilon_A!} \binom{\mathbf{n}}{\mathbf{n}_A} A_\epsilon^{n_A + \pi \epsilon_A} \otimes \mathcal{R}_A T_{\epsilon + \epsilon_A}^{n - n_A}.$$

We extend this map to $\hat{\mathcal{T}}_-$ by multiplicativity regarding the forest product. Then one can turn this map into a coproduct $\Delta^- : \mathcal{T}_- \rightarrow \mathcal{T}_- \otimes \mathcal{T}_-$ and obtain a Hopf algebra for \mathcal{T}_- endowed with this coproduct and the forest product see [6, Prop. 5.35] and [6, Cor. 6.37]. The main difference here is that we do not consider extended decorations, but the results for the Hopf algebra are the same as in [6].

Using the definition of Δ^- , one can write a recursive formulation for $\tilde{\mathcal{A}}_-$ in which one doesn't see any tensor product. It is convenient to introduce the *reduced coaction* $\tilde{\Delta}^- \tau = \Delta^- \tau - \tau \otimes \mathbb{1} - \mathbb{1} \otimes \tau$. Then, using Sweedler's notation, if $\tilde{\Delta}^- \tau = \sum_{(\tau)} \tau' \otimes \tau''$ one has

$$\tilde{\mathcal{A}}_- \tau = -\tau - \sum_{(\tau)} (\tilde{\mathcal{A}}_- \tau') \tau''.$$

Proposition 4.4. For a decorated tree T_ϵ^n with negative degree, one has the relation

$$\tilde{\mathcal{A}}_- T_\epsilon^n = -T_\epsilon^n - \sum_{A \in \mathfrak{A}^*(T)} \sum_{\epsilon_A, n_A} \frac{1}{\epsilon_A!} \binom{\mathbf{n}}{\mathbf{n}_A} \tilde{\mathcal{A}}_- A_\epsilon^{n_A + \pi \epsilon_A} \cdot \mathcal{R}_A T_{\epsilon + \epsilon_A}^{n - n_A},$$

where $\mathfrak{A}^*(T) = \mathfrak{A}(T) \setminus \{\mathbb{1}, T\}$.

PROOF: The proof follows from a straightforward manipulation of the definitions:

$$\begin{aligned} \tilde{\mathcal{A}}_- T_\epsilon^n &= -\hat{\mathcal{M}}_-(\tilde{\mathcal{A}}_- \otimes \text{id})(\Delta^- T_\epsilon^n - T_\epsilon^n \otimes \mathbb{1}) \\ &= -\hat{\mathcal{M}}_-(\tilde{\mathcal{A}}_- \otimes \text{id})(\mathbb{1} \otimes T_\epsilon^n) - \hat{\mathcal{M}}_-(\tilde{\mathcal{A}}_- \otimes \text{id})\tilde{\Delta}^- T_\epsilon^n \\ &= -T_\epsilon^n - \sum_{A \in \mathfrak{A}^*(T)} \sum_{\epsilon_A, n_A} \frac{1}{\epsilon_A!} \binom{\mathbf{n}}{\mathbf{n}_A} \tilde{\mathcal{A}}_- A_\epsilon^{n_A + \pi \epsilon_A} \cdot \mathcal{R}_A T_{\epsilon + \epsilon_A}^{n - n_A}, \end{aligned}$$

where we have treated separately the cases $A = \mathbb{1}$ and $A = T$. \square

The construction of the twisted antipode can be substantially simplified by using Proposition 4.1. Indeed, one has the property $\Delta^- I_E \subset I_E \otimes \hat{\mathcal{T}}_- + \mathcal{T}_- \otimes I_E$, which makes I_E a kind of biideal associated to Δ^- . Therefore, Δ^- is a well-defined map from \mathcal{T}_-^E into $\mathcal{T}_-^E \otimes \hat{\mathcal{T}}_-^E$, where $\mathcal{T}_-^E = \mathcal{T}_- / I_E$ and $\hat{\mathcal{T}}_-^E = \hat{\mathcal{T}}_- / I_E$ (in other words, if $\tau' - \tau \in I_E$, then $\Delta^-(\tau') - \Delta^-(\tau)$ belongs to $I_E \otimes \hat{\mathcal{T}}_- + \mathcal{T}_- \otimes I_E$, and thus equivalence classes modulo I_E are mapped into equivalence classes).

In what follows, we will use the notation $\tilde{\mathcal{A}}_-^E$ when $\tilde{\mathcal{A}}_-$ is considered as acting on \mathcal{T}_-^E . As the consequence of the biideal property, we get

Proposition 4.5. *One has $c_\varepsilon(\tau) = E(\tilde{\mathcal{A}}_- \tau) = E(\tilde{\mathcal{A}}_-^E \tau)$.*

PROOF: This follows from Proposition 4.1, which implies $I_E \subset \ker E$. \square

Proposition 4.6. *If we consider Δ^- as a map from \mathcal{T}_-^E into $\mathcal{T}_-^E \otimes \hat{\mathcal{T}}_-^E$, then it reduces to an extraction-contraction map with some restrictions: for any tree $\tau \in \mathcal{T}_-^E$, we have*

$$\Delta^- \tau = \sum_{\tau_1 \dots \tau_n \subset_E \tau} \tau_1 \dots \tau_n \otimes \tau / (\tau_1 \dots \tau_n),$$

where \subset_E means that we consider all the subforests $\tau_1 \dots \tau_n$ of τ such that the trees τ_i belong to \mathcal{T}_-^E , and $\tau / (\tau_1 \dots \tau_n)$ denotes the tree obtained by contracting τ_1, \dots, τ_n to a single node. Therefore, one can define a multiplicative map $\tilde{\mathcal{A}}_-^E$ for the forest product as

$$\tilde{\mathcal{A}}_-^E \tau = -\tau - \sum_{\mathbb{1} \not\subset \tau_1 \dots \tau_n \not\subset_E \tau} \tilde{\mathcal{A}}_-^E(\tau_1 \dots \tau_n) \cdot \tau / (\tau_1 \dots \tau_n). \quad (4.7)$$

PROOF: The simplification for Δ^- and $\tilde{\mathcal{A}}_-^E$ comes from the precise description of \mathcal{T}_-^E which is composed of full and almost full binary trees. Therefore, $\Delta^- \tau$ does not contain any sum on the node decorations and there remains only the extraction-contraction procedure. \square

Remark 4.7. The very simple expression (4.7) for the twisted antipode is a direct consequence of the fact that we may remove trees with one X_i as a node decoration. This expression may be useful for numerical computations of the constants. \diamond

Example 4.8. We have $\tilde{\mathcal{A}}_-^E(\hat{\diamond}) = -\hat{\diamond}$, since no nontrivial tree can be extracted. Therefore, we obtain

$$\begin{aligned} \tilde{\mathcal{A}}_-^E \left(\begin{array}{c} \bullet \\ \diagup \quad \diagdown \\ \bullet \quad \bullet \\ \diagup \quad \diagdown \\ \bullet \quad \bullet \end{array} \right) &= - \begin{array}{c} \bullet \\ \diagup \quad \diagdown \\ \bullet \quad \bullet \\ \diagup \quad \diagdown \\ \bullet \quad \bullet \end{array} - 4 \tilde{\mathcal{A}}_-^E(\hat{\diamond}) \cdot \begin{array}{c} \bullet \\ \diagup \quad \diagdown \\ \bullet \quad \bullet \\ \diagup \quad \diagdown \\ \bullet \quad \bullet \end{array} - 4 \tilde{\mathcal{A}}_-^E(\hat{\diamond} \cdot \hat{\diamond}) \cdot \begin{array}{c} \bullet \\ \diagup \quad \diagdown \\ \bullet \quad \bullet \end{array} \\ &= - \begin{array}{c} \bullet \\ \diagup \quad \diagdown \\ \bullet \quad \bullet \\ \diagup \quad \diagdown \\ \bullet \quad \bullet \end{array} + 4 \hat{\diamond} \cdot \begin{array}{c} \bullet \\ \diagup \quad \diagdown \\ \bullet \quad \bullet \\ \diagup \quad \diagdown \\ \bullet \quad \bullet \end{array} - 4 \hat{\diamond} \cdot \hat{\diamond} \cdot \begin{array}{c} \bullet \\ \diagup \quad \diagdown \\ \bullet \quad \bullet \end{array}, \end{aligned} \quad (4.8)$$

where $\hat{\diamond} \cdot \hat{\diamond} \in \mathcal{T}_-$ and $\begin{array}{c} \bullet \\ \diagup \quad \diagdown \\ \bullet \quad \bullet \end{array} \in \hat{\mathcal{T}}_- \setminus \mathcal{T}_-$. \clubsuit

4.2 From expectations to Feynman diagrams

We now discuss the computation of expectations $E(\tau)$, starting with some examples.

Example 4.9. It follows from (4.3) and (4.4) that

$$(\mathbf{\Pi}^\varepsilon \dagger)(0) = \int K_\rho(-z) \xi^\varepsilon(z) dz = \int K_\rho^\varepsilon(-z) \xi(dz),$$

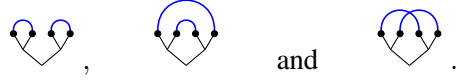
where we have assumed that $\xi^\varepsilon = \varrho^\varepsilon * \xi$ for a scaled mollifier ϱ^ε , and defined $K_\rho^\varepsilon = K_\rho * \varrho^\varepsilon$. Since this is a centred Gaussian random variable, we have $E(\uparrow) = 0$, in accordance with Proposition 4.1. It then follows from the defining property of space-time white noise that

$$\begin{aligned} E(\heartsuit) &= \mathbb{E}\{(\mathbf{\Pi}^\varepsilon \heartsuit)(0)\} = \mathbb{E}\{(\mathbf{\Pi}^\varepsilon \uparrow)(0)^2\} \\ &= \int K_\rho^\varepsilon(-z_1)K_\rho^\varepsilon(-z_2)\mathbb{E}\{\xi(dz_1)\xi(dz_2)\} \\ &= \int K_\rho^\varepsilon(-z_1)^2 dz_1 . \end{aligned} \quad (4.9) \quad \clubsuit$$

Example 4.10. A more complicated example is

$$\begin{aligned} E(\heartsuit \heartsuit) &= \mathbb{E}\{(\mathbf{\Pi}^\varepsilon \heartsuit \heartsuit)(0)^2\} \\ &= \mathbb{E}\left\{\left(\int K_\rho(-z)K_\rho^\varepsilon(z-z_1)K_\rho^\varepsilon(z-z_2)\xi(dz_1)\xi(dz_2) dz\right)^2\right\} . \end{aligned}$$

Wick calculus implies that $\mathbb{E}\{\xi(dz_1)\xi(dz_2)\xi(d\bar{z}_1)\xi(d\bar{z}_2)\}$ is a sum of three terms, which can be symbolised by the pairings



The first pairing yields

$$\left(\int K_\rho(-z)K_\rho^\varepsilon(z-z_1)^2 dz dz_1\right)^2 = 0 ,$$

owing to the fact that K_ρ integrates to zero. By symmetry, the second and third pairing yield the same value, namely

$$\int K_\rho(-z)K_\rho^\varepsilon(z-z_1)K_\rho^\varepsilon(\bar{z}-z_1)K_\rho(-\bar{z})K_\rho^\varepsilon(z-z_2)K_\rho^\varepsilon(\bar{z}-z_2) dz d\bar{z} dz_1 dz_2 .$$

It is convenient to represent such an integral graphically by the diagram



where small black vertices denote integration variables, the large green vertex denotes the point 0, solid arrows denote kernels K_ρ , and broken arrows denote kernels K_ρ^ε . The benefit of the graphical representation (4.10), besides saving space, is that it will allow to represent in a more visual way the extraction-contraction operations associated with renormalisation. \clubsuit

These examples motivate the following definition, which is a particular case of [21, Def. 2.1].

Definition 4.11 (Feynman diagram). A Feynman diagram (or, more precisely, a vacuum diagram) is a finite oriented graph $\Gamma = (\mathcal{V}, \mathcal{E})$, with a distinguished node $v^* \in \mathcal{V}$, and in which each edge $e \in \mathcal{E}$ has a type \mathfrak{t} belonging to a finite set of types \mathfrak{L} . With each type $\mathfrak{t} \in \mathfrak{L}$, we associate a degree $\deg(\mathfrak{t}) \in \mathbb{R}$ and a kernel $K_{\mathfrak{t}} : \mathbb{R}^{d+1} \setminus \{0\} \rightarrow \mathbb{R}$. The degree of Γ is defined by

$$\deg(\Gamma) = (\rho + d)(|\mathcal{V}| - 1) + \sum_{e \in \mathcal{E}} \deg(e) , \quad (4.11)$$

where $|\mathcal{V}|$ denotes the cardinality of \mathcal{V} and $\deg(e) = \deg(\mathfrak{t}(e))$. The value of the diagram $\Gamma = (\mathcal{V}, \mathcal{E})$ is defined as

$$E(\Gamma) = \int_{(\mathbb{R}^{d+1})^{\mathcal{V} \setminus v^*}} \prod_{e \in \mathcal{E}} K_{\mathfrak{t}(e)}(z_{e_+} - z_{e_-}) dz, \quad (4.12)$$

where each oriented edge is written $e = (e_-, e_+) \in \mathcal{V}^2$, and $z_{v^*} = 0$.

The graph in (4.10) is an example of Feynman diagram, with a set of types \mathfrak{L} consisting of 2 types corresponding to the kernels K_ρ and K_ρ^ε . We define their degrees by

$$\deg(\longrightarrow) = \deg(\dashrightarrow) = -d. \quad (4.13)$$

To each symbol $\tau \in T$ without decorations, we associate a linear combination of Feynman diagrams in the following way.

Definition 4.12 (Pairing). *Let $\tau \in T \setminus I_E$ be a symbol without decorations, and denote its set of leaves by N_τ . A pairing of τ is a partition P of N_τ into two-elements blocks. We denote the set of pairings of τ by $\mathcal{P}_\tau^{(2)}$. Then $\Gamma(\tau, P)$ is the Feynman diagram obtained by merging the leaves of a same block, and assigning to every edge adjacent to a former leaf the type K_ρ^ε , and to all other edges the type K_ρ .*

Proposition 4.13. *Let $\tau \in T \setminus I_E$. If τ has p leaves and q edges, then each $\Gamma(\tau, P)$ has $q + 1 - \frac{p}{2}$ vertices and q edges. Therefore,*

$$\deg(\Gamma(\tau, P)) = |\tau|_s \Big|_{\kappa=0} \quad (4.14)$$

holds for any $P \in \mathcal{P}_\tau^{(2)}$. In addition, we have

$$E(\tau) = \sum_{P \in \mathcal{P}_\tau^{(2)}} E(\Gamma(\tau, P)). \quad (4.15)$$

PROOF: By (3.2), we have $|\tau|_s = -\frac{p}{2}(\rho + d) + \rho q - p\kappa$. Since τ is a tree, it has $q + 1$ nodes, and therefore $q + 1 - p$ inner nodes. When contracting the p leaves pairwise, one obtains a Feynman diagram with q edges of type K_ρ or K_ρ^ε , and $q + 1 - p + \frac{p}{2}$ vertices. Therefore its degree is given by $-qd + (\rho + d)(q - \frac{p}{2})$, which agrees with (4.14). The relation (4.15) is then a direct consequence of the rules (4.4) defining the model and Wick calculus. \square

The following simple result shows that we can limit the analysis to Feynman diagrams which are at least 2-connected.

Lemma 4.14. *If Γ is 1-connected (i.e., if one can split Γ into two disjoint graphs by removing one edge), then $E(\Gamma) = 0$.*

PROOF: If $\Gamma = (\mathcal{V}, \mathcal{E})$ is 1-connected, then there exist two vertex-disjoint subgraphs $\Gamma_1 = (\mathcal{V}_1, \mathcal{E}_1)$ and $\Gamma_2 = (\mathcal{V}_2, \mathcal{E}_2)$ such that $\mathcal{V} = \mathcal{V}_1 \cup \mathcal{V}_2$ and $\mathcal{E} = \mathcal{E}_1 \cup \mathcal{E}_2 \cup \{e_0\}$. By a linear change of variables, we may arrange that $e_0 = (v^*, v_1)$ where $v_1 \in \mathcal{V}_1$. We thus obtain

$$E(\Gamma) = \int_{(\mathbb{R}^{d+1})^{\mathcal{V}_1}} K_{\mathfrak{t}(e_0)}(z_1) \prod_{e \in \mathcal{E}_1} K_{\mathfrak{t}(e)}(z_{e_+} - z_{e_-}) dz E(\Gamma_2).$$

Performing the change of variables $z_v = \bar{z}_v + z_1$ for all $v \in \mathcal{V}_1 \setminus \{v_1\}$, we can factor out the integral over z_1 . This integral vanishes by construction. \square

4.3 Simplification rules for Feynman diagrams

Integrals of the type encountered above can be somewhat simplified by using the fact that P_ρ is the kernel of a Markov semigroup, describing a rotationally symmetric ρ -stable Lévy process (see for instance [32]). While this is not essential for the general argument, it reduces the size of diagrams and thus improves the graphical representation. It also allows to compute the explicit expressions for the renormalisation constants A_0 and \bar{A}_0 given in (2.8) and (2.9).

Lemma 4.15. *Assume the scaled mollifier has the form $\varrho^\varepsilon(t, x) = \varepsilon^{-(\rho+d)} \varrho(\varepsilon^{-\rho}t, \varepsilon^{-1}x)$, where $\varrho(t, x) = \varrho_0(t)\varrho_1(x)$ is even in x , supported in a ball of scaled radius 1, and integrates to 1. Then K_ρ^ε satisfies the following properties for all $(t, x) \in \mathbb{R}^{d+1}$:*

1. *Chapman–Kolmogorov equation: there exists a function $R_1^\varepsilon : \mathbb{R}^{d+2} \rightarrow \mathbb{R}$, uniformly bounded and integrable in its first two arguments, such that*

$$\int K_\rho^\varepsilon(t, x-y)K_\rho^\varepsilon(s, y) dy = \tilde{K}_\rho^\varepsilon(t+s, x) + R_1^\varepsilon(t, s, x), \quad (4.16)$$

where $\tilde{K}_\rho^\varepsilon = K_\rho^\varepsilon * \varrho^\varepsilon = K_\rho * \varrho^\varepsilon * \varrho^\varepsilon$ is a kernel with a different mollifier;

2. *Green function: there exists a uniformly bounded function $R_2^\varepsilon : \mathbb{R}^{d+1} \rightarrow \mathbb{R}$ such that*

$$\int_t^\infty K_\rho^\varepsilon(s, x) ds = -(G_\rho *_x P_\rho^\varepsilon)(t, x) + R_2^\varepsilon(t, x), \quad (4.17)$$

where $G_\rho = (\Delta^{\rho/2})^{-1}$ is the Green function of the fractional Laplacian, $P_\rho^\varepsilon = P_\rho * \varrho^\varepsilon$ and $*_x$ denotes convolution in space.

PROOF: For the first property, we use the Chapman–Kolmogorov relation $P_\rho(t, \cdot) *_x P_\rho(s, \cdot) = P_\rho(t+s, \cdot)$ to obtain

$$\begin{aligned} K_\rho(t, \cdot) *_x K_\rho(s, \cdot) &= K_\rho(t+s, \cdot) + R_\rho(t, s, \cdot) \\ &\quad - K_\rho(t, \cdot) *_x R_\rho(s, \cdot) - R_\rho(t, \cdot) *_x K_\rho(s, \cdot) - R_\rho(t, \cdot) *_x R_\rho(s, \cdot). \end{aligned}$$

Using the fact that R_ρ is bounded and that K_ρ and $R_\rho = P_\rho - K_\rho$ are integrable (P_ρ being integrable and K_ρ having compact support), one obtains that all terms involving R_ρ are bounded. The relation (4.16) then follows upon convolving twice with ϱ^ε . The last relations follows from the fact that

$$\Delta^{\rho/2} \int_t^\infty P_\rho(s, \cdot) ds = \int_t^\infty \Delta^{\rho/2} e^{s\Delta^{\rho/2}} ds = e^{s\Delta^{\rho/2}} \Big|_t^\infty = -P_\rho(t, \cdot).$$

Convolving with G_ρ , we obtain

$$\int_t^\infty P_\rho(s, x) ds = -G_\rho *_x P_\rho(t, x).$$

The result then follows by decomposing P_ρ on the left-hand side into $K_\rho + R_\rho$, and convolving with ϱ^ε . \square

Applying these properties to (4.9), we obtain

$$E(\heartsuit) = \iint K_\rho^\varepsilon(-t, -x)K_\rho^\varepsilon(-t, x) dx dt = \int \tilde{K}_\rho^\varepsilon(-2t, 0) dt + \mathcal{O}(1) = \frac{1}{2}G_\rho^\varepsilon(0) + \mathcal{O}(1),$$

where $G_\rho^\varepsilon = \varrho_1^\varepsilon *_x G_\rho$, $\mathcal{O}(1)$ denotes a constant bounded uniformly in ε , and we used the fact that $P_\rho(0, x) = \delta(x)$. Note that this implies the expression (2.8) for the counterterm associated with \heartsuit . The expression (2.9) for \bar{A}_0 is obtained by a similar argument applied to the element \spadesuit .

Lemma 4.16. *There exists a uniformly bounded function $R_3^\varepsilon : \mathbb{R}^{2(d+1)} \rightarrow \mathbb{R}$ such that*

$$\begin{aligned} \int K_\rho^\varepsilon(z_1 - z) K_\rho^\varepsilon(z_2 - z) dz &= \int K_\rho^\varepsilon(z - z_1) K_\rho^\varepsilon(z - z_2) dz \\ &= -\frac{1}{2} (G_\rho^\varepsilon *_x \tilde{P}_\rho^\varepsilon)(|t_1 - t_2|, x_1 - x_2) + R_3^\varepsilon(z_1, z_2), \end{aligned} \quad (4.18)$$

where $\tilde{P}_\rho^\varepsilon = P_\rho^\varepsilon * \varrho^\varepsilon$.

PROOF: The first two terms in (4.18) are equal, as can be seen by a change of variables $z \mapsto -z$. Using (4.16) and setting $s = t_1 + t_2 - 2t$, we obtain that

$$\begin{aligned} \int K_\rho^\varepsilon(z_1 - z) K_\rho^\varepsilon(z_2 - z) dz &= \int K_\rho^\varepsilon(t_1 - t, x_1 - x) K_\rho^\varepsilon(t_2 - t, x_2 - x) 1_{\{t < t_1 \wedge t_2\}} dt dx + R_{3,1}^\varepsilon(z_1, z_2) \\ &= \int K_\rho^\varepsilon(t_1 + t_2 - 2t, x_1 - x_2) 1_{\{t < t_1 \wedge t_2\}} dt + R_{3,2}^\varepsilon(z_1, z_2) \\ &= \frac{1}{2} \int_{|t_1 - t_2|}^{\infty} K_\rho^\varepsilon(s, x_1 - x_2) ds + R_{3,2}^\varepsilon(z_1, z_2) \end{aligned}$$

for some uniformly bounded remainders $R_{3,1}^\varepsilon$ and $R_{3,2}^\varepsilon$. The result follows from (4.17). \square

We represent (4.18) symbolically, for $\varepsilon = 0$ and $\varepsilon \neq 0$, by

$$\begin{aligned} \begin{array}{c} z_1 \longleftarrow \bullet \longrightarrow z_2 \\ \bullet \longrightarrow \bullet \longleftarrow z_2 \end{array} &= -\frac{1}{2} \begin{array}{c} z_1 \text{---} \bullet \text{---} z_2 \\ \bullet \text{---} \bullet \text{---} z_2 \end{array}, \\ \begin{array}{c} z_1 \text{---} \bullet \text{---} z_2 \\ \bullet \text{---} \bullet \text{---} z_2 \end{array} &= -\frac{1}{2} \begin{array}{c} z_1 \text{---} \bullet \text{---} z_2 \\ \bullet \text{---} \bullet \text{---} z_2 \end{array}, \end{aligned} \quad (4.19)$$

where we do not put arrows on edges representing kernels that are symmetric in both variables, and discard terms bounded uniformly in ε .

Example 4.17. Applying Lemma 4.16 to (4.10), and using the fact that the root, marked by the green vertex, can be moved to a different node by a linear change of variables in the integral, we obtain

$$E(\begin{array}{c} \bullet \bullet \bullet \\ \diagdown \diagup \\ \bullet \\ \diagup \diagdown \\ \bullet \bullet \bullet \end{array}) = -\frac{1}{4} \begin{array}{c} \bullet \bullet \bullet \\ \diagdown \diagup \\ \bullet \\ \diagup \diagdown \\ \bullet \bullet \bullet \end{array}.$$

Here and below, we will sometimes make a slight abuse of notation, by identifying a Feynman diagram Γ with its value $E(\Gamma)$. A similar computation yields

$$E(\begin{array}{c} \bullet \bullet \bullet \\ \diagdown \diagup \\ \bullet \\ \diagup \diagdown \\ \bullet \bullet \bullet \end{array}) = 2 \begin{array}{c} \bullet \bullet \bullet \\ \diagdown \diagup \\ \bullet \\ \diagup \diagdown \\ \bullet \bullet \bullet \end{array} = \frac{1}{2} \begin{array}{c} \bullet \bullet \bullet \\ \diagdown \diagup \\ \bullet \\ \diagup \diagdown \\ \bullet \bullet \bullet \end{array}$$

Moving the root and introducing the new kernel

$$\begin{array}{c} 0 \\ \bullet \text{---} \bullet \end{array} \xrightarrow{z} \begin{array}{c} 0 \\ \bullet \text{---} \bullet \end{array}, \quad (4.20)$$

we obtain

$$E(\text{diagram}) = \frac{1}{2} \text{diagram} . \quad (4.21)$$

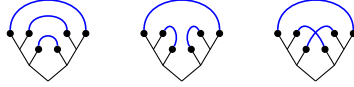
Proceeding in the same way, we obtain for instance

$$E(\text{diagram}) = \frac{1}{8} \text{diagram} + \frac{1}{4} \text{diagram} + \frac{1}{4} \text{diagram} \quad (4.22)$$

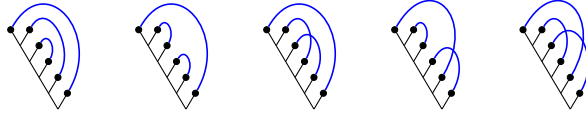
and

$$E(\text{diagram}) = -\frac{1}{4} \left[\text{diagram} + \text{diagram} + \text{diagram} + \text{diagram} + \text{diagram} \right] .$$

The corresponding pairings are



for the first three diagrams, and



for the last five. ♣

Definition 4.11 can be applied to this setting, by expanding the set of types \mathcal{L} by 3 new elements, with degrees

$$\begin{aligned} \deg(\text{red zigzag}) &= \deg(\text{red zigzag}) = \rho - d \\ \deg(\text{purple wavy}) &= 2\rho - d . \end{aligned} \quad (4.23)$$

The associated kernels are $G_\rho *_{x} \tilde{P}_\rho$, $G_\rho^\varepsilon *_{x} \tilde{P}_\rho^\varepsilon$ and $K_\rho * G_\rho^\varepsilon *_{x} \tilde{P}_\rho^\varepsilon$. We will say that a Feynman diagram is *reduced* if the reduction rules (4.19) and (4.20) have been applied. Then Proposition 4.13 extends as follows.

Proposition 4.18. *Let $\tau \in T \setminus I_E$. If τ has p leaves and q edges, then each reduced $\Gamma(\tau, P)$ has $q - p$ vertices. The relation (4.14) still holds in this case, while (4.15) becomes*

$$E(\tau) = \sum_{P \in \mathcal{P}_\tau^{(2)}} \left(-\frac{1}{2} \right)^{1 + \frac{p}{2}} E(\Gamma(\tau, P)) + \mathcal{O}(1) , \quad (4.24)$$

where $\mathcal{O}(1)$ denotes a constant uniform in ε .

PROOF: Recall that the unreduced Feynman diagram has q edges of type K_ρ or K_ρ^ε , and $q + 1 - p + \frac{p}{2}$ vertices. Since τ cannot be a planted tree, the number of reductions is equal to $1 + \frac{p}{2}$, each decreasing by 1 the number of edges and vertices, which is why each reduced $\Gamma(\tau, P)$ has $q - p$ vertices. The degree is conserved by the reductions. The relation (4.24) is then a direct consequence of Lemma 4.16 and (4.19). □

5 Forests

5.1 Zimmermann's forest formula

The aim of this and the following section is to derive upper bounds for the expectations $E(\tilde{\mathcal{A}}_-\tau)$ when $\tau \in T_-$. We want to prove that

$$|E(\tilde{\mathcal{A}}_-\tau)| \leq C f(\tau) \varepsilon^{|\tau|_s}, \quad (5.1)$$

where the constant C does not depend on τ , ε or ρ , and $f(\tau)$ is a function to be determined, which depends on the structure of the tree τ .

A nice feature is that one can define a twisted antipode $\tilde{\mathcal{A}}_-$ acting on Feynman diagrams of negative degree, which is essentially the same as in [21], and reduces in this case to a mere extraction/contraction of divergent subdiagrams. In the sequel, we will use the same notation for this antipode as the one on trees. From the context, it will be clear which one is used. Denote by \mathcal{G} the vector space spanned by all admissible Feynman diagrams (not necessarily connected), and by \mathcal{G}_- the subspace spanned by diagrams of negative degree. We say that $\Gamma' = (\mathcal{V}', \mathcal{E}')$ is a subgraph of $\Gamma = (\mathcal{V}, \mathcal{E})$ if $\mathcal{E}' \subset \mathcal{E}$, and \mathcal{V}' contains all vertices in \mathcal{V} which belong to at least one edge $e \in \mathcal{E}'$. Then we define the twisted antipode to be the map $\tilde{\mathcal{A}}_- : \mathcal{G}_- \rightarrow \mathcal{G}$ given by

$$\tilde{\mathcal{A}}_-\Gamma = -\Gamma - \sum_{\bar{\Gamma} \subsetneq \Gamma} \tilde{\mathcal{A}}_-\bar{\Gamma} \cdot \Gamma/\bar{\Gamma},$$

where the sum runs over all not necessarily connected subgraphs of negative degree, and $\Gamma/\bar{\Gamma}$ denotes the graph obtained by contracting $\bar{\Gamma}$ to a single vertex.

Remark 5.1. The name twisted antipode is again related to the fact that one can introduce a Hopf algebra structure on (decorated) graphs, see [21, Section 2.3], which generalises the extraction-contraction Hopf algebra on undecorated graphs introduced by Connes and Kreimer in [12, 13]. The twisted antipode differs from the antipode of that Hopf algebra because of the use of a coaction instead of a coproduct, meaning that the extracted graphs $\bar{\Gamma}$ and the contracted graphs $\Gamma/\bar{\Gamma}$ are not in the same space: while the former have negative degree, the latter can have arbitrary degree. \diamond

Proposition 5.2. *One has*

$$E(\tilde{\mathcal{A}}_-\tau) = \sum_{P \in \mathcal{P}_\tau^{(2)}} E(\tilde{\mathcal{A}}_-\Gamma(\tau, P)).$$

PROOF: It follows from Propositions 4.5 and 4.6 that

$$E(\tilde{\mathcal{A}}_-\tau) = -E(\tau) - \sum_{\mathbb{1} \subsetneq \tau_1 \dots \tau_n \subsetneq E\tau} E(\tilde{\mathcal{A}}_-(\tau_1 \dots \tau_n) \cdot \tau / (\tau_1 \dots \tau_n)).$$

We then apply Proposition 4.13 to the expectations on the right-hand side and by an inductive argument, we get

$$\begin{aligned} E(\tilde{\mathcal{A}}_-\tau) &= - \sum_{P \in \mathcal{P}_\tau^{(2)}} E(\Gamma(\tau, P)) \\ &\quad - \sum_{\mathbb{1} \subsetneq \tau_1 \dots \tau_n \subsetneq E\tau} \prod_{i=1}^n \sum_{P_i \in \mathcal{P}_{\tau_i}^{(2)}} E(\tilde{\mathcal{A}}_-\Gamma(\tau_i, P_i)) \sum_{P_{n+1} \in \mathcal{P}_{\tau_{n+1}}^{(2)}} E(\Gamma(\tau_{n+1}, P_{n+1})) \end{aligned}$$

where $\tau_{n+1} = \tau / (\tau_1 \cdot \dots \cdot \tau_n)$. Indeed, one has

$$\mathcal{P}_\tau^{(2)} = \bigcup_{\mathbb{1} \not\subseteq \tau_1 \dots \tau_n \not\subseteq E\tau} \left\{ \bigsqcup_{i=1}^{n+1} P_i : P_i \in \mathcal{P}_{\tau_i}^{(2)} \right\} \bigsqcup \hat{\mathcal{P}}_\tau^{(2)}$$

where $\hat{\mathcal{P}}_\tau^{(2)}$ contains the pairings without any subdiagrams that could be extracted via $\tilde{\mathcal{A}}_-$. Moreover, any subdiagram of $\Gamma(\tau, P)$ is of the form $\Gamma(\bar{\tau}, \bar{P})$ where $\bar{\tau}$ is a subtree of τ and \bar{P} is a subpairing of P . \square

Example 5.3. Consider the symbol $\tau = \begin{array}{c} \bullet \\ \diagup \quad \diagdown \\ \bullet \quad \bullet \\ \diagup \quad \diagdown \\ \bullet \quad \bullet \end{array}$. The effect of the twisted antipode on τ has been determined in Example 4.8, and $E(\tau)$ is given in (4.22). Applying the twisted antipode directly to (4.22), we find

$$E(\tilde{\mathcal{A}}_-(\begin{array}{c} \bullet \\ \diagup \quad \diagdown \\ \bullet \quad \bullet \\ \diagup \quad \diagdown \\ \bullet \quad \bullet \end{array})) = -E(\begin{array}{c} \bullet \\ \diagup \quad \diagdown \\ \bullet \quad \bullet \\ \diagup \quad \diagdown \\ \bullet \quad \bullet \end{array}) + \frac{1}{2} \begin{array}{c} \bullet \\ \diagup \quad \diagdown \\ \bullet \quad \bullet \\ \diagup \quad \diagdown \\ \bullet \quad \bullet \end{array} \begin{array}{c} \bullet \\ \diagup \quad \diagdown \\ \bullet \quad \bullet \\ \diagup \quad \diagdown \\ \bullet \quad \bullet \end{array} - \frac{1}{4} \left(\begin{array}{c} \bullet \\ \diagup \quad \diagdown \\ \bullet \quad \bullet \\ \diagup \quad \diagdown \\ \bullet \quad \bullet \end{array} \right)^2 \begin{array}{c} \bullet \\ \diagup \quad \diagdown \\ \bullet \quad \bullet \\ \diagup \quad \diagdown \\ \bullet \quad \bullet \end{array}. \quad (5.2)$$

Indeed, one easily checks that since $\rho > \rho_c = d/3$, the only nontrivial subgraph of negative degree in (4.22) is the ‘‘bubble’’ having two edges, one of type K_ρ and one of type $G_\rho^\varepsilon *_{x} \tilde{P}_\rho^\varepsilon$. The expression (5.2) is indeed equivalent to the one obtained by transforming the expression (4.8) for $\tilde{\mathcal{A}}_-^E(\tau)$ into Feynman diagrams.

Note that the degree of all diagrams in (4.22) is $7\rho - 3d$, while the total degree of the two extracted diagrams in (5.2) is $2(2\rho - d) < 7\rho - 3d$. This is an instance of the degree of subdivergences being worse than the degree of the whole diagram. \clubsuit

Remark 5.4. If γ is any (non-reduced) diagram with $n + 1$ vertices and q edges, then its degree can be written as

$$\deg(\gamma) = (\rho + d)n - qd = (4n - 3q)\frac{d}{3} + n(\rho - \rho_c).$$

In particular, if γ is of the form $\Gamma(\tau, P)$, one has

$$\deg(\gamma) = -\frac{2}{3}d + \frac{3m - 1}{2}(\rho - \rho_c), \quad \deg(\gamma) = -\frac{1}{3}d + \frac{3\bar{m} + 1}{2}(\rho - \rho_c),$$

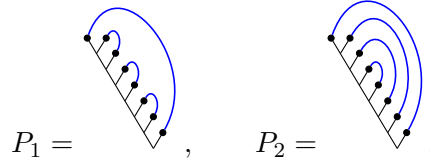
respectively, for full and almost full binary trees, where m, \bar{m} are such that τ has $2m$ edges in the first case, and $2\bar{m} + 1$ edges in the second case. Note that in both cases, the degree is a strictly increasing function of the number of edges.

For practical counting of degrees, it is sometimes useful to consider the limiting case $\rho \searrow \rho_c$, and to use $\frac{d}{3}$ as degree unit. Then edges of the three types in (4.13) and (4.23) count for $-3, -2$ and -1 respectively, while vertices have weight $+4$. Similarly, for trees $\tau \in \mathcal{T}_-$, edges have weight $+1$ and leaves have weight -2 . \diamond

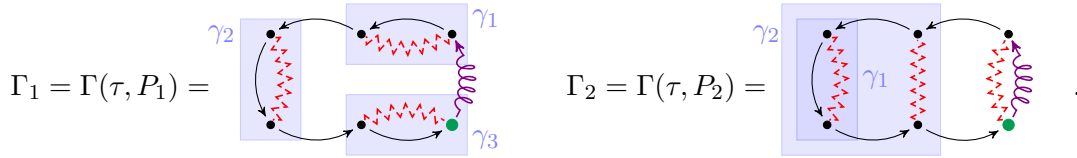
Proposition 5.2 allows to reduce the estimation of the coefficients $c_\varepsilon(\tau)$ to the problem of estimating the value of Feynman diagrams. The difficulty is that the twisted antipode is essential to obtain a bound of the form (5.1): such a bound is not true in general for $E(\tau)$, because, as the above example shows, Feynman diagrams $\Gamma(\tau, P)$ may contain subdiagrams whose degree is strictly less than the degree of $\Gamma(\tau, P)$. In order to deal with this difficulty, our plan is now to adapt the approach of [21] to the present situation. While we will use its formalism, the main novelty is an adaptation of the proof of [21, Thm. 3.1] in order to derive ε -dependent bounds for Feynman diagrams given in Proposition 6.1 below. This proposition can be considered as one of the main results of this work, as the bound it provides is new and was not proved in [21].

Definition 5.5 (Forests). Let Γ be a Feynman diagram, and denote by \mathcal{G}_Γ^- the set of all connected subgraphs $\bar{\Gamma} \subset \Gamma$ of negative degree. We denote by $<$ the partial order on \mathcal{G}_Γ^- defined by inclusion. A subset $\mathcal{F} \subset \mathcal{G}_\Gamma^-$ is called a forest if any two elements of \mathcal{F} are either comparable by $<$, or vertex-disjoint. The set of forests on Γ is denoted by \mathcal{F}_Γ^- . Given a forest \mathcal{F} and two graphs $\bar{\Gamma}, \bar{\Gamma}_1 \in \mathcal{F}$, we say that $\bar{\Gamma}_1$ is a child of $\bar{\Gamma}$ if $\bar{\Gamma}_1 < \bar{\Gamma}$, and there is no $\bar{\Gamma}_2 \in \mathcal{F}$ such that $\bar{\Gamma}_1 < \bar{\Gamma}_2 < \bar{\Gamma}$. In that case, $\bar{\Gamma}$ is called the parent of $\bar{\Gamma}_1$.

Example 5.6. Let τ be the comb with eight leaves, and consider the following pairings:



The corresponding Feynman diagrams are given by



The diagram Γ_1 has 3 identical divergent bubbles $\gamma_1, \gamma_2, \gamma_3$, indicated by shaded frames. The left-hand bubble γ_2 is part of two overlapping subdivergences, each consisting of two bubbles and the joining edge. However, these subdiagrams are 1-connected, and thus do not matter in the analysis. If we restrict our attention to the set $\mathcal{G}_{\Gamma_1, E}^-$ of subgraphs with non-vanishing expectation, we obtain indeed a forest $\mathcal{G}_{\Gamma_1, E}^- = \{\Gamma_1, \gamma_1, \gamma_2, \gamma_3, \emptyset\}$. The corresponding parent-child relationship graph consists of the parent Γ_1 and its three children $\gamma_1, \gamma_2, \gamma_3$.

The diagram Γ_2 has two nested subdivergences: a bubble γ_1 , and the bubble together with the 3 adjacent edges, denoted γ_2 . In this case again, the set $\mathcal{G}_{\Gamma_2, E}^-$ is a forest, while the associated graph is a linear graph with parent Γ , child γ_2 and grandchild γ_1 . ♣

In what follows, we will occasionally need decorated Feynman diagrams $\bar{\Gamma}_\epsilon^n$, though as in the case of trees, decorations will play almost no role. Such a diagram is defined by a graph $\Gamma = (\mathcal{V}, \mathcal{E})$ with a distinguished node $v^* \in \mathcal{V}$, a node decoration $\mathbf{n} : \mathcal{V} \rightarrow \mathbb{N}_0^{d+1}$ and a vertex decoration $\epsilon : \mathcal{E} \rightarrow \mathbb{N}_0^{d+1}$. The degree of $\bar{\Gamma}_\epsilon^n$ is defined as

$$\deg(\bar{\Gamma}_\epsilon^n) = (\rho + d)(|\mathcal{V}| - 1) + \sum_{v \in \mathcal{V}} |\mathbf{n}(v)|_s + \sum_{e \in \mathcal{E}} [\deg(e) - |\epsilon(e)|_s], \quad (5.3)$$

and its value is given by

$$E(\bar{\Gamma}_\epsilon^n) = \int_{(\mathbb{R}^{d+1})^{\mathcal{V} \setminus v^*}} \prod_{e \in \mathcal{E}} \partial^{\epsilon(e)} K_{t(e)}(z_{e_+} - z_{e_-}) \prod_{w \in \mathcal{V} \setminus v^*} (z_w - z_{v^*})^{n(w)} dz. \quad (5.4)$$

Note that when the decorations \mathbf{n} and ϵ vanish identically, (5.3) and (5.4) reduce to the expressions (4.11) and (4.12) for undecorated Feynman diagrams. Given a divergent subdiagram $\gamma \in \mathcal{G}_\Gamma^-$, we define an extraction-contraction operator \mathcal{C}_γ by

$$\mathcal{C}_\gamma \bar{\Gamma}_\epsilon^n = \sum_{\epsilon_\gamma, \mathbf{n}_\gamma} \mathbf{1}_{\deg(\gamma_\epsilon^{n_\gamma + \pi \epsilon_\gamma}) < 0} \frac{(-1)^{|\text{out } \epsilon_\gamma|}}{\epsilon_\gamma!} \binom{\mathbf{n}}{\mathbf{n}_\gamma} \gamma_\epsilon^{n_\gamma + \pi \epsilon_\gamma} \cdot \mathcal{R}_\gamma \bar{\Gamma}_{\epsilon + \epsilon_\gamma}^{n - n_\gamma}, \quad (5.5)$$

where $\pi\epsilon_\gamma$ and \mathcal{R}_γ are defined in the same way as for decorated trees in (4.6), and $|\text{out } \epsilon_\gamma|$ is the number of derivatives on outgoing edges from γ . This operator can be naturally extended to undecorated diagrams Γ , by identifying them with $\bar{\Gamma}_\epsilon^n$ with $n = 0$ and $\epsilon = 0$. Note that in that case, the sum over n_γ disappears in (5.5). The main difference with the case of trees is that ϵ_γ has a different support: it is supported on the edges (x, y) such that either x or y belongs to the vertex set $\mathcal{V}(\gamma)$. Therefore, one gets a minus sign for each derivative on outgoing edges. In the case of a tree, by contrast, ϵ_γ is supported only on the incoming edges. However, using this representation does not make any difference. Indeed, by taking v_* to be the root of the underlying tree behind the construction of γ , one obtains a vanishing contribution whenever one puts a monomial at v_* and a derivative on the only outgoing edge at v_* .

We can now define a forest extraction operator $\mathcal{C}_\mathcal{F}$ recursively by setting $\mathcal{C}_\emptyset\Gamma = \Gamma$ and

$$\mathcal{C}_\mathcal{F}\Gamma = \mathcal{C}_{\mathcal{F}\setminus\varrho(\mathcal{F})} \prod_{\gamma \in \varrho(\mathcal{F})} \mathcal{C}_\gamma\Gamma ,$$

where $\varrho(\mathcal{F})$ denotes the set of roots of γ in the graph of parent-child relationships. Then Zimmermann's forest formula states that

$$\tilde{\mathcal{A}}_-\Gamma = - \sum_{\mathcal{F} \in \mathcal{F}_\Gamma^-} (-1)^{|\mathcal{F}|} \mathcal{C}_\mathcal{F}\Gamma , \quad (5.6)$$

cf. [21, Prop. 3.3]. In the particular case where \mathcal{G}_Γ^- is itself a forest, (5.6) can be rewritten as

$$\tilde{\mathcal{A}}_-\Gamma = -\mathcal{R}_{\mathcal{G}_\Gamma^-}\Gamma ,$$

where \mathcal{R} is defined recursively by $\mathcal{R}_\emptyset\Gamma = \Gamma$ and

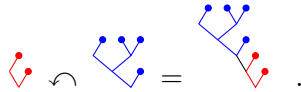
$$\mathcal{R}_\mathcal{F}\Gamma = \mathcal{R}_{\mathcal{F}\setminus\varrho(\mathcal{F})} \prod_{\gamma \in \varrho(\mathcal{F})} (\text{id} - \mathcal{C}_\gamma)\Gamma , \quad (5.7)$$

which turns out to be simpler to handle than (5.6). This is a consequence of the ‘‘inclusion–exclusion identity’’

$$\prod_{i \in A} (\text{id} - X_i) = \sum_{B \subset A} (-1)^{|B|} \prod_{j \in B} X_j$$

valid for any finite set A , and operators $\{X_i : i \in A\}$, cf. [21, (3.3)]. In general, however, \mathcal{G}_Γ^- is *not* a forest, so that (5.7) does not hold. This is the problem of overlapping subdivergences: a divergent subgraph $\bar{\Gamma} \subset \Gamma$ can be part of two different divergent subgraphs $\bar{\Gamma}_1$ and $\bar{\Gamma}_2$, none of which is included in the other one.

The above example suggests that in our case, $\mathcal{G}_{\Gamma,E}^-$ may always be a forest, so that (5.7) is applicable. In order to establish this fact, we define a grafting operation on trees. If τ_1 and τ_2 are two non-planted trees, with τ_1 being almost full, we denote by $\tau_1 \curvearrowright \tau_2$ the tree obtained by joining the root of τ_2 to the vertex of τ_1 of degree 2 which is not the root. For instance, we have



Note that this operation is associative, but not commutative.

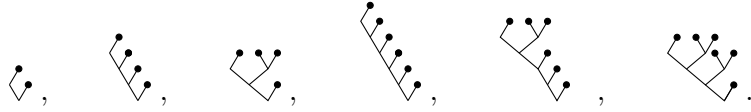
The following observation allows to characterise divergent subgraphs.

Lemma 5.7. *Let τ be a full binary tree with an even number of leaves. Then there exists a pairing P such that $\Gamma(\tau, P)$ is at least 2-connected, and a divergent subdiagram $\bar{\Gamma} = \Gamma(\bar{\tau}, \bar{P}) \subsetneq \Gamma$, if and only if $\bar{\tau}$ is an almost full binary tree of negative degree, having an even number of leaves, and which does not contain the root of τ .*

PROOF: Assume first that $\bar{\tau}$ is an almost full binary tree of negative degree, not containing the root and with an even number of leaves. Let \bar{P} be any pairing of the leaves of $\bar{\tau}$ and $\bar{\Gamma} = \Gamma(\bar{\tau}, \bar{P})$. Then $\tau = \tau_0 \frown \bar{\tau} \frown \tau_1$, where τ_0 is almost full and τ_1 is full. By pairing at least one leaf of τ_0 and one leaf of τ_1 , we obtain a 2-connected diagram Γ .

Conversely, assume $\Gamma(\tau, P)$ is at least 2-connected, with a divergent subdiagram $\bar{\Gamma} = \Gamma(\bar{\tau}, \bar{P})$. Then $\bar{\tau}$ cannot contain the root of τ . Indeed, if this were the case, $\bar{\tau}$ would necessarily be an almost full binary tree (being divergent and a proper subtree of τ), so that $\bar{\tau}$ and $\tau_1 = \tau \setminus \bar{\tau}$ would be connected by a single edge. Since P cannot connect leaves of $\bar{\tau}$ to leaves of τ_1 , Γ would be 1-connected. Similarly, if $\tau = \tau_0 \frown \bar{\tau}$, we would obtain a 1-connected diagram. Thus τ has to be of the form $\tau = \tau_0 \frown \bar{\tau} \frown \tau_1$, showing that $\bar{\tau}$ is almost full and does not contain the root of τ . \square

Example 5.8. Some examples of subtrees $\bar{\tau}$ leading to divergent subdiagrams are



One can check that they do not lead to any overlapping subdivergences. \clubsuit

Proposition 5.9. *Assume a Feynman diagram $\Gamma(\tau, P)$ has two overlapping subdivergences Γ_1 and Γ_2 . Then Γ_1 and Γ_2 are 1-connected. As a consequence, $\mathcal{G}_{\Gamma, E}^-$ is always a forest.*

PROOF: Assume there exist 3 subdivergences $\bar{\Gamma}, \Gamma_1, \Gamma_2$, such that $\Gamma_1 \setminus \Gamma_2$ and $\Gamma_2 \setminus \Gamma_1$ are both non-empty and $\bar{\Gamma} \subset \Gamma_1 \cap \Gamma_2$. Then there exist subtrees $\bar{\tau}, \tau_1, \tau_2$ such that $\tau_1 \setminus \tau_2 \neq \emptyset, \tau_2 \setminus \tau_1 \neq \emptyset, \bar{\tau} \subset \tau_1 \cap \tau_2$ and each diagram is obtained by restricting the pairing P , e.g. $\bar{\Gamma} = \Gamma(\bar{\tau}, P|_{\bar{\tau}})$. In particular, P can only pair leaves of $\bar{\tau}$.

The previous lemma shows that we must have

$$\tau_1 = \tau_{1,-} \frown \bar{\tau} \frown \tau_{1,+} \quad \text{and} \quad \tau_2 = \tau_{2,-} \frown \bar{\tau} \frown \tau_{2,+} .$$

Since $\tau_1 \setminus \tau_2 \neq \emptyset$ and $\tau_2 \setminus \tau_1 \neq \emptyset$, we may assume without restricting the generality that $\tau_{2,-} \subsetneq \tau_{1,-}$ and $\tau_{1,+} \subsetneq \tau_{2,+}$. Since the leaves of $\tau_{1,-} \setminus \tau_{2,-}$ cannot be paired with those of τ_2 , they have to be paired among themselves. But this results in Γ_1 and Γ_2 being 1-connected, by definition of the grafting operation. Therefore, they do not belong to $\mathcal{G}_{\Gamma, E}^-$ by Lemma 4.14. \square

Remark 5.10. Another consequence of Lemma 5.7 is that a divergent subdiagram $\gamma \subsetneq \Gamma$ has a degree strictly larger than $-\frac{d}{3}$. Therefore, in dimension $d \leq 3$, the operator $\mathcal{C}_\gamma \Gamma$ defined in (5.5) reduces to a simple extraction-contraction, while in dimension $d \in \{4, 5\}$, the sum also contains terms $\gamma^{\pi \epsilon \gamma}$ with edge decorations ϵ of degree at most 1. However, the value (5.4) of these additional terms vanishes by symmetry. \diamond

5.2 Hepp sectors and forest intervals

In this section, we present the main tools and definitions for renormalising Feynman diagrams: Hepp sectors, safe and unsafe forests, and forest intervals. All these notions have originally been introduced in the physics literature, see for instance [33, Chapter II.3] for an overview. We follow

mainly [21], where these notions have been reformulated in connection with [6, 8]. They first appear in the context of singular SPDEs in [8], and were imported from [15]. A first important concept in order to evaluate Feynman diagrams is the one of Hepp sector (cf. [21, proof of Prop. 2.4]).

Definition 5.11 (Hepp sector). *Fix a finite set \mathcal{V} and a bounded set $\Lambda \subset \mathbb{R}^{d+1}$. With any point configuration $z \in \Lambda^{\mathcal{V}}$, one can associate a binary tree $T = T(z)$, whose leaves are given by \mathcal{V} , and a function $\mathbf{n} = \mathbf{n}(z)$ defined on the inner nodes of T and taking values in \mathbb{N}_0 , with the following properties:*

- $u \mapsto \mathbf{n}_u$ is increasing when going from the root to the leaves of T ,
- for any leaves $v, \bar{v} \in \mathcal{V}$, one has

$$\|z_v - z_{\bar{v}}\|_s \asymp 2^{-\mathbf{n}_u} ,$$

where $u = v \wedge \bar{v}$ is the first common ancestor of v and \bar{v} in T and \asymp is a shorthand notation for

$$C^{-1}2^{-\mathbf{n}_u} \leq \|z_v - z_{\bar{v}}\|_s \leq C2^{-\mathbf{n}_u} , \quad (5.8)$$

where the constant C only depends on the size of Λ .

Writing $\mathbf{T} = (T, \mathbf{n})$ for these data, the Hepp sector $D_{\mathbf{T}} \subset \Lambda^{\mathcal{V}}$ is defined as the set of configurations $z \in \Lambda^{\mathcal{V}}$ for which $(T(z), \mathbf{n}(z)) = \mathbf{T}$.

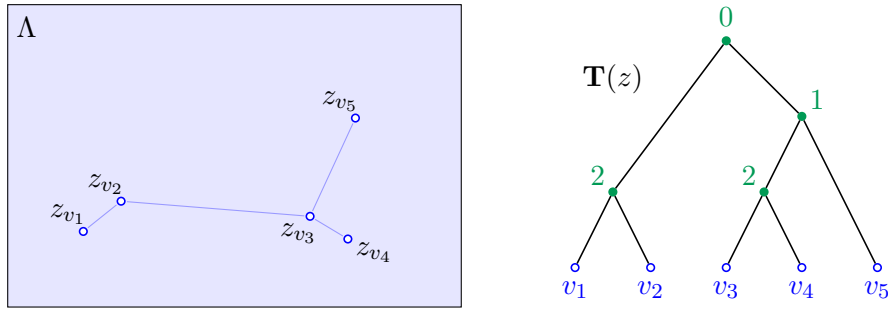
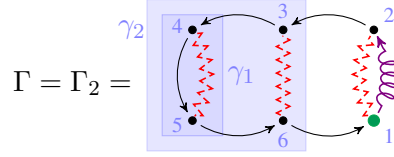


FIGURE 3: A point configuration $z \in \Lambda^{\mathcal{V}}$ with its minimal spanning tree (left), and the associated labelled tree $\mathbf{T} = (T(z), \mathbf{n}(z))$ (right). Here $\mathcal{V} = \{v_1, v_2, v_3, v_4, v_5\}$, and node decorations \mathbf{n} are shown in green. For instance, $\mathbf{n}_{v_1 \wedge v_2} = 2$, so that z_{v_1} and z_{v_2} are at a distance of order 2^{-2} , while $\mathbf{n}_{v_3 \wedge v_5} = 1$, so that z_{v_3} and z_{v_5} are at a distance of order 2^{-1} .

The main idea is that in each Hepp sector, the kernels have a given order of magnitude. Since the Hepp sectors provide a partition of $\Lambda^{\mathcal{V}}$, the value of the Feynman diagram can be written as a sum of integrals over individual Hepp sectors, so that it suffices to obtain uniform bounds on the products of kernels valid in each sector.

In order to exploit cancellations, it turns out to be necessary to adapt the way contractions are performed to the particular Hepp sector, cf. [21, Section 3.2]. If Γ is a Feynman diagram (possibly with decorations) and γ is a divergent subdiagram of Γ , one defines a new diagram $\mathcal{C}_\gamma \Gamma$ as in (5.5), but with the following differences. First the vertices of Γ are given an arbitrary order, and its edges e are assigned an additional label $\partial(e) = 0$ indicating their depth. Instead of extracting the subdiagram γ , all edges of Γ adjacent to γ are reconnected to the first vertex of γ (according to the chosen order), while the depth $\partial(e)$ of all edges e of γ is incremented by 1. Finally, when applying $\mathcal{C}_\gamma \Gamma$ to a diagram having edges of strictly positive depth, we set $\mathcal{C}_\gamma \Gamma = 0$ unless all edges adjacent to γ have a smaller depth than those of γ .

Example 5.12. Let



be the second diagram in Example 5.6 (without decorations \mathbf{n} and ϵ). We order the vertices counterclockwise, starting at the green vertex, as indicated by blue labels. Assume furthermore that $d \leq 3$, so that \mathcal{C}_γ does not create any terms with nontrivial decoration. Then we have

$$\mathcal{C}_{\gamma_1}\Gamma = \text{diagram}, \quad \mathcal{C}_{\gamma_2}\Gamma = \text{diagram}, \quad (5.9)$$

where violet edge labels denote the depth $\vartheta(e)$ (we do not indicate zero depths). Extracting both subdiagrams, we obtain

$$\mathcal{C}_{\gamma_1}\mathcal{C}_{\gamma_2}\Gamma = \mathcal{C}_{\gamma_2}\mathcal{C}_{\gamma_1}\Gamma = \text{diagram}. \quad (5.10)$$

Note that \mathcal{C}_{γ_1} and \mathcal{C}_{γ_2} commute. Given a forest $\mathcal{F} \subset \mathcal{G}_\Gamma^-$, one can thus define in an unambiguous way the operator $\mathfrak{K}_\mathcal{F}$ performing all contractions \mathcal{C}_γ with $\gamma \in \mathcal{F}$. We denote by σ the bijection between vertices and edges of $\mathfrak{K}_\mathcal{F}\Gamma$ and those of Γ .

We now fix a Hepp sector $D_\mathbf{T}$, $\mathbf{T} = (T, \mathbf{n})$ and a forest $\mathcal{F} \subset \mathcal{G}_\Gamma^-$, which we assume to be *full* in the sense that all $\gamma \in \mathcal{F}$ contain all edges of Γ joining two vertices of γ . As in [21, Section 3.2], we construct a partition $\mathcal{P}_\mathbf{T}$ of \mathcal{G}_Γ^- into subsets which are adapted to the particular Hepp sector. The first step is to define, for each edge e of Γ , the common ancestor of the extremities of e viewed as an element of $\mathfrak{K}_\mathcal{F}\Gamma$, that is

$$v_e = \sigma(\sigma^{-1}(e)_-) \wedge \sigma(\sigma^{-1}(e)_+).$$

Then the integer

$$\text{scale}_\mathbf{T}^\mathcal{F}(e) = \mathbf{n}_{v_e}$$

measures the distance between the extremities of e in $\mathfrak{K}_\mathcal{F}\Gamma$. For $\gamma \in \mathcal{F}$, define

$$\text{int}_\mathbf{T}^\mathcal{F}(\gamma) = \inf_{e \in \mathcal{E}_\gamma^\mathcal{F}} \text{scale}_\mathbf{T}^\mathcal{F}(e), \quad \text{ext}_\mathbf{T}^\mathcal{F}(\gamma) = \sup_{e \in \partial \mathcal{E}_\gamma^\mathcal{F}} \text{scale}_\mathbf{T}^\mathcal{F}(e),$$

where $\mathcal{E}_\gamma^\mathcal{F}$ denotes the set of edges belonging to γ , but not to any of its children in \mathcal{F} , while $\partial \mathcal{E}_\gamma^\mathcal{F}$ denotes the set of edges adjacent to γ belonging to its parent $\mathcal{A}(\gamma)$ in \mathcal{F} . If γ is a root of \mathcal{F} , we set $\mathcal{A}(\gamma) = \Gamma$. Thus $\text{int}_\mathbf{T}^\mathcal{F}(\gamma)$ describes the longest distance between points in γ without its children, while $\text{ext}_\mathbf{T}^\mathcal{F}(\gamma)$ describes the shortest distance between points in γ and those in its parent in \mathcal{F} . Examples 5.14, 6.5 and 6.12 below provide illustrations of these concepts.

Definition 5.13 (Safe and unsafe forests).

- A subdiagram $\gamma \in \mathcal{F}$ is safe in \mathcal{F} if

$$\text{ext}_{\mathbf{T}}^{\mathcal{F}}(\gamma) \geq \text{int}_{\mathbf{T}}^{\mathcal{F}}(\gamma)$$

and unsafe otherwise.

- A subdiagram γ of Γ is safe (resp. unsafe) for \mathcal{F} if $\mathcal{F} \cup \{\gamma\}$ is a full forest and γ is safe (resp. unsafe) in $\mathcal{F} \cup \{\gamma\}$.
- A forest \mathcal{F} is safe if every $\gamma \in \mathcal{F}$ is safe in \mathcal{F} .

Loosely speaking, a subdiagram γ is thus unsafe if the diameter of γ (without its children) is much shorter than the distance between γ and its parent. In other words, children are unsafe if they are small and far away from their parents.

Example 5.14. Consider again the diagram Γ of the previous example, with the forest $\mathcal{F} = \{\gamma_1, \gamma_2\}$. Then for most edges $e = (e_-, e_+)$ we have $\text{scale}_{\mathbf{T}}^{\mathcal{F}}(e) = \mathbf{n}_{e_- \wedge e_+}$, except for the two cases

$$\text{scale}_{\mathbf{T}}^{\mathcal{F}}((5, 6)) = \mathbf{n}_{4 \wedge 6}, \quad \text{scale}_{\mathbf{T}}^{\mathcal{F}}((6, 1)) = \mathbf{n}_{3 \wedge 1}.$$

Indeed, the edges $(5, 6)$ and $(6, 1)$ are exactly those which are reconnected when applying $\mathfrak{R}_{\mathcal{F}}$. It follows that γ_1 is safe in \mathcal{F} if and only if

$$\mathbf{n}_{3 \wedge 4} \vee \mathbf{n}_{4 \wedge 6} \geq \mathbf{n}_{4 \wedge 5}, \quad (5.11)$$

and one checks that this is also the condition for γ_1 to be safe in $\{\gamma_1\}$ (that is, for $\{\gamma_1\}$ to be a safe forest). The condition for γ_2 to be safe in \mathcal{F} reads

$$\mathbf{n}_{2 \wedge 3} \vee \mathbf{n}_{3 \wedge 1} \geq \mathbf{n}_{3 \wedge 4} \wedge \mathbf{n}_{4 \wedge 6} \wedge \mathbf{n}_{3 \wedge 6}. \quad (5.12)$$

This time, it turns out that γ_2 is safe in the forest $\{\gamma_2\}$ if and only if

$$\mathbf{n}_{2 \wedge 3} \vee \mathbf{n}_{3 \wedge 1} \geq \mathbf{n}_{3 \wedge 4} \wedge \mathbf{n}_{4 \wedge 5} \wedge \mathbf{n}_{5 \wedge 6} \wedge \mathbf{n}_{3 \wedge 6},$$

because of the difference between $\hat{\mathcal{C}}_{\gamma_2}$ and $\hat{\mathcal{C}}_{\gamma_1} \hat{\mathcal{C}}_{\gamma_2}$. Note, however, that the ultrametricity of $\mathbf{n}_{\cdot \wedge \cdot}$ implies that $\mathbf{n}_{4 \wedge 6} \geq \mathbf{n}_{4 \wedge 5} \wedge \mathbf{n}_{5 \wedge 6}$, so that if γ_2 is safe in \mathcal{F} , then it is also safe in $\{\gamma_2\}$. ♣

This example shows that the property of being safe or unsafe may depend on the choice of forest \mathcal{F} . A crucial property, shown in [21, Lemma 3.6], is the following. If \mathcal{F}_s is a safe full forest, and

$$\mathcal{F}_u = \{\gamma \in \mathcal{G}_{\Gamma}^- : \gamma \text{ is unsafe for } \mathcal{F}_s\}, \quad (5.13)$$

then $\mathcal{F}_s \cup \mathcal{F}_u \in \mathcal{F}_{\Gamma}^-$ is a full forest, and every $\gamma \in \mathcal{F}_s$ is safe in $\mathcal{F}_s \cup \mathcal{F}_u$, while every $\gamma \in \mathcal{F}_u$ is unsafe in $\mathcal{F}_s \cup \mathcal{F}_u$. This implies in particular that any full forest $\mathcal{F} \subset \mathcal{G}_{\Gamma}^-$ has a unique decomposition $\mathcal{F} = \mathcal{F}_s \cup \mathcal{F}_u$, where \mathcal{F}_s is safe and \mathcal{F}_u is given by (5.13). Moreover, the properties of being safe/unsafe and the construction of \mathcal{F}_u depend only on the structure of the tree T , and not on the scale assignment \mathbf{n} defining \mathbf{T} .

The last step to construct the partition $\mathcal{P}_{\mathbf{T}}$ relies on the notion of forest interval, cf. [21, Section 3.1]. In general, forest intervals have two purposes: one of them is to deal with overlapping divergences, and the other one is to simplify the combinatorics when dealing with unsafe forests. In our model, we do not have overlapping divergences, but forest intervals are still useful to deal with unsafe forests. Moreover, they will allow us to obtain estimates on $c_e(\tau)$ that can be extended to cases with overlapping divergences.

Definition 5.15 (Forest interval). Let $\underline{\mathbb{M}} \subset \overline{\mathbb{M}}$ be two forests in \mathcal{F}_Γ^- . A forest interval is a subset $\mathbb{M} \subset \mathcal{F}_\Gamma^-$ defined by

$$\mathbb{M} = [\underline{\mathbb{M}}, \overline{\mathbb{M}}] = \{ \mathcal{F} \in \mathcal{F}_\Gamma^- : \underline{\mathbb{M}} \subset \mathcal{F} \subset \overline{\mathbb{M}} \}.$$

Alternatively, we have

$$\mathbb{M} = \{ \underline{\mathbb{M}} \cup \mathcal{F} : \mathcal{F} \subset \delta(\mathbb{M}) \},$$

where $\delta(\mathbb{M}) = \overline{\mathbb{M}} \setminus \underline{\mathbb{M}}$ is a forest such that $\delta(\mathbb{M}) \cap \underline{\mathbb{M}} = \emptyset$.

Given a Hepp sector $D_{\mathbf{T}}$, $\mathbf{T} = (T, \mathbf{n})$, we write $\mathcal{F}_\Gamma^{(s)}(T)$ for the set of all safe full forests in Γ . Then we have a partition

$$\mathcal{P}_{\mathbf{T}} = \{ [\mathcal{F}_s, \mathcal{F}_s \cup \mathcal{F}_u] : \mathcal{F}_s \in \mathcal{F}_\Gamma^{(s)}(T) \}, \quad (5.14)$$

where \mathcal{F}_u is defined by (5.13). The point of $\mathcal{P}_{\mathbf{T}}$ is that Zimmermann's forest formula (5.7) can be rewritten as

$$\mathcal{R}\Gamma = \mathcal{R}_{\mathcal{G}_\Gamma^-}\Gamma = \sum_{\mathbb{M}_i \in \mathcal{P}_{\mathbf{T}}} \hat{\mathcal{R}}_{\mathbb{M}_i}\Gamma, \quad (5.15)$$

where

$$\hat{\mathcal{R}}_{\mathbb{M}}\Gamma = \prod_{\gamma \in \delta(\mathbb{M})} (\text{id} - \hat{\mathcal{C}}_\gamma) \prod_{\bar{\gamma} \in \underline{\mathbb{M}}} (-\hat{\mathcal{C}}_{\bar{\gamma}})\Gamma.$$

Here, the factors $(\text{id} - \hat{\mathcal{C}}_\gamma)$ are interpreted as renormalising the subdiagrams in $\delta(\mathbb{M})$, and the factors $(-\hat{\mathcal{C}}_{\bar{\gamma}})$ as extracting those in $\underline{\mathbb{M}}$.

Example 5.16. Continuing with the previous example, there are 4 cases to be considered.

1. If $\{\gamma_1, \gamma_2\}$ is a safe forest, then we have seen that both $\{\gamma_1\}$ and $\{\gamma_2\}$ are safe. We thus have

$$\mathcal{F}_\Gamma^{(s)}(T) = \{ \emptyset, \{\gamma_1\}, \{\gamma_2\}, \{\gamma_1, \gamma_2\} \},$$

and the corresponding partition is simply

$$\mathcal{P}_{\mathbf{T}} = \{ [\emptyset, \emptyset], [\{\gamma_1\}, \{\gamma_1\}], [\{\gamma_2\}, \{\gamma_2\}], [\{\gamma_1, \gamma_2\}, \{\gamma_1, \gamma_2\}] \},$$

which is in fact identical with $\mathcal{F}_\Gamma^{(s)}(T)$. Thus (5.15) becomes

$$\mathcal{R}\Gamma = \Gamma - \hat{\mathcal{C}}_{\gamma_1}\Gamma - \hat{\mathcal{C}}_{\gamma_2}\Gamma + \hat{\mathcal{C}}_{\gamma_1}\hat{\mathcal{C}}_{\gamma_1}\Gamma, \quad (5.16)$$

which is indeed compatible with (5.7).

2. If $\{\gamma_1\}$ is safe, but γ_2 is unsafe for $\{\gamma_1\}$, then $\{\gamma_2\}$ may be safe or unsafe. In the former case, we have

$$\begin{aligned} \mathcal{F}_\Gamma^{(s)}(T) &= \{ \emptyset, \{\gamma_1\}, \{\gamma_2\} \}, \\ \mathcal{P}_{\mathbf{T}} &= \{ [\emptyset, \emptyset], [\{\gamma_1\}, \{\gamma_1, \gamma_2\}], [\{\gamma_2\}, \{\gamma_2\}] \}, \\ \mathcal{R}\Gamma &= \Gamma - (\text{id} - \hat{\mathcal{C}}_{\gamma_2})\hat{\mathcal{C}}_{\gamma_1}\Gamma - \hat{\mathcal{C}}_{\gamma_2}\Gamma \end{aligned} \quad (5.17)$$

while in the latter case,

$$\begin{aligned} \mathcal{F}_\Gamma^{(s)}(T) &= \{ \emptyset, \{\gamma_1\} \}, \\ \mathcal{P}_{\mathbf{T}} &= \{ [\{\gamma_1\}, \{\gamma_1, \gamma_2\}], [\emptyset, \{\gamma_2\}] \}, \\ \mathcal{R}\Gamma &= -(\text{id} - \hat{\mathcal{C}}_{\gamma_2})\hat{\mathcal{C}}_{\gamma_1}\Gamma + (\text{id} - \hat{\mathcal{C}}_{\gamma_2})\Gamma. \end{aligned} \quad (5.18)$$

Naturally, the expressions (5.17) and (5.18) are equivalent to (5.16), but the point is that the terms in each expression can be controlled individually.

3. If $\{\gamma_2\}$ is safe, but γ_1 is unsafe for $\{\gamma_2\}$, then $\{\gamma_1\}$ is unsafe. Hence

$$\begin{aligned}\mathcal{F}_\Gamma^{(s)}(T) &= \{\emptyset, \{\gamma_2\}\}, \\ \mathcal{P}_\Gamma &= \{[\emptyset, \{\gamma_1\}], [\{\gamma_2\}, \{\gamma_1, \gamma_2\}]\}, \\ \mathcal{R}\Gamma &= (\text{id} - \hat{\mathcal{C}}_{\gamma_1})\Gamma - (\text{id} - \hat{\mathcal{C}}_{\gamma_1})\hat{\mathcal{C}}_{\gamma_2}\Gamma.\end{aligned}$$

4. Finally, if both $\{\gamma_1\}$ and $\{\gamma_2\}$ are unsafe, then

$$\begin{aligned}\mathcal{F}_\Gamma^{(s)}(T) &= \{\emptyset\}, \\ \mathcal{P}_\Gamma &= \{[\emptyset, \{\gamma_1, \gamma_2\}]\}, \\ \mathcal{R}\Gamma &= (\text{id} - \hat{\mathcal{C}}_{\gamma_1})(\text{id} - \hat{\mathcal{C}}_{\gamma_2})\Gamma.\end{aligned}$$

♣

6 Bounds on $E(\tilde{\mathcal{A}}_-^E \tau)$

Combining Zimmermann's forest formula (5.15), our choice (5.14) of partition of \mathcal{F}_Γ^- , and the expression (4.12) for the expectation of a Feynman diagram, we obtain (cf. [21, Section 3.2])

$$E(\tilde{\mathcal{A}}_- \Gamma(\tau, P)) = - \sum_T \sum_{\mathcal{F}_s \in \mathcal{F}_\Gamma^{(s)}(T)} \sum_{\mathbf{n}} \int_{D_\Gamma} (\mathcal{W}^K \hat{\mathcal{R}}_{[\mathcal{F}_s, \mathcal{F}_s \cup \mathcal{F}_u]} \Gamma(\tau, P))(z) dz, \quad (6.1)$$

where the sums run over all binary trees T with $|\mathcal{V}|$ leaves, and all increasing node labels \mathbf{n} of T . Here

$$(\mathcal{W}^K \hat{\Gamma}_\varepsilon^n)(z) = \prod_{e \in \mathcal{E}} \partial^{e(e)} K_{t(e)}(z_{\sigma(e_+)} - z_{\sigma(e_-)}) \prod_{w \in \mathcal{V} \setminus v_*} (z_{\sigma(w)} - z_{\sigma(v_*)})^{n(w)}$$

corresponds to the integrand in (5.4) (recall that σ is the bijection between vertices and edges of $\mathfrak{K}_{\mathcal{F}_s} \Gamma$ and Γ), and v_* is by definition the first vertex in the component of $\mathfrak{K}_{\mathcal{F}_s} \Gamma$ containing w . An upper bound for (6.1) is given by

$$|E(\tilde{\mathcal{A}}_- \Gamma(\tau, P))| \leq \sum_T \sum_{\mathcal{F}_s \in \mathcal{F}_\Gamma^{(s)}(T)} \sum_{\mathbf{n}} \sup_{z \in D_\Gamma} |(\mathcal{W}^K \hat{\mathcal{R}}_{[\mathcal{F}_s, \mathcal{F}_s \cup \mathcal{F}_u]} \Gamma(\tau, P))(z)| C_0^{|\mathcal{V}_\Gamma|} \prod_{v \in T} 2^{-(\rho+d)\mathbf{n}_v}.$$

Here $|\mathcal{V}_\Gamma|$ is the number of vertices of the graph $\Gamma(\tau, P)$, C_0 is a constant depending only on the size of Λ through the definition 5.11 of Hepp sectors, and $C_0^{|\mathcal{V}_\Gamma|}$ times the product corresponds to the volume of the Hepp sector D_Γ . The aim of this section is to prove the following bound.

Proposition 6.1. *There exists a constant K_1 , depending only on the kernels K_t , such that for any safe forest $\mathcal{F}_s \in \mathcal{F}_\Gamma^{(s)}(T)$,*

$$\sum_{\mathbf{n}} \sup_{z \in D_\Gamma} |(\mathcal{W}^K \hat{\mathcal{R}}_{[\mathcal{F}_s, \mathcal{F}_s \cup \mathcal{F}_u]} \Gamma)(z)| \prod_{v \in T} 2^{-(\rho+d)\mathbf{n}_v} \leq \begin{cases} K_1^{|\mathcal{E}|} \varepsilon^{\deg(\Gamma)} [\log(\varepsilon^{-1})]^\zeta & \text{if } \deg \Gamma < 0, \\ K_1^{|\mathcal{E}|} [\log(\varepsilon^{-1})]^{1+\zeta} & \text{if } \deg \Gamma = 0, \end{cases}$$

where $\zeta \in \{0, 1\}$ is the number of children of Γ in \mathcal{F}_s having degree 0.

The existence of the exponent ζ has no influence on the main result, because $\zeta = 1$ occurs only for very few diagrams. The fact that $\zeta \in \{0, 1\}$ is shown in Lemma 6.11 below.

The proof of Proposition 6.1 follows rather closely the one given in [21, Section 3.2]. There are a few differences, due to the facts that we work with a non-Euclidean scaling, and that the

Feynman diagrams we consider have no legs. Owing to the special structure of the equations we consider, decorations of vertices and edges can be almost entirely avoided, they only arise in one estimate involving unstable forests (cf. Section 6.2).

We first need to quantify the singularity of the kernels. Similarly to [19, 21], we use the notation

$$\|K_t\| = \sup_{|k|_s \leq 2} \sup_z \frac{|\partial^k K_t(z)|}{\|z\|_s^{\deg t - |k|_s}}.$$

It then follows from [19, Lemma 10.7] that there exists a constant C_t such that

$$|K_t^\varepsilon(z)| \leq C_t \|K_t\| (\|z\|_s \vee \varepsilon)^{\deg t}$$

holds uniformly in $\varepsilon \in (0, 1]$. We will write K_0 for the maximal value of $C_t \|K_t\|$ for all kernels involved. Indeed t runs over a finite set of types, so that the maximum is finite.

A difference with [21] is that we have to deal explicitly with the fact that some kernels are regularised, and others are not. To indicate this, we attach to each edge $e \in \mathcal{E}$ an additional label $\text{reg}(e)$ with value 0 if e corresponds to a bare kernel, and with value 1 if it corresponds to a mollified kernel, and we write

$$\mathcal{E}^\circ = \{e \in \mathcal{E} : \text{reg}(e) = 0\}, \quad \mathcal{E}^\varepsilon = \{e \in \mathcal{E} : \text{reg}(e) = 1\}.$$

6.1 The case $\mathcal{F}_u = \emptyset$

As in [21], we start by discussing the case $\mathcal{F}_u = \emptyset$. First note that according to Remark 5.10, any diagram with nontrivial decorations obtained by applying an operator $\hat{\mathcal{C}}_\gamma$ has zero expectation. Therefore we may simply set

$$\hat{\mathcal{R}}_{[\mathcal{F}_s, \mathcal{F}_s \cup \mathcal{F}_u]} \Gamma = \prod_{\gamma \in \mathcal{F}_s} (-\hat{\mathcal{C}}_\gamma) \Gamma = (-1)^{|\mathcal{F}_s|} \mathfrak{R}_{\mathcal{F}_s} \Gamma.$$

Lemma 6.2. *For any inner node $v \in T$, define*

$$\begin{aligned} \eta^\circ(v) &= \rho + d + \sum_{e \in \mathcal{E}^\circ} \deg(e) \mathbf{1}_{e^\uparrow}(v), \\ \eta^\varepsilon(v) &= \sum_{e \in \mathcal{E}^\varepsilon} \deg(e) \mathbf{1}_{e^\uparrow}(v), \end{aligned} \tag{6.2}$$

where $e^\uparrow = \sigma(e_-) \wedge \sigma(e_+)$ is the last common ancestor of the vertices of e seen as an edge of Γ . Let

$$f(v, \mathbf{n}_v) = \eta^\circ(v) \mathbf{n}_v + \eta^\varepsilon(v) [\mathbf{n}_v \wedge n_\varepsilon], \tag{6.3}$$

where n_ε is the smallest integer such that $2^{-n_\varepsilon} \leq \varepsilon$. Then there exists a constant $\bar{K}_0 \geq K_0$ such that

$$\sum_{\mathbf{n}} \sup_{z \in D_{\mathbf{T}}} |(\mathscr{W}^K \mathfrak{R}_{\mathcal{F}_s} \Gamma)(z)| \prod_{v \in T} 2^{-(\rho+d)\mathbf{n}_v} \leq \bar{K}_0^{|\mathcal{E}|} C^{-\deg \Gamma} \sum_{\mathbf{n}} \prod_{v \in T} 2^{-f(v, \mathbf{n}_v)}, \tag{6.4}$$

where C is the constant appearing in the relation (5.8) characterising Hepp sectors.

PROOF: The definitions of Hepp sectors and of K_0 imply that uniformly over $z \in D_{\mathbf{T}}$, one has

$$|(\mathscr{W}^K \mathfrak{R}_{\mathcal{F}_s} \Gamma)(z)| \leq K_0^{|\mathcal{E}|} C^{-\sum_{e \in \mathcal{E}} \deg(e)} \prod_{e \in \mathcal{E}^\circ} 2^{-\mathbf{n}(e^\uparrow) \deg(e)} \prod_{e \in \mathcal{E}^\varepsilon} 2^{-\mathbf{n}(e^\uparrow) \wedge n_\varepsilon \deg(e)}.$$

Since only edges of negative degree give an unbounded contribution, the term $C^{-\sum_{e \in \mathcal{E}} \deg(e)}$ can be bounded by $C^{-\deg \Gamma}$, enlarging if necessary the value of K_0 . Now it suffices to observe that

$$\begin{aligned} -\log_2 \prod_{e \in \mathcal{E}^\circ} 2^{-\mathbf{n}(e^\uparrow) \deg(e)} &= \sum_{v \in T} \sum_{e \in \mathcal{E}^\circ} \deg(e) \mathbf{1}_{e^\uparrow}(v) \mathbf{n}_v = \sum_{v \in T} [\eta^\circ(v) - \rho - d] \mathbf{n}_v, \\ -\log_2 \prod_{e \in \mathcal{E}^\varepsilon} 2^{-\mathbf{n}(e^\uparrow) \wedge n_\varepsilon \deg(e)} &= \sum_{v \in T} \sum_{e \in \mathcal{E}^\varepsilon} \deg(e) \mathbf{1}_{e^\uparrow}(v) [\mathbf{n}_v \wedge n_\varepsilon] = \sum_{v \in T} \eta^\varepsilon(v) [\mathbf{n}_v \wedge n_\varepsilon]. \end{aligned}$$

Substituting in the left-hand side of (6.4) yields the result. \square

Our aim is now to bound the quantity

$$\sum_{\mathbf{n}} \prod_{v \in T} 2^{-f(v, \mathbf{n}_v)} \quad (6.5)$$

by a recursive argument, starting from the leaves of T . The argument is somewhat similar to the one given in [25, Lemma A.10], but with an explicit control of the bound's dependence on the properties of the graph Γ .

Given an inner node v of T , we say that w is an *offspring* of v if $w > v$, and there exists no \bar{w} with $w > \bar{w} > v$ (we do not use the term child to avoid confusion with the notion of child in \mathcal{F}_s). We denote the set of offspring of v by $\mathcal{O}(v)$. Note that since T is a binary tree, $\mathcal{O}(v)$ has at most two elements.

For any $v \in T$ and $\mathbf{n}_v \in \mathbb{N}_0$, we introduce the notation

$$\mathcal{S}_v(\mathbf{n}_v) = \sum_{\bar{\mathbf{n}} \geq \mathbf{n}_v} \prod_{w > v} 2^{-f(w, \bar{\mathbf{n}}_w)},$$

where the sum runs over all increasing node decorations $\bar{\mathbf{n}}$ of $\{w : w > v\}$. We can rewrite this as

$$\mathcal{S}_v(\mathbf{n}_v) = \prod_{w_i \in \mathcal{O}(v)} \widehat{\mathcal{S}}_{w_i}(\mathbf{n}_v), \quad (6.6)$$

where

$$\widehat{\mathcal{S}}_w(\mathbf{n}_v) = \sum_{\bar{\mathbf{n}} \geq \mathbf{n}_v} \prod_{\bar{w} \geq w} 2^{-f(\bar{w}, \bar{\mathbf{n}}_{\bar{w}})} = \sum_{\mathbf{n}_w \geq \mathbf{n}_v} 2^{-f(w, \mathbf{n}_w)} \mathcal{S}_w(\mathbf{n}_w). \quad (6.7)$$

Then (6.5) is equal to $\widehat{\mathcal{S}}_\emptyset(0)$, where \emptyset denotes the root of T . Our plan is now to compute the quantities $\widehat{\mathcal{S}}_w(\mathbf{n}_v)$ inductively, starting from the leaves of T . In order to initialise the induction, we set $\widehat{\mathcal{S}}_\ell(\mathbf{n}_v) = 1$ on the leaves ℓ of T . (Equivalently, one could set $\mathcal{S}_v(\mathbf{n}_v) = 1$ for all nodes v of T with no offspring.) Then we have the following recursive bound.

Lemma 6.3. *Let v be an inner node of T . Assume that there exist non-negative functions α, β, γ and $\bar{\alpha}, \bar{\beta}$ such that the relation*

$$\widehat{\mathcal{S}}_w(\mathbf{n}_v) \lesssim \begin{cases} 2^{\alpha(w)n_\varepsilon} 2^{-\beta(w)\mathbf{n}_v} (n_\varepsilon - \mathbf{n}_v)^{\gamma(w)} & \text{if } \mathbf{n}_v < n_\varepsilon \\ 2^{\bar{\alpha}(w)n_\varepsilon} 2^{-\bar{\beta}(w)\mathbf{n}_v} & \text{if } \mathbf{n}_v \geq n_\varepsilon \end{cases} \quad (6.8)$$

holds for all $w \in \mathcal{O}(v)$. Assume furthermore that one has

$$\eta^\circ(v) + \sum_{w_i \in \mathcal{O}(v)} \bar{\beta}(w_i) > 0, \quad (6.9)$$

$$\alpha(w_i) - \beta(w_i) \geq \bar{\alpha}(w_i) - \bar{\beta}(w_i) \quad \forall w_i \in \mathcal{O}(v), \quad (6.10)$$

and define

$$\eta(v) = \eta^\circ(v) + \eta^\varepsilon(v), \quad \lambda(v) = \eta(v) + \sum_{w_i \in \mathcal{O}(v)} \beta(w_i). \quad (6.11)$$

Let u be the parent of v , that is, the unique u such that $v \in \mathcal{O}(u)$. Then $\widehat{\mathcal{S}}_v(\mathbf{n}_u)$ satisfies the analogue of (6.8), with exponents given as follows:

$$\alpha(v) = \begin{cases} \sum_{w_i \in \mathcal{O}(v)} \alpha(w_i) - \lambda(v) & \text{if } \lambda(v) < 0, \\ \sum_{w_i \in \mathcal{O}(v)} \alpha(w_i) & \text{otherwise,} \end{cases} \quad (6.12)$$

while

$$\beta(v) = \begin{cases} 0 & \text{if } \lambda(v) \leq 0, \\ \lambda(v) & \text{otherwise,} \end{cases} \quad (6.13)$$

and

$$\gamma(v) = \begin{cases} 0 & \text{if } \lambda(v) < 0, \\ \sum_{w_i \in \mathcal{O}(v)} \gamma(w_i) + 1 & \text{if } \lambda(v) = 0, \\ \sum_{w_i \in \mathcal{O}(v)} \gamma(w_i) & \text{otherwise.} \end{cases} \quad (6.14)$$

Finally, we have

$$\begin{aligned} \bar{\alpha}(v) &= \sum_{w_i \in \mathcal{O}(v)} \bar{\alpha}(w_i) - \eta^\varepsilon(v), \\ \bar{\beta}(v) &= \sum_{w_i \in \mathcal{O}(v)} \bar{\beta}(w_i) + \eta^\circ(v). \end{aligned} \quad (6.15)$$

PROOF: Combining (6.6) and (6.7), we obtain

$$\widehat{\mathcal{S}}_v(\mathbf{n}_u) = \sum_{\mathbf{n}_v \geq \mathbf{n}_u} 2^{-f(v, \mathbf{n}_v)} \prod_{w_i \in \mathcal{O}(v)} \widehat{\mathcal{S}}_{w_i}(\mathbf{n}_v).$$

Consider first the case $\mathbf{n}_u \geq n_\varepsilon$. Using (6.8) and the definition (6.3) of $f(v, \mathbf{n}_v)$, we get

$$\widehat{\mathcal{S}}_v(\mathbf{n}_u) \lesssim 2^{\bar{\alpha}(v)n_\varepsilon} \sum_{\mathbf{n}_v \geq \mathbf{n}_u} 2^{-\bar{\beta}(v)\mathbf{n}_v}$$

with $\bar{\alpha}(v)$ and $\bar{\beta}(v)$ given by (6.15). By Condition (6.9), one can sum the geometric series, yielding the claimed bound.

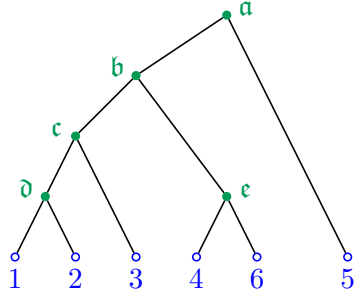
For $\mathbf{n}_u < n_\varepsilon$, we decompose the sum into two parts, yielding

$$\widehat{\mathcal{S}}_v(\mathbf{n}_u) \lesssim 2^{\sum_i \alpha(w_i)n_\varepsilon} \sum_{\mathbf{n}_v = \mathbf{n}_u}^{n_\varepsilon - 1} 2^{-\lambda(v)\mathbf{n}_v} (n_\varepsilon - \mathbf{n}_v)^{\sum_i \gamma(w_i)} + 2^{\bar{\alpha}(v)n_\varepsilon} \sum_{\mathbf{n}_v \geq n_\varepsilon} 2^{-\bar{\beta}(v)\mathbf{n}_v}.$$

The first sum can be evaluated using the bound

$$\sum_{n=n_0}^{N-1} (N-n)^\gamma 2^{-\eta n} \lesssim \begin{cases} (N-n_0)^\gamma 2^{-\eta n_0} & \text{if } \eta > 0, \\ (N-n_0)^{\gamma+1} & \text{if } \eta = 0, \\ 2^{-\eta N} & \text{if } \eta < 0, \end{cases}$$

valid for any $n_0 < N \in \mathbb{N}$, $\eta \in \mathbb{R}$ and $\gamma > 0$. The second sum has order $2^{(\bar{\alpha}(v) - \bar{\beta}(v))n_\varepsilon}$, and is negligible thanks to Condition (6.10). \square



e	$\sigma(e)$	e^\uparrow	$\deg(e)$	$\text{reg}(e)$
(1, 2)	(1, 2)	d	-1	1
(1, 2)	(1, 2)	d	-2	1
(2, 3)	(2, 3)	c	-3	0
(3, 1)	(6, 1)	c	-3	0
(3, 4)	(3, 4)	b	-3	0
(4, 6)	(5, 6)	e	-3	0
(3, 6)	(3, 6)	b	-2	1
(4, 5)	(4, 5)	a	-3	0
(4, 5)	(4, 5)	a	-2	1

FIGURE 4: A tree T defining a Hepp sector D_T for the diagram $\mathfrak{K}_{\mathcal{F}_s} \Gamma$ in (5.10). The table shows, for each edge e , its image $\sigma(e) = (\sigma(e)_-, \sigma(e)_+)$, the ancestor e^\uparrow , the degree of e measured in units of $\frac{d}{3}$ in the limit $\rho \searrow \rho_c$, and the index showing whether the edge has been mollified. Since there can be multiple edges between two given vertices, they have been colour-coded according to their type.

v	$\eta^\circ(v)$	$\eta^\varepsilon(v)$	$\eta(v)$	$\eta_{\geq}(v)$	$\lambda(v)$	$\alpha(v)$	$\beta(v)$	$\gamma(v)$	$\bar{\alpha}(v)$	$\bar{\beta}(v)$
e	1	0	1	1	1	0	1	0	0	1
d	4	-3	1	1	1	0	1	0	3	4
c	-2	0	-2	-1	-1	1	0	0	3	2
b	1	-2	-1	-1	0	1	0	1	5	4
a	1	-2	-1	-2	-1	2	0	0	7	5

TABLE 1: Coefficients appearing in the recursive computation described in Lemma 6.3, in the case of the Hepp tree T given in Figure 4. The first four exponents are defined in (6.2), (6.11) and (6.16). All coefficients are shown in units of $\frac{d}{3}$ and in the limit $\rho \searrow \rho_c$.

Example 6.4. Consider again the diagram of Example 5.12, with the forest $\mathcal{F} = \{\gamma_1, \gamma_2\}$. Consider a Hepp sector D_T such that T has the structure given in Figure 4. The forest \mathcal{F} is safe according to (5.11) and (5.12). Table 1 shows the values of the different exponents, computed iteratively starting from the leaves of the tree T , in the limit $\rho \searrow \rho_c$. In particular, we obtain

$$\sum_{\mathbf{n}} \prod_{v \in T} 2^{-f(v, \mathbf{n}_v)} = \widehat{\mathcal{S}}_a(0) \lesssim 2^{\alpha(a)n_\varepsilon} = 2^{2dn_\varepsilon/3} \leq \varepsilon^{-2d/3},$$

which is indeed equal to $\varepsilon^{\deg \Gamma}$ in that limit. A similar computation can be made for any $\rho > \rho_c$. ♣

Let us now examine the inductive bounds in more detail. The initialisation is made by setting all functions $\alpha, \beta, \gamma, \bar{\alpha}$ and $\bar{\beta}$ equal to zero on the leaves of T . Combining the recursive relations (6.12) and (6.13), we obtain

$$\alpha(v) - \beta(v) = \sum_{w_i \in \mathcal{O}(v)} (\alpha(w_i) - \beta(w_i)) - \eta(v).$$

Together with the initial values on the leaves, this yields

$$\alpha(v) - \beta(v) = - \sum_{w \geq v} \eta(w) =: -\eta_{\geq}(v) \tag{6.16}$$

for all nodes v of T . In the same way, (6.15) yields

$$\bar{\alpha}(v) - \bar{\beta}(v) = -\eta_{\geq}(v).$$

This shows in particular that Condition (6.10) is always satisfied. Regarding Condition (6.9), we observe that (6.15) implies

$$\bar{\beta}(v) = \sum_{w \geq v} \eta^\circ(w) =: \eta_{\geq}^\circ(v).$$

We thus have to show that $\eta_{\geq}^\circ(v)$ is strictly positive on all inner vertices v if T , and to bound $\eta_{\geq}^\circ(v)$ below in order to control (6.5). To do this, we will import some further notations from [21]. For $\gamma \in \mathcal{F}_s \cup \{\Gamma\}$, we write $\mathfrak{K}(\gamma) = (\mathcal{V}_\gamma, \mathcal{E}_\gamma)$ for the subgraph of $\mathfrak{K}_{\mathcal{F}_s} \Gamma$ with edge set $\mathcal{E}_\gamma = \sigma^{-1}(\mathcal{E}(\gamma \setminus \mathcal{C}(\gamma)))$, where $\mathcal{C}(\gamma)$ denotes the set of children of γ in \mathcal{F}_s . Given an inner vertex $v \in T$, we let $\Gamma_0 = \Gamma_0(v) = (\mathcal{V}_0, \mathcal{E}_0)$ be the subgraph of $\mathfrak{K}_{\mathcal{F}_s} \Gamma$ containing all vertices $w \in \mathcal{V}$ such that $\sigma(w) \geq v$. Note that this implies

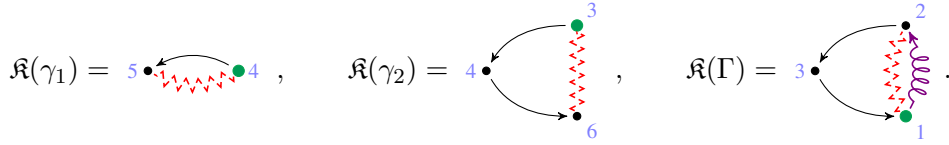
$$e \in \mathcal{E}_0(v) \Leftrightarrow e^\uparrow \geq v.$$

In addition, we have

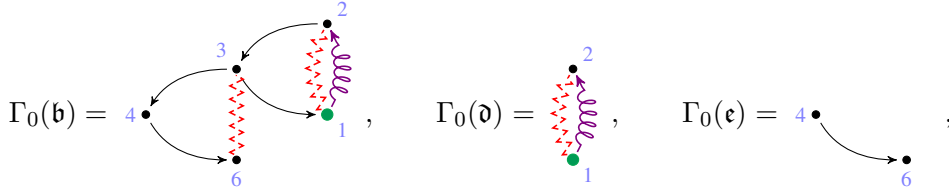
$$\text{scale}_{\mathbf{T}^s}(e) > \text{scale}_{\mathbf{T}^s}(\bar{e}),$$

and thus $e^\uparrow > \bar{e}^\uparrow$, for all $e \in \mathcal{E}_0$ and all \bar{e} adjacent to Γ_0 in $\mathfrak{K}_{\mathcal{F}_s} \Gamma$.

Example 6.5. Continuing with Example 6.4, we have



Examples of subgraphs $\Gamma_0(v)$ are



while $\Gamma_0(\epsilon) = \mathfrak{K}(\Gamma)$ and $\Gamma_0(\mathfrak{a}) = \mathfrak{K}_{\mathcal{F}_s} \Gamma$ is the diagram given in (5.10). ♣

Lemma 6.6. *Let v be an inner vertex of T such that $\Gamma_0(v)$ is non-empty. Then the quantity $\eta_{\geq}(v)$ satisfies the following properties :*

1. $\eta_{\geq}(v) = \deg(\Gamma)$ if $v = \emptyset$ is the root of T , and $\eta_{\geq}(v) \geq \deg(\Gamma)$ otherwise;
2. if $v > \emptyset$, then $\eta_{\geq}(v) = \deg(\Gamma)$ happens only if Γ has at least one child $\gamma \in \mathcal{C}(\Gamma)$ satisfying $\deg(\gamma) = 0$, and $\Gamma_0(v) = \bigcup_{\bar{\gamma}} \mathfrak{K}(\bar{\gamma})$, where the union runs over all $\bar{\gamma}$ which are not descendants of a child with vanishing degree;
3. if $\mathcal{O}(v) = \{w_1, w_2\}$, then there exists at least one $i \in \{1, 2\}$ such that $\eta_{\geq}(w) > 0$ for all $w \geq w_i$.

If, furthermore, Γ has at least one regularised edge, then there exists a constant $\kappa > 0$ such that

$$\eta_{\geq}^\circ(v) = \sum_{w \geq v} \eta^\circ(w) \geq \kappa. \quad (6.17)$$

PROOF: Since T is a tree, $\{w \geq v\}$ has $|\mathcal{V}_0| - 1$ elements, so that we can write

$$\eta_{\geq}(v) = (\rho + d)(|\mathcal{V}_0| - 1) + \sum_{e \in \mathcal{E} \cap \mathcal{E}_0} \deg(e).$$

By construction, the $\mathfrak{K}(\gamma)$ have disjoint edge sets, and two $\mathfrak{K}(\gamma)$ can share at most one vertex. We can thus decompose

$$\eta_{\geq}(v) = \sum_{\gamma \in \mathcal{F}_s \cup \{\Gamma\}} \eta_{\geq, \gamma}(v), \quad (6.18)$$

where

$$\eta_{\geq, \gamma}(v) = (\rho + d)(|\mathcal{V}_0 \cap \mathcal{V}_\gamma| - 1) + \sum_{e \in \mathcal{E}_\gamma \cap \mathcal{E}_0} \deg(e).$$

As in [21], we say that $\gamma \in \mathcal{F}_s \cup \{\Gamma\}$ is

- *full* if $\mathcal{E}_\gamma \cap \mathcal{E}_0 = \mathcal{E}_\gamma$;
- *empty* if $\mathcal{E}_\gamma \cap \mathcal{E}_0 = \emptyset$;
- *normal* in all other cases.

By [21, Lemma 3.7], a full γ cannot have an empty parent, and

$$\eta_{\geq, \gamma}(v) = \begin{cases} \deg(\gamma) - \sum_{\bar{\gamma} \in \mathcal{C}(\gamma)} \deg(\bar{\gamma}) & \text{if } \gamma \text{ is full,} \\ 0 & \text{if } \gamma \text{ is empty,} \\ \deg(\hat{\gamma}) - \sum_{\bar{\gamma} \in \mathcal{C}_*(\gamma)} \deg(\bar{\gamma}) & \text{if } \gamma \text{ is normal,} \end{cases} \quad (6.19)$$

where $\mathcal{C}_*(\gamma)$ is the set of children $\bar{\gamma}$ of γ such that $\mathfrak{K}(\bar{\gamma})$ shares a vertex with $\Gamma_0(v)$, and $\hat{\gamma}$ is the subdiagram of Γ with edge set $\sigma(\mathcal{E}_\gamma \cap \mathcal{E}_0) \cup \bigcup_{\bar{\gamma} \in \mathcal{C}_*(\gamma)} \mathcal{E}(\bar{\gamma})$. The fact that γ is safe implies that $\deg(\hat{\gamma}) > 0$, and is also used to prove the absence of empty parent.

The result follows by considering all possibilities for the types of the subgraphs γ .

- A first case occurs when no $\gamma \in \mathcal{F}_s \cup \{\Gamma\}$ is full. Since Γ_0 is not empty, the γ cannot all be empty, so that $\eta_{\geq}(v)$ is a non-empty sum of strictly positive terms. Therefore, $\eta_{\geq}(v) > 0$.
- A second case occurs when Γ is not full, but there exists at least one subgraph $\gamma \subsetneq \Gamma$ which is full. Since the parent of γ is not empty, the negative term $\deg(\gamma)$ is compensated by the corresponding term stemming from its parent. Since Γ is not full, there must exist a full subgraph γ whose parent is normal. Since the inequality for normal subgraphs is strict, we have again $\eta_{\geq}(v) > 0$.
- It remains to consider the case where Γ is full (which does not occur in [21]). The case of all $\gamma \subset \Gamma$ also being full can only occur when $v = \emptyset$ (because only in that case is $\Gamma_0(v)$ equal to $\mathfrak{K}_{\mathcal{F}_s}(\gamma)$), and leads to the sum being equal to $\deg(\Gamma)$.

Consider next the case when there is no normal subgraph. Then all subgraphs are full or empty. Since a full subgraph cannot have an empty parent, we obtain $\eta_{\geq}(v) = \deg(\Gamma) - \sum_i \deg(\gamma_i)$, where the γ_i are all empty subgraphs with a full parent. This shows in particular that $\eta_{\geq}(v) \geq \deg(\Gamma)$ if v is not the root. Equality can only hold when all γ_i have zero degree. These γ_i must all be children of Γ , since Lemma 5.7 and Remark 5.4 imply that the degree of strict subdiagrams, which all arise from almost full trees, is strictly increasing in terms of their number of edges. In addition, all $\gamma \subset \gamma_i$ are empty, so that the second property follows.

The only remaining case occurs when there exists a $\gamma \subsetneq \Gamma$ which is normal. Then one obtains $\eta_{\geq}(v) \geq \deg(\Gamma) - \deg(\gamma) + \deg(\hat{\gamma}) > \deg(\Gamma)$.

To prove the third property of η_{\geq} , we note that since the edge sets $\mathcal{E}_0(w_1)$ and $\mathcal{E}_0(w_2)$ are disjoint, Γ cannot be full for both $\Gamma_0(w_1)$ and $\Gamma_0(w_2)$. Since $\mathcal{E}_0(w) \subset \mathcal{E}(w_i)$ for all $w \geq w_i$, there is at least one i such that Γ is not full for any $\Gamma_0(w)$ such that $w \geq w_i$. Therefore, $\eta_{\geq}(w) > 0$ for these w .

It remains to prove (6.17). Here we note that $\eta_{\geq}^{\circ}(v)$ can be written as the sum of $\eta_{\geq, \gamma}^{\circ}(v)$, where

$$\eta_{\geq, \gamma}^{\circ}(v) = (\rho + d)(|\mathcal{V}_0 \cap \mathcal{V}_{\gamma}| - 1) + \sum_{e \in \mathcal{E}^{\circ} \cap \mathcal{E}_{\gamma}} \deg(e).$$

We define full, empty and normal subgraphs as above, but with \mathcal{E}_0 replaced by $\mathcal{E}_0 \cap \mathcal{E}^{\circ}$. Since Γ admits at least one regularised edge, it cannot be full. The same argument as above thus shows that $\eta_{\geq}^{\circ}(v)$ is strictly positive. \square

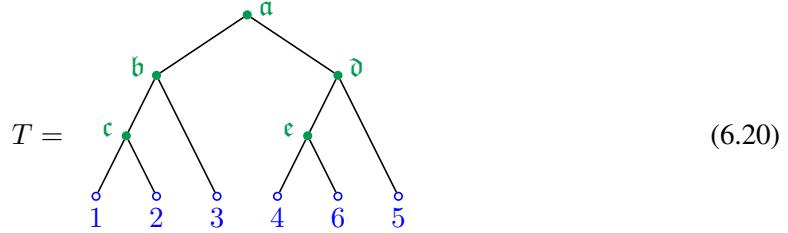
Remark 6.7. It follows from Lemma 5.7 that for any subtree $\bar{\tau} \subsetneq \tau$ of negative degree, τ has at least two leaves that do not belong to $\bar{\tau}$. As a consequence, for any divergent subdiagram $\gamma \subsetneq \Gamma$, $\Gamma \setminus \gamma$ admits at least one regularised edge. Therefore, the assumption that $\mathfrak{R}(\Gamma)$ admit at least one regularised edge is indeed satisfied in our situation. \diamond

Example 6.8. We illustrate the lemma and the notions of full, normal and empty subgraphs used in its proof on Example 6.5:

- for $\Gamma_0(\mathfrak{a})$, all $\gamma \in \mathcal{F}_s \cup \{\Gamma\}$ are full;
- for $\Gamma_0(\mathfrak{b})$, Γ and γ_2 are full, while γ_1 is empty;
- for $\Gamma_0(\mathfrak{c})$, Γ is full, while γ_2 and γ_1 are empty;
- for $\Gamma_0(\mathfrak{d})$, Γ is normal, and the other graphs are empty;
- for $\Gamma_0(\mathfrak{e})$, γ_2 is normal, and the other graphs are empty.

The first three cases lead to $\eta_{\geq}(v) \leq 0$, since there is no normal subgraph. The last two cases lead to $\eta_{\geq}(v) > 0$, since there is no full subgraph (compare with Table 1).

Consider now the case where the Hepp tree is of the form



The forest $\mathcal{F} = \{\gamma_1, \gamma_2\}$ is again safe, and we have in particular $\Gamma_0(\mathfrak{b}) = \mathfrak{R}(\Gamma)$. This shows that for $\Gamma_0(\mathfrak{b})$, Γ is full, and γ_1 and γ_2 are empty. If $\rho = \frac{2}{5}d$, then $\deg(\Gamma) = \deg(\gamma_2) = 0$, and we are in a situation where Property 2. of Lemma 6.6 applies: we have $\eta_{\geq}(\mathfrak{a}) = \eta_{\geq}(\mathfrak{b}) = 0$, while $\eta_{\geq}(v) > 0$ for $v \in \{\mathfrak{c}, \mathfrak{d}, \mathfrak{e}\}$. \clubsuit

Corollary 6.9. *There exists a constant K_1 , depending only on \bar{K}_0 and d , such that*

$$\sum_{\mathfrak{n}} \sup_{z \in D_{\mathfrak{T}}} |(\mathcal{W}^K \mathfrak{R}_{\mathcal{F}_s} \Gamma)(z)| \prod_{v \in T} 2^{-(\rho+d)\mathfrak{n}_v} \leq \begin{cases} K_1^{|\mathcal{E}|} \varepsilon^{\deg(\Gamma)} [\log(\varepsilon^{-1})]^{\zeta} & \text{if } \deg \Gamma < 0, \\ K_1^{|\mathcal{E}|} [\log(\varepsilon^{-1})]^{1+\zeta} & \text{if } \deg \Gamma = 0, \end{cases} \quad (6.21)$$

where ζ is the number of children of Γ in \mathcal{F}_s having degree 0.

PROOF: The lower bound (6.17) on η_{\geq}° shows that Condition (6.9) is satisfied, so that Lemma 6.3 applies for all inner vertices of T . Combining (6.16) with the induction relations (6.12) and (6.13), we obtain

$$\alpha(v) = \max \left\{ -\eta_{\geq}(v), \sum_{w_i \in \mathcal{O}(v)} \alpha(w_i) \right\}. \quad (6.22)$$

We claim that in fact, we have

$$\alpha(v) \leq \max(\{0\} \cup \{-\eta_{\geq}(w) : w \geq v\}) . \quad (6.23)$$

This relation is clearly true if v has no offspring. We now proceed by induction, and assume that (6.23) holds for all $w_i \in \mathcal{O}(v)$. If all $\alpha(w_i)$ vanish, (6.23) trivially holds. Property 3. of Lemma 6.6 implies that at most one of the $\alpha(w_i)$, say $\alpha(w_1)$, can be strictly positive. Indeed, if v has two offspring w_1 and w_2 , then the property implies that there is at most one offspring, say w_2 , such that $\eta_{\geq}(w) > 0$ for all $w \geq w_2$. But then $\alpha(w_2) = 0$ by the induction assumption. Therefore, $\alpha(v) = \max\{-\eta_{\geq}(v), \alpha(w_1)\}$, and (6.23) follows from the induction assumption.

The result is then a consequence of the fact that (6.5) is bounded by

$$\widehat{\mathcal{S}}_{\emptyset}(0) \lesssim 2^{\alpha(\emptyset)n_\varepsilon} n_\varepsilon^{\gamma(\emptyset)} .$$

Indeed, we have $\alpha(\emptyset) = -\deg(\Gamma)$, as a consequence of Property 1. of Lemma 6.6, which implies

$$\max\{-\eta_{\geq}(w) : w \geq \emptyset\} = -\eta_{\geq}(\emptyset) = -\deg(\Gamma) .$$

Therefore (6.23) yields $\alpha(\emptyset) \leq -\deg(\Gamma)$, but by (6.22) this is actually an equality, because (6.22) implies that $\alpha(\emptyset) \geq -\deg(\Gamma)$. Since $\deg(\Gamma)$ is bounded below by a constant depending only on d , the term $C^{-\deg \Gamma}$ in (6.4) can be incorporated into K_1 .

It remains to determine $\gamma(\emptyset)$. We first note that (6.16) implies

$$\lambda(v) = \eta_{\geq}(v) + \sum_{w_i \in \mathcal{O}(v)} \alpha(w_i) .$$

In the case $\deg(\Gamma) = 0$, we have $\alpha(v) = 0$, and thus $\lambda(v) = \eta_{\geq}(v)$ for all $v \in T$. By Property 3. of Lemma 6.6, at most one of the offspring of v , say w_1 , satisfies $\eta_{\geq}(w_1) = 0$. Therefore, there exists at most one path $(w_0 = \emptyset, w_1, \dots, w_\zeta)$ starting at the root, such that $\eta_{\geq}(w_i) = 0$, and thus $\lambda(w_i) = 0$, for each w_i in the path. On such a path, (6.14) shows that $\gamma(v)$ increases by 1 at each step. Extending this path to any leaf, and using $\gamma = 0$ as initial value on the leaf, we obtain that $\gamma(\emptyset) = \zeta$. By Property 2. of Lemma 6.6, each $\Gamma_0(w_i)$ is of the form $\bigcup_{\bar{\gamma}_i} \mathfrak{R}(\bar{\gamma}_i)$, where the $\bar{\gamma}_i$ are *not* descendants of a given $\gamma_i \in \mathcal{O}(\Gamma)$ with vanishing degree. Since $\Gamma_0(w_{i+1}) \subsetneq \Gamma_0(w_i)$ for each i , ζ is bounded by the number of these γ_i .

In the case $\deg(\Gamma) < 0$, consider the longest sequence $(w_0 = \emptyset, w_1, \dots, w_{\zeta'})$ such that $w_{i+1} \in \mathcal{O}(w_i)$ and $\eta_{\geq}(w_i) \leq 0$ for each i . Then Property 3. of Lemma 6.6 implies that $\eta_{\geq}(v) > 0$ for all other $v \in T$, which yields $\alpha(v) = 0$, $\lambda(v) > 0$ and thus $\gamma(v) = 0$ for those v . For the w_i , we get the induction relations

$$\begin{aligned} \lambda(w_i) &= \eta_{\geq}(w_i) + \alpha(w_{i+1}) , \\ \alpha(w_i) &= \max\{-\eta_{\geq}(w_i), \alpha(w_{i+1})\} \geq \alpha(w_{i+1}) , \\ \gamma(w_i) &= \begin{cases} 0 & \text{if } \lambda(w_i) < 0 , \\ \gamma(w_{i+1}) + 1 & \text{if } \lambda(w_i) = 0 , \\ \gamma(w_{i+1}) & \text{if } \lambda(w_i) > 0 , \end{cases} \end{aligned}$$

with the convention that $\alpha(w_{\zeta'+1}) = \gamma(w_{\zeta'+1}) = 0$. Note that we have the implications

$$\gamma(w_i) \neq 0 \quad \Rightarrow \quad \lambda(w_i) \geq 0 \quad \Leftrightarrow \quad \alpha(w_{i+1}) \geq -\eta_{\geq}(w_i) \quad \Leftrightarrow \quad \alpha(w_i) = \alpha(w_{i+1}) .$$

In addition, γ is incremented only if $\lambda(w_i) = 0$, which happens if and only if $\alpha(w_i) = \alpha(w_{i+1}) = -\eta_{\geq}(w_i)$. It follows that $\gamma(\emptyset)$ is equal to the length $\zeta \leq \zeta'$ of the longest sequence $(w_0, \dots, w_{\zeta-1})$ such that $\eta_{\geq}(w_i) = \deg(\Gamma)$ for all i . Property 2. of Lemma 6.6 again implies that ζ is bounded by the number of children of Γ having degree 0. \square

Example 6.10. Consider again the Hepp sector with tree T as in (6.20) in Example 6.8. As we have seen, when $\rho = \frac{2}{5}$, one has $\deg(\Gamma) = \deg(\gamma_2) = 0$. Therefore, the bound (6.21) has order $(\log(\varepsilon^{-1}))^2$. \clubsuit

Though we find that nontrivial powers of $\log(\varepsilon^{-1})$ can occur, the following result shows that in our situation, these powers cannot exceed the value 2.

Lemma 6.11. *If $\Gamma = \Gamma(\tau, P)$ and τ is an almost full binary tree, then Γ cannot have any children of degree 0, i.e., $\zeta = 0$. If $\Gamma = \Gamma(\tau, P)$ and τ is a full binary tree, then Γ can have at most one child of degree 0, i.e., $\zeta \leq 1$.*

PROOF: Let τ be almost full with $2m + 1$ edges, and assume that Γ contains a subdiagram γ with $\deg(\gamma) = 0$. By Lemma 5.7, γ is of the form $\Gamma(\bar{\tau}, \bar{P})$ with $\bar{\tau}$ an almost full binary tree having $2\bar{m} + 1 < 2m + 1$ edges. By Remark 5.4, we necessarily have $\deg(\gamma) < \deg(\Gamma)$, so that $\deg(\gamma) = 0$ would imply $\deg(\Gamma) > 0$, which is not permitted.

If τ is full with $2m$ edges, then any divergent subdiagram γ results from an almost full tree $\bar{\tau}$ with $2\bar{m} + 1 < 2m$ edges. By Remark 5.4, the condition $\deg(\Gamma) \leq 0 = \deg(\gamma)$ yields $m \leq 2\bar{m} + 1$. If Γ contains ζ non-overlapping divergent subdiagrams of degree 0, they must all have the same number of edges, and we obtain $\zeta(2\bar{m} + 1) < 2m \leq 2(2\bar{m} + 1)$, yielding $\zeta < 2$. \square

6.2 The case $\mathcal{F}_u \neq \emptyset$

We turn now to the case $\mathcal{F}_u \neq \emptyset$, where we can write

$$\hat{\mathcal{R}}_{[\mathcal{F}_s, \mathcal{F}_s \cup \mathcal{F}_u]} \Gamma = (-1)^{|\mathcal{F}_s|} \mathfrak{K}_{\mathcal{F}_s} \prod_{\gamma \in \mathcal{F}_u} (\text{id} - \hat{\mathcal{C}}_\gamma) \Gamma. \quad (6.24)$$

We define as before subgraphs $\mathfrak{K}(\gamma) = (\mathcal{V}_\gamma, \mathcal{E}_\gamma)$ of $\mathfrak{K}_{\mathcal{F}_s}$, except that $\mathcal{C}(\gamma)$ now denotes the set of children of γ in $\mathcal{F}_s \cup \{\gamma\}$. For any $\gamma \in \mathcal{F}_u$, we denote by γ^\uparrow the inner vertex of T such that $\sigma(\mathcal{V}_\gamma) = \{v \in \mathcal{V} : v \geq \gamma^\uparrow\}$, and

$$\gamma^{\uparrow\uparrow} = \sup\{e^\uparrow : e \in \mathcal{E}_{\mathcal{A}(\gamma)} \text{ and } e \sim \mathfrak{K}(\gamma)\}.$$

Recall that $\mathcal{A}(\gamma)$ denotes the parent of γ in \mathcal{F} , while \sim denotes adjacency. In other words, we are considering edges in $\mathcal{E}_{\mathcal{A}(\gamma)}$ which are not in \mathcal{E}_γ . It follows that we necessarily have $\gamma^\uparrow > \gamma^{\uparrow\uparrow}$. Finally, we set

$$N(\gamma) = 1 + \lfloor -\deg(\gamma) \rfloor.$$

Lemma 5.7 implies that all subdivergences γ have a degree $\deg(\gamma) > -\frac{d}{3}$ (cf. Remark 5.4). Thus in space dimensions $d \leq 3$, $N(\gamma)$ is always equal to 1, while for $d \in \{4, 5\}$ it can take the value 2, and is always equal to 2 when ρ is sufficiently close to ρ_c . In the latter case, the operator $\hat{\mathcal{C}}_\gamma$ produces terms with nontrivial node labels, which are here essential for the renormalisation.

Example 6.12. Consider again the diagram of Example 5.12, with the forest $\mathcal{F} = \{\gamma_1, \gamma_2\}$. Consider now a Hepp sector $D_{\mathbf{T}}$ such that T has the structure given in Figure 5. In this example, γ_1 is unsafe, γ_2 is safe, and we have $\gamma_1^\uparrow = \mathfrak{d}$ and $\gamma_1^{\uparrow\uparrow} = \mathfrak{b}$.

If $d \leq 3$, the extraction operation $\hat{\mathcal{C}}_{\gamma_1} \Gamma$ has the same form as in (5.9) in Example 5.12. If

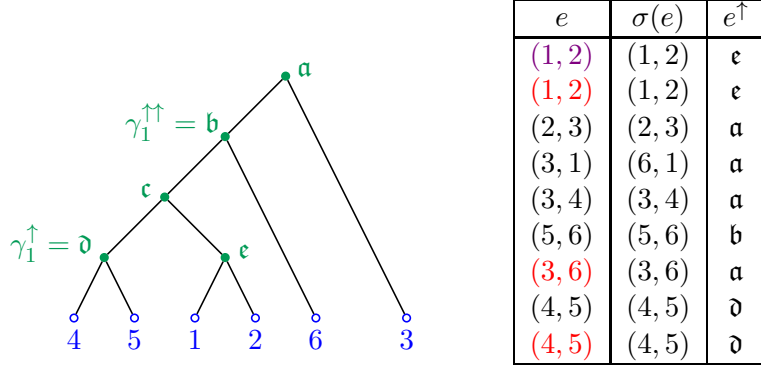


FIGURE 5: A tree T defining a Hepp sector $D_{\mathbf{T}}$ for the diagram $\hat{\mathcal{C}}_{\gamma_2}\Gamma$, cf. (5.9). The table shows, for each edge, its image $\sigma(e) = (\sigma(e)_-, \sigma(e)_+)$, and the ancestor e^\uparrow .

$d \in \{4, 5\}$, it becomes

$$\begin{aligned}
 \hat{\mathcal{C}}_{\gamma_1}\Gamma &= \text{Diagram 1} + \sum_{i=1}^d \text{Diagram 2} \\
 &\quad - \sum_{i=1}^d \text{Diagram 3}, \tag{6.25}
 \end{aligned}$$

where edge and node decorations have been indicated in green (e_i being the i th canonical basis vector). Note that this produces a factor

$$K_\rho(z_4 - z_3) \left[K_\rho(z_6 - z_5) - K_\rho(z_6 - z_4) + \sum_{i=1}^d \partial_i K_\rho(z_6 - z_4) (z_4 - z_5)^{e_i} \right]$$

in the integrand giving the value of $(\text{id} - \hat{\mathcal{C}}_{\gamma_1})\Gamma$, since the terms proportional to $(z_4 - z_{v_\star})^{e_i}$ stemming from the second term in (6.25) are killed because $v_\star = 4$. The point of the whole procedure is that the term in square brackets is bounded by a positive power of $\|z_4 - z_5\|_5$, which is much smaller than $\|z_6 - z_5\|_5$ owing to the fact that γ_1 is unsafe. ♣

Lemma 6.13. *There exists a constant \bar{K}_0 depending only on the kernels K_t such that*

$$\sum_{\mathbf{n}} \sup_{z \in D_{\mathbf{T}}} |(\mathcal{W}^K \hat{\mathcal{R}}_{[\mathcal{F}_s, \mathcal{F}_s \cup \mathcal{F}_u]}\Gamma)(z)| \prod_{v \in T} 2^{-(\rho+d)\mathbf{n}_v} \leq \bar{K}_0^{|\mathcal{E}|} C^{-\text{deg } \Gamma} \sum_{\mathbf{n}} \prod_{v \in T} 2^{-f(v, \mathbf{n}_v)},$$

where

$$f(v, \mathbf{n}_v) = \eta^\circ(v) \mathbf{n}_v + \eta^\varepsilon(v) [\mathbf{n}_v \wedge n_\varepsilon] + \sum_{\gamma \in \mathcal{F}_u} N(\gamma) [\mathbf{1}_{\gamma^\uparrow}(v) - \mathbf{1}_{\gamma^{\uparrow\uparrow}}(v)] \mathbf{n}_v, \tag{6.26}$$

with the same $\eta^\circ(v)$ and $\eta^\varepsilon(v)$ as in (6.2).

PROOF: The difference with the proof of Lemma 6.2 is the presence of the factors $(\text{id} - \hat{\mathcal{C}}_\gamma)$ with γ unsafe in (6.24). These produce a factor

$$\prod_{\substack{e \in \mathcal{E}_{\mathcal{A}}(\gamma) \\ e \sim \mathfrak{K}(\gamma)}} \left[K_{\text{t}(e)}(z_{\sigma(e_+)} - z_{\sigma(e_-)}) - \sum_{|\ell|_s < N(\gamma)} \frac{1}{\ell!} (z_{\sigma(e'_+)} - z_{\sigma(v_*)})^\ell \partial^\ell K_{\text{t}(e)}(z_{\sigma(v_*)} - z_{\sigma(e'_-)}) \right],$$

where e' is the image of e under $\hat{\mathcal{C}}_\gamma$. By the Taylor formula-type bound given in [21, Lemma 3.8], this factor is bounded by

$$K_1 2^{N(\gamma)[\mathbf{n}_{\gamma^\uparrow} - \mathbf{n}_{\gamma^\uparrow}]} \prod_{\substack{e \in \mathcal{E}_{\mathcal{A}}(\gamma) \\ e \sim \mathfrak{K}(\gamma)}} \|z_{\sigma(e_+)} - z_{\sigma(e_-)}\|_s^{\deg(e)},$$

which accounts for the last sum in (6.26). \square

Writing as before $\eta(v) = \eta^\circ(v) + \eta^\varepsilon(v)$, we introduce the notations

$$\hat{\eta}(v) = \eta(v) + \sum_{\gamma \in \mathcal{F}_u} N(\gamma) [\mathbf{1}_{\gamma^\uparrow}(v) - \mathbf{1}_{\gamma^\uparrow\uparrow}(v)], \quad \hat{\eta}_{\geq}(v) = \sum_{w \geq v} \hat{\eta}(w).$$

Lemma 6.14. *The conclusions of Lemma 6.6 still hold in the present situation, with η_{\geq} replaced by $\hat{\eta}_{\geq}$.*

PROOF: The only difference with the proof of Lemma 6.6 is the presence of the sum over diagrams in $\gamma \in \mathcal{F}_u$. We claim that we have the equivalences

$$\begin{aligned} v \leq \gamma^\uparrow &\Leftrightarrow \mathfrak{K}(\gamma) \subset \Gamma_0(v) \cap \mathfrak{K}(\mathcal{A}(\gamma)), \\ v > \gamma^\uparrow\uparrow &\Leftrightarrow \Gamma_0(v) \cap \mathfrak{K}(\mathcal{A}(\gamma)) \subset \mathfrak{K}(\gamma). \end{aligned} \quad (6.27)$$

Indeed, we always have $\mathfrak{K}(\gamma) \subset \mathfrak{K}(\mathcal{A}(\gamma))$, so that the first equivalence follows from the fact that $v \leq \gamma^\uparrow \Leftrightarrow \mathfrak{K}(\gamma) \subset \Gamma_0(v)$. For the second equivalence, we observe that if $e \in \Gamma_0(v) \cap \mathfrak{K}(\mathcal{A}(\gamma))$, then $e^\uparrow \geq v$, and e is either in \mathcal{E}_γ , or adjacent to $\mathfrak{K}(\gamma)$. However, the second case is ruled out if $v > \gamma^\uparrow\uparrow$. Conversely, if $\Gamma_0(v) \cap \mathfrak{K}(\mathcal{A}(\gamma)) \subset \mathfrak{K}(\gamma)$, then any edge $e \sim \mathfrak{K}(\gamma)$ cannot belong to \mathcal{E}_0 , and must thus satisfy $e^\uparrow < v$, which implies that $\gamma^\uparrow\uparrow < v$.

It follows from (6.27) that

$$\sum_{w \geq v} [\mathbf{1}_{\gamma^\uparrow}(w) - \mathbf{1}_{\gamma^\uparrow\uparrow}(w)] = \mathbf{1}_{\gamma^\uparrow\uparrow < v \leq \gamma^\uparrow} = \mathbf{1}_{\mathfrak{K}(\gamma) = \Gamma_0(v) \cap \mathfrak{K}(\mathcal{A}(\gamma))}.$$

Thus, $\hat{\eta}_{\geq}(v)$ satisfies the equivalent of the decomposition (6.18), with

$$\hat{\eta}_{\geq, \gamma}(v) = (\rho + d)(|\mathcal{Y}_0 \cap \mathcal{Y}_\gamma| - 1) + \sum_{e \in \mathcal{E}_\gamma \cap \mathcal{E}_0} \deg(e) + \sum_{\tilde{\gamma} \in \mathcal{F}_u} N(\tilde{\gamma}) \mathbf{1}_{\mathfrak{K}(\tilde{\gamma}) = \Gamma_0(v) \cap \mathfrak{K}(\mathcal{A}(\tilde{\gamma}))}. \quad (6.28)$$

One then shows that the properties (6.19) of full, empty and normal subgraphs still hold in this case. The case of γ being normal requires the presence of the last term in (6.28), to which only $\hat{\gamma}$ contributes, together with the fact that $\deg(\hat{\gamma}) + N(\hat{\gamma}) > 0$. The remainder of the proof is the same as for Lemma 6.6. \square

The analogue of Corollary 6.9 is then proved in the same way as above, completing the proof of Proposition 6.1.

7 Asymptotics

Fix a tree $\tau \in T_-^F$ with p leaves and q edges. It follows from the definition (4.5) of $c_\varepsilon(\tau)$, Propositions 4.5 and 5.2, the decomposition (6.1) into Hepp sectors and Proposition 6.1 that

$$c_\varepsilon(\tau) = (-2)^{-1-\frac{p}{2}} \sum_{P \in \mathcal{P}_\tau^{(2)}} \sum_T \sum_{\mathcal{F}_s \in \mathcal{F}_{\Gamma(\tau, P)}^{(s)}} \mathcal{I}(\tau, P, T, \mathcal{F}_s),$$

where

$$\mathcal{I}(\tau, P, T, \mathcal{F}_s) = \sum_{\mathbf{n}} \int_{D_{\mathbf{T}}} (\mathcal{W}^K \hat{\mathcal{R}}_{[\mathcal{F}_s, \mathcal{F}_s \cup \mathcal{F}_u]} \Gamma(\tau, P))(z) dz$$

satisfies

$$|\mathcal{I}(\tau, P, T, \mathcal{F}_s)| \leq C_0^{|\mathcal{Y}(\Gamma(\tau, P))|} K_1^{|\mathcal{L}(\Gamma(\tau, P))|} \varepsilon^{\deg \Gamma(\tau, P)} [\log(\varepsilon^{-1})]^{\zeta(\Gamma(\tau, P))}$$

(with the convention that $\varepsilon^{\deg \Gamma(\tau, P)}$ is to be replaced by $\log(\varepsilon^{-1})$ if $\deg \Gamma(\tau, P) = 0$). To obtain an upper bound on $|c_\varepsilon(\tau)|$, it thus remains to control the sums over Hepp trees T , permutations P , and safe forests \mathcal{F}_s . Summing over all $\tau \in T_-^F$ will then provide an upper bound on the renormalisation constants.

7.1 Full binary trees

Recall that a full binary tree τ with p leaves has $q = 2p - 2$ edges and $p - 1$ inner vertices. It will be useful to parametrise the set of full binary trees with an even number of leaves by integers k such that $p = 2k + 2$ and $q = 4k + 2$. It follows from Proposition 4.18 that for any pairing P , the corresponding (reduced) Feynman diagram $\Gamma = \Gamma(\tau, P)$ will have $2k$ vertices, $3k$ edges, and degree

$$\begin{aligned} \deg \Gamma(\tau, P) &= (3k + 1)\rho - (k + 1)d \\ &= -\frac{2}{3}d + (3k + 1)(\rho - \rho_c) \quad \forall P \in \mathcal{P}^{(2)}. \end{aligned} \quad (7.1)$$

This degree is negative if and only if

$$k \leq k_{\max} = \frac{d - \rho}{3\rho - d} = \frac{d - \rho}{3(\rho - \rho_c)}. \quad (7.2)$$

We can thus rewrite (7.1) as

$$\deg \Gamma = -(d - \rho) \left(1 - \frac{k}{k_{\max}} \right) =: \alpha_k. \quad (7.3)$$

The number of possible pairings of the $2k + 2$ leaves is equal to $(2k + 1)!! = \prod_{i=0}^k (2i + 1)$. The number of Hepp trees T is bounded above by $(2k - 1)!$, and is reached when T is a comb tree, whose $2k$ leaves can be associated in $(2k - 1)!$ inequivalent ways to the $2k$ vertices of Γ . The number of safe forests \mathcal{F}_s can be bounded as follows.

Lemma 7.1. *There are at most $2^{|\mathcal{G}_\Gamma^-|}$ safe forests in Γ , where the number of divergent subdiagrams satisfies $|\mathcal{G}_\Gamma^-| \leq k$.*

PROOF: Let N_m denote the number of edges of a Feynman diagram Γ having m divergent subdiagrams. Then $N_1 \geq 2$, and $N_{m_1+m_2} \geq N_{m_1} + N_{m_2} + 1$, since elements of a forest have to be strictly included into one another or vertex disjoint. By induction on m , one obtains $N_m \geq 3m - 1$, implying $3|\mathcal{G}_\Gamma^-| - 1 \leq 3k$, and thus $|\mathcal{G}_\Gamma^-| \leq k$. The bound on the number of safe forests then simply follows from the fact that a finite set with n elements has 2^n subsets, and is reached when all forests are safe. \square

Finally, we need to control the number of terms yielding an exponent $\zeta = 1$ rather than $\zeta = 0$. We write $\mathcal{P}_\tau^{(2)} = \mathcal{P}_{\tau,0}^{(2)} \sqcup \mathcal{P}_{\tau,1}^{(2)}$, where $\mathcal{P}_{\tau,i}^{(2)}$ denotes the set of pairings yielding a diagram $\Gamma(\tau, P)$ with $\zeta(\Gamma) = i$. Then we have the following key estimate.

Lemma 7.2. $\mathcal{P}_{\tau,1}^{(2)}$ is non-empty only when k_{\max} is an odd integer and $2k \geq k_{\max} + 1$. In that case, we have

$$\frac{|\mathcal{P}_{\tau,1}^{(2)}|}{|\mathcal{P}_{\tau,0}^{(2)}|} \leq r(k) := \frac{k_{\max}!!(2k - k_{\max})!!}{(2k + 1)!!}. \quad (7.4)$$

Furthermore, we have

$$r(k) \leq M2^{-(2k - k_{\max})} \quad (7.5)$$

for $k_{\max} + 1 \leq 2k \leq 2k_{\max}$, where M is a constant independent of k , ρ and ε .

PROOF: Assume $\Gamma = \Gamma(\tau, P)$ has a child γ having degree 0. By Lemma 5.7, $\gamma = \Gamma(\bar{\tau}, \bar{P})$ where $\bar{\tau}$ is an almost full binary subtree of τ , and \bar{P} is the restriction of P to the leaves of $\bar{\tau}$. Let $\bar{k} < k$ be such that $\bar{\tau}$ has $2\bar{k} + 2$ leaves and $4\bar{k} + 3$ edges. Then we have

$$\deg \gamma = -\frac{1}{3}d + (3\bar{k} + 2)(\rho - \rho_c) = 0.$$

In view of (7.1), this implies

$$2(3\bar{k} + 2)(\rho - \rho_c) = \frac{2}{3}d = (3k + 1)(\rho - \rho_c) - \deg \Gamma,$$

which yields $2\bar{k} + 1 = k_{\max}$ by (7.2) and (7.3). Thus k_{\max} must be an odd integer, and the condition $k > \bar{k}$ yields $2k \geq k_{\max} + 1$. Finally, the number of pairings that do not mix leaves of $\bar{\tau}$ with those of $\tau \setminus \bar{\tau}$ is given by $(2\bar{k} + 1)!!(2k - 2\bar{k} - 1)!! = k_{\max}!!(2k - k_{\max})!!$, which proves (7.4). To prove (7.5), we write $k = xk_{\max}$ and use Stirling's formula to obtain

$$\begin{aligned} \log r(k) &= \frac{k_{\max}}{2} [(2x - 1) \log(2x - 1) - 2x \log(2x)] - \frac{1}{2} \log(x) + \mathcal{O}(1) \\ &\leq -\log(2)(2xk_{\max} - k_{\max}) + \mathcal{O}(1), \end{aligned}$$

where we have used a convexity argument to obtain the last line. \square

Remark 7.3. In what follows, we will always assume that $k_{\max} > 1$. Indeed, for $k_{\max} < 1$ (that is, $\rho > \frac{d}{2}$), the only potentially divergent tree is \blacklozenge , while for $k_{\max} = 1$, the trees with 4 leaves considered in Example 4.17 have degree 0. These cases can be treated “by hand”, in particular the expectation (4.21) can be shown to diverge like $\log(\varepsilon^{-1})$. \diamond

The above combinatorial considerations show that

$$|c_\varepsilon(\tau)| \leq (2k + 1)!!(2k - 1)! C_0^{2k} K_1^{3k} \varepsilon^{\deg \Gamma} [1 + r(k) \log(\varepsilon^{-1})],$$

where $\deg \Gamma$ is given by (7.3), and $\varepsilon^{\deg \Gamma}$ has to be replaced by $\log(\varepsilon^{-1})$ if $\deg \Gamma = 0$. Let us write $C_0^{2k} K_1^{3k} = K_2^{3k}$, where $K_2 = C_0^{2/3} K_1$. It follows from Stirling's formula that

$$\log((2k+1)!(2k-1)!K_1^{3k}\varepsilon^{\deg \Gamma}) \leq 3k \log k + 3k[\log 2 - 1 + \log K_2] - \log(\varepsilon^{-1}) \deg \Gamma + \mathcal{O}(1),$$

where the remainder term $\mathcal{O}(1)$ is independent of k , ρ and ε .

When computing the contribution of full binary trees to the renormalisation counterterm (3.3), we have to take into account the number of these trees, as well as the combinatorial factor $2^{n_{\text{inner}}(\tau) - n_{\text{sym}}(\tau)}$. The latter can be bounded above by 2^{2k+1} , while the former is given by the $(2k+2)$ nd Wedderburn–Etherington number (sequence **A001190** in the On-Line Encyclopedia of Integer Sequences OEIS), cf. [3, Section 4.4.1]. These numbers are known to grow like $k^{-3/2}\beta_2^{-2k}$, where $\beta_2 \simeq 0.4026975$ (OEIS sequence **A240943**) is the radius of convergence of the generating series of the sequence.

The renormalisation counterterm $C_0(\varepsilon, \rho)$ due to full binary trees can thus be written in the form

$$\begin{aligned} C_0(\varepsilon, \rho) = & \sum_{k=0}^{\lfloor k_{\max} \rfloor - 1} A_k \varepsilon^{\alpha_k} + \mathbf{1}_{k_{\max} \in \mathbb{N}} A_{k_{\max}} \log(\varepsilon^{-1}) \\ & + \mathbf{1}_{k_{\max} \in 2\mathbb{N}+1} \left[\sum_{k=(k_{\max}-1)/2}^{k_{\max}-1} A_k \varepsilon^{\alpha_k} r(k) + A_{k_{\max}} r(k_{\max}) \log(\varepsilon^{-1}) \right] \log(\varepsilon^{-1}), \end{aligned} \quad (7.6)$$

where α_k is defined in (7.3) and

$$\begin{aligned} \log|A_k| & \leq 3[k \log k + ak - \frac{1}{2} \log(k+1)] + \mathcal{O}(1), \\ a & = \log 2 - 1 + \log K_2 + \frac{2}{3} \log(\beta_2^{-1}). \end{aligned}$$

As a consequence, we have the bound

$$|A_k \varepsilon^{\alpha_k}| \leq M e^{3F(k)}, \quad (7.7)$$

where M is a constant independent of k , ρ and ε , and

$$F(k) = k \log k + (a - b_\varepsilon)k + b_\varepsilon k_{\max} - \frac{1}{2} \log(k+1), \quad (7.8)$$

with

$$b_\varepsilon = (\rho - \rho_c) \log(\varepsilon^{-1}).$$

Note in particular that $e^{3F(0)} = \varepsilon^{-(d-\rho)}$, and that F is strictly convex.

Proposition 7.4. *Define the threshold*

$$\varepsilon_c(\rho) = \exp \left\{ -\frac{1}{\rho - \rho_c} \left[\log k_{\max} + a - \frac{\log(k_{\max} + 1)}{2k_{\max}} \right] \right\}.$$

Then there exist constants M_1, M_2 , independent of ε and ρ , such that the counterterm $C_0(\varepsilon, \rho)$ satisfies

$$\begin{aligned} C_0(\varepsilon, \rho) & = A_0 \varepsilon^{-(d-\rho)} [1 + R_1(\varepsilon, \rho)] & \text{for } \varepsilon < \varepsilon_c(\rho), \\ |C_0(\varepsilon, \rho)| & \leq M \varepsilon_c(\rho)^{-(d-\rho)} [\log(\varepsilon^{-1}) + R_2(\varepsilon, \rho)] & \text{for } \varepsilon \geq \varepsilon_c(\rho), \end{aligned}$$

where the remainders satisfy

$$|R_1(\varepsilon, \rho)| \leq \frac{M_1}{\rho - \rho_c} \left(\frac{\varepsilon}{\varepsilon_c(\rho)} \right)^{3(\rho - \rho_c)}, \quad |R_2(\varepsilon, \rho)| \leq \frac{M_2}{\rho - \rho_c} \left(\frac{\varepsilon_c(\rho)}{\varepsilon} \right)^{3(\rho - \rho_c)}.$$

PROOF: Since F is convex, we have $F(k) \leq F(0) + Hk$ for all $k \in [0, k_{\max}]$, where

$$H = \frac{F(k_{\max}) - F(0)}{k_{\max}} = \log k_{\max} - b_\varepsilon + a - \frac{1}{2} \frac{\log(k_{\max} + 1)}{k_{\max}}. \quad (7.9)$$

Note that $\varepsilon_c(\rho)$ has been defined in such a way that

$$H = (\rho - \rho_c) \log\left(\frac{\varepsilon}{\varepsilon_c(\rho)}\right),$$

and that $e^{3F(k_{\max})} = \varepsilon_c(\rho)^{-(d-\rho)}$. We will repeatedly use the fact that if $\beta \in \mathbb{R}$ and $N > k_0$ are positive integers, then

$$\sum_{k=k_0}^{N-1} e^{\beta k} \leq \begin{cases} [(N - k_0) \wedge \beta^{-1}] e^{\beta(N-1)} & \text{if } \beta > 0, \\ N - k_0 & \text{if } \beta = 0, \\ [(N - k_0) \wedge |\beta|^{-1}] e^{\beta k_0} & \text{if } \beta < 0. \end{cases} \quad (7.10)$$

In the case $\varepsilon \geq \varepsilon_c(\rho)$, i.e. $H \geq 0$, we rewrite (7.6) as

$$\begin{aligned} C_0(\varepsilon, \rho) - \mathbf{1}_{k_{\max} \in \mathbb{N}} A_{k_{\max}} \log(\varepsilon^{-1}) &= \sum_{k=0}^{\lfloor k_{\max} \rfloor - 1} A_k \varepsilon^{\alpha k} + \sum_{k=(k_{\max}+1)/2}^{k_{\max}-1} A_k \varepsilon^{\alpha k} r(k) \log(\varepsilon^{-1}) \\ &\quad + A_{k_{\max}} r(k_{\max}) [\log(\varepsilon^{-1})]^2 \\ &=: M e^{3F(k_{\max})} [\mathcal{R}_1(\varepsilon, \rho) + \mathcal{R}_2(\varepsilon, \rho) + \mathcal{R}_3(\varepsilon, \rho)], \end{aligned}$$

where the terms \mathcal{R}_2 and \mathcal{R}_3 vanish unless k_{\max} is an odd integer, which we can assume to be at least 3 by Remark 7.3. By (7.7), the leading term $A_{k_{\max}} \log(\varepsilon^{-1})$ has indeed order $\varepsilon_c(\rho)^{-(d-\rho)} \log(\varepsilon^{-1})$. To bound \mathcal{R}_1 , we use (7.10) with $N = \lfloor k_{\max} \rfloor$, $k_0 = 0$ and $\beta = 3H$ to get

$$|\mathcal{R}_1(\varepsilon, \rho)| \lesssim k_{\max} e^{-3H} \lesssim \frac{1}{\rho - \rho_c} \left(\frac{\varepsilon_c(\rho)}{\varepsilon}\right)^{3(\rho - \rho_c)}.$$

Regarding \mathcal{R}_2 , we use (7.5) to get

$$|\mathcal{R}_2(\varepsilon, \rho)| \leq M e^{-3H k_{\max}} e^{k_{\max} \log 2} \sum_{k=(k_{\max}+1)/2}^{k_{\max}-1} e^{(3H-2 \log 2)k} \log(\varepsilon^{-1}).$$

We use (7.10) differently in several regimes. If $3H \leq 1$, we obtain

$$|\mathcal{R}_2(\varepsilon, \rho)| \lesssim e^{-\frac{3}{2}H(k_{\max}-1)} \log(\varepsilon^{-1}) \leq e^{-3H} \log(\varepsilon^{-1}).$$

If $1 < 3H < 2 \log 2$, we get

$$|\mathcal{R}_2(\varepsilon, \rho)| \lesssim k_{\max} e^{-\frac{3}{2}H(k_{\max}-1)} \log(\varepsilon^{-1}) \leq e^{-3H} k_{\max} e^{-\frac{3}{2}(k_{\max}-3)} \log(\varepsilon^{-1}),$$

which yields a bound of the same form, since $k_{\max} e^{-\frac{3}{2}(k_{\max}-3)}$ is bounded uniformly in $k_{\max} \geq 3$. If $3H \geq 2 \log 2$, we have

$$|\mathcal{R}_2(\varepsilon, \rho)| \lesssim e^{-3H} k_{\max} 2^{-k_{\max}} \log(\varepsilon^{-1}).$$

Note that in all three regimes, we have $|\mathcal{R}_2(\varepsilon, \rho)| \lesssim e^{-3H} \log(\varepsilon^{-1})$. Regarding \mathcal{R}_3 , we observe that it is bounded by $r(k_{\max}) \log(\varepsilon^{-1})^2$, showing that

$$e^{3H} |\mathcal{R}_3(\varepsilon, \rho)| \lesssim \frac{2^{-k_{\max}}}{\varepsilon_c(\rho)^{3(\rho-\rho_c)}} \varepsilon^{3(\rho-\rho_c)} [\log(\varepsilon^{-1})]^2.$$

For fixed ρ , the right-hand side is maximal for $\varepsilon = \varepsilon_* = e^{-2/(3(\rho-\rho_c))}$. Therefore, by definition of k_{\max} and $\varepsilon_c(\rho)$, we have

$$e^{3H} |\mathcal{R}_3(\varepsilon, \rho)| \lesssim \frac{2^{-k_{\max}}}{\varepsilon_c(\rho)^{3(\rho-\rho_c)}} \frac{4e^{-2}}{9(\rho-\rho_c)^2} \lesssim 2^{-k_{\max}} k_{\max}^3 k_{\max}^2,$$

which is bounded uniformly in $k_{\max} \geq 1$. Therefore, we have $|\mathcal{R}_3(\varepsilon, \rho)| \lesssim e^{-3H}$, completing the proof for $\varepsilon > \varepsilon_c(\rho)$.

It remains to consider the case $\varepsilon < \varepsilon_c(\rho)$, i.e. $H < 0$. Here we decompose

$$\begin{aligned} C_0(\varepsilon, \rho) - A_0 \varepsilon^{\alpha_0} &= \sum_{k=1}^{\lfloor k_{\max} \rfloor - 1} A_k \varepsilon^{\alpha_k} + A_{k_{\max}} \log(\varepsilon^{-1}) \\ &\quad + \sum_{k=(k_{\max}+1)/2}^{k_{\max}-1} A_k \varepsilon^{\alpha_k} r(k) \log(\varepsilon^{-1}) + A_{k_{\max}} r(k_{\max}) [\log(\varepsilon^{-1})]^2 \\ &=: M e^{3F(0)} [\mathcal{R}_1(\varepsilon, \rho) + \mathcal{R}_2(\varepsilon, \rho) + \mathcal{R}_3(\varepsilon, \rho) + \mathcal{R}_4(\varepsilon, \rho)], \end{aligned}$$

where \mathcal{R}_3 and \mathcal{R}_4 vanish unless k_{\max} is an odd integer. Applying (7.10) with $N = \lfloor k_{\max} \rfloor$, $k_0 = 1$ and $\beta = 3H$, we obtain

$$|\mathcal{R}_1(\varepsilon, \rho)| \lesssim k_{\max} e^{3H} \lesssim \frac{1}{\rho - \rho_c} \left(\frac{\varepsilon}{\varepsilon_c(\rho)} \right)^{3(\rho-\rho_c)}.$$

Using (7.7), we find

$$|\mathcal{R}_2(\varepsilon, \rho)| \leq e^{3H k_{\max}} \log(\varepsilon^{-1}) = \left(\frac{\varepsilon}{\varepsilon_c(\rho)} \right)^{d-\rho} \log(\varepsilon^{-1}).$$

Regarding \mathcal{R}_3 , using again (7.10) we get

$$|\mathcal{R}_3(\varepsilon, \rho)| \lesssim e^{\frac{3}{2}H(k_{\max}+1)} \log(\varepsilon^{-1}) = \left(\frac{\varepsilon}{\varepsilon_c(\rho)} \right)^{\frac{3}{2}(k_{\max}+1)(\rho-\rho_c)} \log(\varepsilon^{-1}).$$

Finally, by (7.5) we also have

$$|\mathcal{R}_4(\varepsilon, \rho)| \leq \left(\frac{\varepsilon}{\varepsilon_c(\rho)} \right)^{d-\rho} 2^{-k_{\max}} [\log(\varepsilon^{-1})]^2.$$

Since $k_{\max} > 1$, we have $d - \rho > 3(\rho - \rho_c)$, so that \mathcal{R}_2 and \mathcal{R}_4 are negligible with respect to \mathcal{R}_1 . In addition, \mathcal{R}_3 only occurs when $k_{\max} \geq 3$, and then it is also dominated by \mathcal{R}_1 . \square

7.2 Almost full binary trees

It remains to consider the case of almost full binary trees without decorations X_i , as the contribution of almost full binary trees with a decoration X_i vanishes by symmetry.

Almost full trees with an even number of leaves can be parametrised by an integer k such that these trees have $p = 2k + 2$ leaves and $q = 4k + 3$ edges. The corresponding reduced Feynman diagrams have $2k + 1$ vertices, $3k + 1$ edges, and degree

$$\deg \Gamma(\tau, P) = (3k + 2)\rho - (k + 1)d \quad \forall P \in \mathcal{P}^{(2)} .$$

The main difference with the case of full trees is that the maximal value of k for $\deg \Gamma(\tau, P)$ to be negative is now

$$\bar{k}_{\max} = \frac{d - 2\rho}{3\rho - d} = \frac{d - 2\rho}{3(\rho - \rho_c)} ,$$

which is smaller than k_{\max} by a factor approaching 2 as $\rho \searrow \rho_c$. Furthermore, Lemma 7.2 shows that ζ always vanishes in this case. The remaining combinatorial arguments remain unchanged, with the result that

$$C_1(\varepsilon, \rho) = \sum_{k=0}^{\bar{k}_{\max}-1} \bar{A}_k \varepsilon^{\bar{\alpha}_k} + \mathbf{1}_{\bar{k}_{\max} \in \mathbb{N}} \bar{A}_{\bar{k}_{\max}} \log(\varepsilon^{-1}) ,$$

where

$$\bar{\alpha}_k = -(d - 2\rho) \left(1 - \frac{k}{\bar{k}_{\max}} \right)$$

and $|\bar{A}_k \varepsilon^{\bar{\alpha}_k}| \leq M e^{3\bar{F}(k)}$ with

$$\bar{F}(k) = k \log k + (a - b_\varepsilon)k + b_\varepsilon \bar{k}_{\max} - \frac{1}{2} \log(k + 1) .$$

It thus suffices to modify the threshold value of ε to obtain the result.

7.3 A remark on lower bounds

The results we have obtained provide upper bounds on the counterterms. Obtaining matching lower bounds seems out of reach at this stage, because, as we have seen, the behaviour in $\varepsilon^{\deg \Gamma(\tau, P)}$ of the terms $c_\varepsilon(\tau)$ is a consequence of cancellations of more singular terms in Zimmermann's forest formula.

However, we can at least argue that among the many terms contributing to the counterterms $C_0(\varepsilon, \rho)$ and $C_1(\varepsilon, \rho)$, there exist terms which are bounded above *and* below by a quantity of the same order. This does not of course exclude that cancellations among these terms exist, which ultimately make the counterterms much smaller. However, such a scenario seems unlikely, unless some hidden symmetries have been overlooked.

Indeed, assume that τ is a regular binary tree (cf. (3.5)). Then $n_{\text{inner}}(\tau) = n_{\text{sym}}(\tau)$, so that the contribution of τ to $C_0(\varepsilon, \rho)$ is given by

$$c_\varepsilon(\tau) = E(\tilde{\mathcal{A}}_-^E \tau) = \sum_{P \in \mathcal{P}_\tau^{(2)}} E(\tilde{\mathcal{A}}_- \Gamma(\tau, P)) .$$

It follows from Lemma 5.7 that $\Gamma(\tau, P)$ cannot have any divergent strict subdiagram, since a regular binary tree does not contain any almost full binary subtree. Therefore, (6.1) reduces to

$$E(\tilde{\mathcal{A}}_- \Gamma(\tau, P)) = - \sum_T \sum_{\mathbf{n}} \int_{D_T} (\mathcal{W}^K \Gamma(\tau, P))(z) dz .$$

It is known that whenever $\rho < d$, the fractional heat kernel P_ρ is given by the Riesz kernel which has a constant sign. This sign is not conserved by the decomposition (4.1) of the kernel into its singular and smooth parts, but one can add a bounded, compactly supported term to K_ρ in such a way that K_ρ has a constant sign, and without changing the divergent part of the integrals. Therefore, we obtain

$$|E(\tilde{\mathcal{A}}_-\Gamma(\tau, P))| \geq a \sum_T K_2^{|\mathcal{E}|} \varepsilon^{\deg(\Gamma)}$$

for a constant $a > 0$. Since the number of pairings P and of Hepp trees T have the same factorial behaviour as above, we indeed obtain for $c_\varepsilon(\tau)$ an asymptotic behaviour in $\varepsilon_c(\rho)^{-(d-\rho)} \log(\varepsilon^{-1})$.

7.4 Extension to other parameter regimes

In this section, we extend the results to the more general family of equations

$$\partial_t u - \gamma \Delta^{\rho/2} u = g u^2 + \sigma \xi, \quad (7.11)$$

where γ , g and σ are parameters measuring the strength of each component of the equation, that is, the smoothing effect given by the fractional Laplacian, the nonlinearity u^2 and the noise ξ . Our aim is to understand how the model behaves when one lets these parameters vary, and to determine some potentially interesting parameter regimes.

The extension can actually be done in two equivalent ways: using directly the BPHZ renormalisation on the parameter-dependent equation (7.11), or using a scaling argument for the original equation (1.1). We will briefly outline both arguments, which will serve as a reality check of the results. Using the BPHZ renormalisation (3.3) on (7.11), one obtains the renormalised equation

$$\partial_t u - \gamma \Delta^{\rho/2} u = g u^2 + C^{\gamma, g, \sigma}(\varepsilon, \rho, u) + \sigma \xi^\varepsilon, \quad (7.12)$$

where the new counterterm is given by

$$C^{\gamma, g, \sigma}(\varepsilon, \rho, u) = C_0^{\gamma, g, \sigma}(\varepsilon, \rho) + C_1^{\gamma, g, \sigma}(\varepsilon, \rho) u$$

with

$$C_0^{\gamma, g, \sigma}(\varepsilon, \rho) = \sum_{\tau \text{ full}} c_\varepsilon^{\gamma, \sigma}(\tau) g^{n_{\text{inner}}(\tau)} 2^{\bar{n}(\tau)},$$

$$C_1^{\gamma, g, \sigma}(\varepsilon, \rho) = \sum_{\tau \text{ almost full}} c_\varepsilon^{\gamma, \sigma}(\tau) g^{n_{\text{inner}}(\tau)} 2^{\bar{n}(\tau)},$$

and $\bar{n}(\tau) = n_{\text{inner}}(\tau) - n_{\text{sym}}(\tau)$. The new renormalisation constant $c_\varepsilon^{\gamma, \sigma}$ associated to a tree τ is given by

$$c_\varepsilon^{\gamma, \sigma}(\tau) = \sigma^{n_{\text{leaves}}(\tau)} c_\varepsilon^\gamma(\tau),$$

where $n_{\text{leaves}}(\tau)$ is the number of leaves of τ . Here in the notation $c_\varepsilon^\gamma(\tau)$, we stress that the value of the renormalisation constant depends on γ via the scaled Green function $K_\rho^{(\gamma)} = (\partial_t - \gamma \Delta^{\rho/2})^{-1}$ of the fractional Laplacian that now appears on every edge of the tree τ . One key property that we use in the sequel is

$$K_\rho^{(\gamma)}(t, x) = K_\rho(\gamma t, x).$$

Indeed, since $f(t, x) = (K_\rho * h)(t, x)$ satisfies the equation $\partial_t f - \Delta^{\rho/2} f = h$, setting $\bar{h}(t, x) = \gamma h(\gamma t, x)$ it is easy to check that

$$\bar{f}(t, x) = f(\gamma t, x) = \int_{\mathbb{R}} \int_{\mathbb{R}^d} K_\rho(\gamma(t-s), x-y) \bar{h}(s, y) dy ds$$

satisfies $\partial_t \bar{f} - \gamma \Delta^{\rho/2} \bar{f} = \bar{h}$. Then, performing a linear change of variable for all time integrals in the definition (4.12) of $E(\Gamma)$, we get

$$c_\varepsilon^\gamma(\tau) = \frac{1}{\gamma^{\nu_\tau - 1}} c_\varepsilon(\tau)$$

where ν_τ is the number of nodes of the Feynman diagram $\Gamma(\tau, P)$ associated with τ .

- If τ is a full tree with p leaves and $q = 2p - 2$ edges, then we have

$$\nu_\tau = q + 1 - \frac{p}{2} = \frac{3}{2}p - 1, \quad n_{\text{inner}}(\tau) = p - 1.$$

Therefore, we obtain

$$C_0^{\gamma, g, \sigma}(\varepsilon, \rho) = \sum_p \frac{g^{p-1} \sigma^p}{\gamma^{\frac{3}{2}p-2}} \sum_{\tau \text{ full with } p \text{ leaves}} c_\varepsilon(\tau) 2^{\bar{n}(\tau)}. \quad (7.13)$$

- If τ is an almost full tree with p leaves and $q = 2p - 1$ edges, then we have

$$\nu_\tau = \frac{3}{2}p, \quad n_{\text{inner}}(\tau) = p,$$

yielding

$$C_1^{\gamma, g, \sigma}(\varepsilon, \rho) = \sum_p \frac{g^p \sigma^p}{\gamma^{\frac{3}{2}p-1}} \sum_{\tau \text{ almost full with } p \text{ leaves}} c_\varepsilon(\tau) 2^{\bar{n}(\tau)}. \quad (7.14)$$

The second argument allowing to obtain (7.13) and (7.14) is based on scaling. If u satisfies the renormalised equation

$$\partial_t u - \Delta^{\rho/2} u = u^2 + C(\varepsilon, \rho, u) + \xi^\varepsilon,$$

then for any $\lambda > 0$ and $\alpha, \beta \in \mathbb{R}$, $\bar{u}(t, x) = \lambda^\alpha u(\lambda^\beta t, \lambda x)$ solves the equation

$$\partial_t \bar{u} - \lambda^{\beta-\rho} \Delta^{\rho/2} \bar{u} = \lambda^{\beta-\alpha} \bar{u}^2 + \lambda^{\alpha+\beta} C(\varepsilon, \rho, \lambda^{-\alpha} \bar{u}) + \lambda^{\alpha+\beta} \xi_{\lambda^\beta, \lambda}^\varepsilon, \quad (7.15)$$

where

$$\begin{aligned} \xi_{\lambda^\beta, \lambda}^\varepsilon(t, x) &= \xi^\varepsilon(\lambda^\beta t, \lambda x) \\ &= \frac{1}{\varepsilon^{\rho+d}} \int_{\mathbb{R}^{d+1}} \varrho\left(\frac{\lambda^\beta t - t'}{\varepsilon^\rho}, \frac{\lambda x - x'}{\varepsilon}\right) \xi(dt', dx') \\ &= \frac{1}{\bar{\varepsilon}^{\rho+d}} \int_{\mathbb{R}^{d+1}} \lambda^{\beta-\rho} \varrho\left(\frac{\lambda^{\beta-\rho}(t - t'')}{\bar{\varepsilon}^\rho}, \frac{x - x''}{\bar{\varepsilon}}\right) \xi(\lambda^\beta dt'', \lambda dx''). \end{aligned}$$

In the last line, we have set $\varepsilon = \lambda \bar{\varepsilon}$, and made the change of variables $t' = \lambda^\beta t''$, $x' = \lambda x''$. By the scaling property of space-time white noise, this is equal in law to

$$\frac{\lambda^{-\frac{\beta}{2} - \frac{d}{2}}}{\bar{\varepsilon}^{\rho+d}} \int_{\mathbb{R}^{d+1}} \lambda^{\beta-\rho} \varrho\left(\frac{\lambda^{\beta-\rho}(t - t'')}{\bar{\varepsilon}^\rho}, \frac{x - x''}{\bar{\varepsilon}}\right) \xi(dt'', dx'') = \lambda^{-\frac{\beta}{2} - \frac{d}{2}} \tilde{\xi}^{\bar{\varepsilon}}(t, x),$$

where $\tilde{\xi}^{\bar{\varepsilon}} = \tilde{\varrho}^{\bar{\varepsilon}} * \xi$ is defined like ξ^ε , but using $\tilde{\varrho}(t, x) = \lambda^{\beta-\rho} \varrho(\lambda^{\beta-\rho} t, x)$ as new mollifier. Thus (7.15) is indeed of the form (7.12) with parameters

$$\gamma = \lambda^{\beta-\rho}, \quad g = \lambda^{\beta-\alpha}, \quad \sigma = \lambda^{\alpha + \frac{\beta}{2} - \frac{d}{2}}. \quad (7.16)$$

Using the expression (3.3) of $C(\varepsilon, \rho, u)$, we find

$$\lambda^{\alpha+\beta} C(\lambda\bar{\varepsilon}, \rho, \lambda^{-\alpha}\bar{u}) = \lambda^{\alpha+\beta} \sum_{\tau \text{ full}} c_{\lambda\bar{\varepsilon}}(\tau) 2^{\bar{n}(\tau)} + \lambda^\beta \sum_{\tau \text{ almost full}} c_{\lambda\bar{\varepsilon}}(\tau) 2^{\bar{n}(\tau)} u$$

If $\deg(\tau) < 0$, then

$$c_\varepsilon(\tau) \sim \varepsilon^{\deg(\tau)}, \quad c_{\lambda\bar{\varepsilon}}(\tau) \sim \bar{\varepsilon}^{\deg(\tau)} \lambda^{\deg(\tau)},$$

which implies that $c_{\lambda\bar{\varepsilon}} = \lambda^{\deg(\tau)} c_{\bar{\varepsilon}}(\tau)$ (note that since $\log(\lambda\bar{\varepsilon}) = \log \lambda + \log \bar{\varepsilon}$, logarithmic divergences do not change the leading order of $c_\varepsilon(\tau)$). In the case of τ being a full tree with $p = 2k + 2$ leaves, by (7.1) we have

$$\deg(\tau) = (3k + 1)\rho - (k + 1)d = \frac{3}{2}p(\rho - \rho_c) - 2\rho$$

where we have used the fact that $\rho_c = \frac{d}{3}$. For almost full trees, we obtain

$$\deg(\tau) = (3k + 2)\rho - (k + 1)d = \frac{3}{2}p(\rho - \rho_c) - \rho.$$

It follows that (7.15) becomes

$$\partial_t \bar{u} - \gamma \Delta^{\rho/2} \bar{u} = g \bar{u}^2 + \bar{C}_0(\bar{\varepsilon}, \rho) + \bar{C}_1(\bar{\varepsilon}, \rho) \bar{u} + \sigma \xi^{\bar{\varepsilon}}$$

with

$$\begin{aligned} \bar{C}_0(\bar{\varepsilon}, \rho) &= \lambda^{\alpha+\beta} \sum_p \lambda^{\frac{3}{2}p(\rho-\rho_c)-2\rho} \sum_{\tau \text{ full with } p \text{ leaves}} c_{\bar{\varepsilon}}(\tau) 2^{\bar{n}(\tau)}, \\ \bar{C}_1(\bar{\varepsilon}, \rho) &= \lambda^\beta \sum_p \lambda^{\frac{3}{2}p(\rho-\rho_c)-\rho} \sum_{\tau \text{ almost full with } p \text{ leaves}} c_{\bar{\varepsilon}}(\tau) 2^{\bar{n}(\tau)}. \end{aligned}$$

By (7.16), these expressions for the counterterms are indeed equivalent to (7.13) and (7.14).

It remains to prove the relations (2.10) and (2.11). For full binary trees, setting as before $p = 2k + 2$, we obtain from (7.13) that

$$C_0^{\gamma, g, \sigma}(\varepsilon, \rho) = \sum_{k=0}^{\lfloor k_{\max} \rfloor - 1} \frac{g^{2k+1} \sigma^{2k+2}}{\gamma^{3k+1}} f(k) = \frac{g\sigma^2}{\gamma} \sum_{k=0}^{\lfloor k_{\max} \rfloor - 1} \delta^k f(k),$$

where $f(k)$ is as on the right-hand side of (7.6) and $\delta = g^2 \sigma^2 \gamma^{-3}$. We can now proceed as in the proof of Proposition 7.4, replacing $F(k)$ defined in (7.8) by $\hat{F}(k) = F(k) + \frac{1}{3}k \log \delta$, and H in (7.9) by $\hat{H} = H + \frac{1}{3} \log \delta$. Note that \hat{F} is still convex.

For $\varepsilon > \varepsilon_c$, the sum is dominated by $k = k_{\max}$, and yields the same bound as for $C_0^{1,1,1}(\varepsilon, \rho) = C_0(\varepsilon, \rho)$, up to an additional factor

$$\frac{g\sigma^2}{\gamma} \delta^{k_{\max}} = \left(\frac{g^2 \sigma^2}{\gamma^3} \right)^{k_{\max}} \frac{g\sigma^2}{\gamma}.$$

For $\varepsilon < \varepsilon_c$, the sum is dominated by the term $k = 0$, which has the same scaling behaviour as $C_0(\varepsilon, \rho)$, up to an additional factor $g\sigma^2 \gamma^{-1}$. An analogous argument applies to the expression (2.11) for $C_1^{\gamma, g, \sigma}(\varepsilon, \rho)$.

Contents

1	Introduction	1
2	Model and results	3
3	Model space and renormalised equation	9
4	Canonical model	11
4.1	Simplifying the twisted antipode	12
4.2	From expectations to Feynman diagrams	15
4.3	Simplification rules for Feynman diagrams	18
5	Forests	21
5.1	Zimmermann’s forest formula	21
5.2	Hepp sectors and forest intervals	25
6	Bounds on $E(\tilde{\mathcal{A}}^E\tau)$	30
6.1	The case $\mathcal{F}_u = \emptyset$	31
6.2	The case $\mathcal{F}_u \neq \emptyset$	39
7	Asymptotics	42
7.1	Full binary trees	42
7.2	Almost full binary trees	47
7.3	A remark on lower bounds	47
7.4	Extension to other parameter regimes	48

References

[1] M. Aizenman and H. Duminil-Copin. Marginal triviality of the scaling limits of critical 4D Ising and ϕ_4^4 models. *Ann. of Math.*, 194(1):163–235, 2021.

[2] N. Berglund and C. Kuehn. Regularity structures and renormalisation of FitzHugh–Nagumo SPDEs in three space dimensions. *Electron. J. Probab.*, 21:Paper No. 18, 48, 2016.

[3] N. Berglund and C. Kuehn. Model spaces of regularity structures for space-fractional SPDEs. *J. Stat. Phys.*, 168(2):331–368, 2017.

[4] Y. Bruned, A. Chandra, I. Chevyrev, and M. Hairer. Renormalising SPDEs in regularity structures. *J. Eur. Math. Soc. (JEMS)*, 23(3):869–947, 2021.

[5] Y. Bruned, F. Gabriel, M. Hairer, and L. Zambotti. Geometric stochastic heat equations. *J. Amer. Math. Soc. (JAMS)*, 35(1):1–80, 2022.

[6] Y. Bruned, M. Hairer, and L. Zambotti. Algebraic renormalisation of regularity structures. *Invent. Math.*, 215(3):1039–1156, Mar 2019.

[7] D. Brydges, J. Dimock, and T. R. Hurd. A non-Gaussian fixed point for ϕ^4 in $4 - \epsilon$ dimensions. *Comm. Math. Phys.*, 198(1):111–156, 1998.

[8] A. Chandra and M. Hairer. An analytic BPHZ theorem for regularity structures. [arXiv:1612.08138](https://arxiv.org/abs/1612.08138), 2016.

[9] A. Chandra, M. Hairer, and H. Shen. The dynamical sine-Gordon model in the full subcritical regime. [arXiv:1808.02594](https://arxiv.org/abs/1808.02594), 2018.

[10] L. Chiarini and C. Landim. A one-dimensional non-local singular SPDE. [arXiv:1912.11869](https://arxiv.org/abs/1912.11869), 2019.

- [11] A. Connes and D. Kreimer. Hopf algebras, renormalization and noncommutative geometry. In *Quantum field theory: perspective and prospective (Les Houches, 1998)*, volume 530 of *NATO Sci. Ser. C Math. Phys. Sci.*, pages 59–108. Kluwer Acad. Publ., Dordrecht, 1999.
- [12] A. Connes and D. Kreimer. Renormalization in quantum field theory and the Riemann-Hilbert problem. I. The Hopf algebra structure of graphs and the main theorem. *Comm. Math. Phys.*, 210(1):249–273, 2000.
- [13] A. Connes and D. Kreimer. Renormalization in quantum field theory and the Riemann-Hilbert problem. II. The β -function, diffeomorphisms and the renormalization group. *Comm. Math. Phys.*, 216(1):215–241, 2001.
- [14] A. Deya. On a modelled rough heat equation. *Probab. Theory Related Fields*, 166(1-2):1–65, 2016.
- [15] J. Feldman, R. Magnen, V. Rivasseau, and R. Seneor. Bounds on renormalized Feynman graphs. *Comm. Math. Phys.*, 100(1):23–55, 1985.
- [16] R. A. Fisher. The advance of advantageous genes. *Ann. of Eugenics*, 7:335–369, 1937.
- [17] Y. Gu and W. Xu. Moments of 2D parabolic Anderson model. *Asymptot. Anal.*, 108(3):151–161, 2018.
- [18] M. Hairer. Solving the KPZ equation. *Ann. Math.*, 178(2):559–664, 2013.
- [19] M. Hairer. A theory of regularity structures. *Invent. Math.*, 198(2):269–504, 2014.
- [20] M. Hairer. The motion of a random string. [arXiv:1605.02192](https://arxiv.org/abs/1605.02192). To appear in Proceedings of the XVIII ICMP, 2016.
- [21] M. Hairer. An analyst’s take on the BPHZ theorem. In *Comput. Combin. Dyn. Stoch. Control*, pages 429–476, Cham, 2018. Springer International Publishing.
- [22] M. Hairer and C. Labbé. A simple construction of the continuum parabolic Anderson model on \mathbf{R}^2 . *Electron. Commun. Probab.*, 20:no. 43, 11, 2015.
- [23] M. Hairer and C. Labbé. Multiplicative stochastic heat equations on the whole space. *J. Eur. Math. Soc. (JEMS)*, 20(4):1005–1054, 2018.
- [24] M. Hairer and É. Pardoux. A Wong-Zakai theorem for stochastic PDEs. *J. Math. Soc. Japan*, 67(4):1551–1604, 2015.
- [25] M. Hairer and J. Quastel. A class of growth models rescaling to KPZ. *Forum Math. Pi*, 6:112, 2018.
- [26] M. Hairer and H. Shen. The dynamical sine-Gordon model. *Comm. Math. Phys.*, 341(3):933–989, 2016.
- [27] M. Hairer and H. Shen. A central limit theorem for the KPZ equation. *Ann. Probab.*, 45(6B):4167–4221, 2017.
- [28] M. Hairer and W. Xu. Large scale behaviour of 3D continuous phase coexistence models. *Comm. Pure Appl. Math.*, 71(4):688–746, Apr. 2018.
- [29] M. Hairer and W. Xu. Large-scale limit of interface fluctuation models. *Ann. Probab.*, 47(6):3478–3550, Apr. 2019.
- [30] M. Hoshino. KPZ equation with fractional derivatives of white noise. *Stoch. Partial Differ. Equ. Anal. Comput.*, 4(4):827–890, 2016.
- [31] A. N. Kolmogorov, I. G. Petrovsky, and N. S. Piskunov. Etude de l’équation de la diffusion avec croissance de la quantité de matière et son application à un problème biologique. *Bulletin Université d’Etat à Moscou (Bjul. Moskowskogo Gos. Univ.)*, Série internationale, section A 1, page 1–26, 1937.
- [32] M. Kwaśnicki. Ten equivalent definitions of the fractional Laplace operator. *Fractional Calculus & Applied Analysis*, 20(1):7–51, 2017.
- [33] V. Rivasseau. *From Perturbative to Constructive Renormalization*. 2 edition. Princeton, N.J: Princeton University Press., 1991.

- [34] R. Zhu and X. Zhu. Three-dimensional Navier-Stokes equations driven by space-time white noise. *J. Differential Equations*, 259(9):4443–4508, 2015.

Nils Berglund
Institut Denis Poisson (IDP)
Université d’Orléans, Université de Tours, CNRS – UMR 7013
Bâtiment de Mathématiques, B.P. 6759
45067 Orléans Cedex 2, France
E-mail address: `nils.berglund@univ-orleans.fr`

Yvain Bruned
Institut Elie Cartan de Lorraine (IECL)
Université de Lorraine, CNRS–UMR 7502
Faculté des Sciences et Technologies
Campus, Boulevard des Aiguillettes
54506 Vandœuvre-lès-Nancy
E-mail address: `yvain.bruned@univ-lorraine.fr`